INFORMATION TO USERS

This manuscript has been reproduced from the microfilm master. UMI films the text directly from the original or copy submitted. Thus, some thesis and dissertation copies are in typewriter face, while others may be from any type of computer printer.

The quality of this reproduction is dependent upon the quality of the copy submitted. Broken or indistinct print, colored or poor quality illustrations and photographs, print bleedthrough, substandard margins, and improper alignment can adversely affect reproduction.

In the unlikely event that the author did not send UMI a complete manuscript and there are missing pages, these will be noted. Also, if unauthorized copyright material had to be removed, a note will indicate the deletion.

Oversize materials (e.g., maps, drawings, charts) are reproduced by sectioning the original, beginning at the upper left-hand corner and continuing from left to right in equal sections with small overlaps. Each original is also photographed in one exposure and is included in reduced form at the back of the book.

Photographs included in the original manuscript have been reproduced xerographically in this copy. Higher quality 6" x 9" black and white photographic prints are available for any photographs or illustrations appearing in this copy for an additional charge. Contact UMI directly to order.

UMI

A Bell & Howell Information Company
300 North Zeeb Road, Ann Arbor MI 48106-1346 USA
313/761-4700 800/521-0600

WILD-TYPE AND MUTANT 2,2-DIALKYLGLYCINE DECARBOXYLASES: THE CATALYTIC ROLE OF ACTIVE SITE GLUTAMINE 52 INVESTIGATED BY SITE-DIRECTED MUTAGENESIS AND COMPUTER ANALYSIS

A

THESIS

Presented to the Faculty

Of the University of Alaska Fairbanks

In Partial Fulfillment of the Requirements

For the Degree of

DOCTOR OF PHILOSOPHY

By

See-Tarn Woon, B. Sc. (Technology)

Fairbanks, Alaska

August 1998

WILD-TYPE AND MUTANT 2,2-DIALKYLGLYCINE DECARBOXYLASES: THE CATALYTIC ROLE OF ACTIVE SITE GLUTAMINE 52 INVESTIGATED BY SITE-DIRECTED MUTAGENESIS AND COMPUTER ANALYSIS

By

See-Tarn Woon

RECOMMENDED:

Advisory Committee Chair

Departmental Head

APPROVED:

Dean, College of Science, Engineering and Mathematics

Dean of Graduate School

8-11-98

Date

ABSTRACT

The ability of pyridoxal 5'-phosphate (PLP)-dependent 2,2-dialkylglycine decarboxylase (DGD) to catalyze decarboxylation and transamination of amino acids at a single active site depends on the subsite within the active site that cleaves α-H and α-COO^- bonds. As observed in the crystal structure, the strategic position of glutamine 52 at the active site suggests a role in enhancing decarboxylation via formation of a hydrogen bond to the substrate carboxyl group. Supporting evidence for this hypothesis is provided by studies with glutamine 52 active site mutants, computer modeling and protein sequence analyses.

Ten mutant DGDs containing alanine, asparagine, aspartate, arginine, glutamate, glycine, histidine, leucine, lysine, and tryptophan at position 52 were produced. All, except the histidine mutant, exhibited decreased rates of decarboxylation compared to wild-type. Histidine and asparagine mutants showed measurable decarboxylation rates. These results and that of wild-type DGD suggest that hydrogen bonding with the substrate is required for decarboxylation. Mutants incapable of hydrogen bonding to the substrate, such as alanine, leucine and tryptophan mutants, showed negligible decarboxylation reactions.

Transamination rates increased for some mutants and decreased for others. These data imply that the DGD subsite is influenced by the presence of glutamine 52.

Furthermore, there is evidence showing that the subsite environment of wild-type DGD, the histidine and the glutamate mutants are different; the three DGD forms exhibited different chromophores at around λ_{max} of 500 nm when treated with 2-methylalanine or L-alanine in the presence of 3% glycerol. These results have important implications for other PLP-dependent enzymes, such as ornithine aminotransferase and γ-aminobutyrate aminotransferase. Since protein sequence alignment indicates DGD is homologous to the two aminotransferases, mutations at amino acid position corresponding to glutamine 52 of DGD at the active sites of these aminotransferases could disrupt the functionality of the enzymes.

Protein sequence alignment showed that all but one of the PLP-dependent aminotransferases lack residues at position 52 capable of hydrogen bonding with the substrate carboxyl group, further re-affirming the role of glutamine 52 in decarboxylation.

TABLE OF CONTENTS

LIST OF FIGURES

Page

Page

Page

LIST OF TABLES

Page

LIST OF APPENDICES

Page

LIST OF ABBREVIATIONS

2MA	2-methylalanine
AT	aminotransferase
AAT	aspartate aminotransferase
CAPS	3-(cyclohexylamino)-propanesulfonic acid
CHES	2-(N-cyclohexylamino)ethanesulfonic acid
D-ala	D-alanine
Da	Dalton
DEAE	diethylaminoethyl
DEPC	diethyl pyrocarbonate
DGD	2,2-dialkylglycine decarboxylase
HEPES	N-(2-hydroxyethyl)piperazine-N'-2-ethanesulfonic acid
IPTG	isopropyl β–D-thiogalactopyranoside
kDa	kilodalton
L-ala	L-alanine
MES	2-(N-morpholino)ethanesulfonic acid
MOPS	morpholinopropanesulfonic acid
NMWL	nominal molecular weight limit
OrnAT	ornithine aminotransferase
PLP	pyridoxal 5'-phosphate
PMP	pyridoxamine 5'-phosphate
ppGaNTase	UDP-*N*-acetyl-D-galactosamine : polypeptide N-acetylgalactosaminyl-transferase
pyr	pyruvate
SDS	sodium dodecyl sulfate
TAPS	N-tris(hydroxymethyl)methyl-3-aminopropanesulfonic acid
TEA	triethanolamine
WT	wild-type
X-gal	5-bromo, 4-chloro, 3-indolyl β-D-galactoside

ACKNOWLEDGMENTS

I would like to thank my research advisor, Dr. John Keller, for his support and encouragement throughout my coursework and research project. Many thanks to my committee members: Dr. Joan Braddock, Dr. Thomas Clausen and Dr. Lawrence Duffy for their assistance during my graduate study at UAF.

I must say that I have had lots of fun working with my labmates (Lilly Allen-Daley, Pao-Yu Chi and Honghong Sun) throughout the years. Life is fairly interesting when one is in an all-ladies research lab! I am also grateful to Sheila Chapin for keeping lots of affairs within the university system in order for me and Marlys Schneider for putting up with my continuous "Do you happen to have such and such (mostly chemicals or lab equipment) in your lab?" type questions. I would also like to acknowledge the financial assistance from the Graduate School (University Fellowship) and the Department of Chemistry and Biochemistry.

Finally I wish to thank my family for their love and support during my graduate studies.

Chapter 1

Literature review

1.1. Discovery of vitamin B_6

The early 1930s marked the beginning of a series of notable events that unraveled the mystery of vitamin B_6[1]. The early work was reviewed by Snell (1986), Leklem (1991) and Snell (1994). In 1932, a compound with the formula $C_8H_{11}O_3N$ was first isolated in rice polishings. Two years later, Gyorgy discovered the compound could prevent rat pellagra and named the factor vitamin B_6 to distinguish it from vitamin B_3, B_4 and B_5. The first successful isolation of pure crystalline vitamin B_6 was reported in 1938 (Snell, 1994). One year later, the crystal was identified as 3-hydroxy-4, 5-dihydroxymethyl-2-methylpyridine and was chemically synthesized (Snell, 1994). The pyridine derivative was eventually named pyridoxine, a terminology introduced by Gyorgy in 1939. Other major forms of vitamin B_6 were identified in studies involving microorganisms (Leklem, 1991; Snell, 1994). Snell and coworkers found that pyridoxal and pyridoxamine, but not pyridoxine, supported and enhanced microbial growth (Snell et al., 1942). These findings led to chemical synthesis of the two newly discovered pyridoxine derivatives in 1944

[1] Recommended as the generic name for all 3-hydroxy-2-methylpyridine derivatives (IUPAC-IUB Commission on Biochemical Nomenclature, 1973)

[Snell (1944) and Harris et al. (1944) cited in Leklem (1991)]. The availability of the three forms of vitamin B_6 paved the way for further research into the properties of the vitamin (Figure 1).

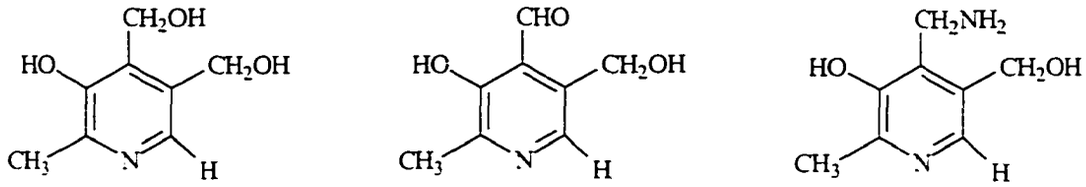

pyridoxine (PN) pyridoxal (PL) pyridoxamine (PM)

Figure 1. Structures of pyridoxine, pyridoxal and pyridoxamine.

During his initial investigations into *Streptococcus faecalis* tyrosine decarboxylase conducted in 1940, Gale concluded that enzyme production was dependent on substrate and a factor in the growth media, which was later identified as pyridoxine [Gale (1946) cited in Snell (1994)]. This was the first clue of an enzyme related to vitamin B_6. Studies with a crude preparation of *S. faecalis* tyrosine decarboxylase provided evidence that phosphorylated or 'activated' pyridoxal was required for enzyme functionality (Gunsalus et al., 1944). Coupled with improved chemical synthesis of phosphorylated pyridoxal, Gunsalus and colleagues also concluded that the coenzyme is a monophospho-pyridoxal. In 1945, Gale and Baddiley showed that pyridoxal phosphate activates arginine, lysine, ornithine and tyrosine apodecarboxylases (Snell, 1986). Attention was then shifted to explaining the possible role of pyridoxal phosphate in

biological reactions. In that same year, Snell demonstrated reversible non-enzymatic transamination between pyridoxal and amino acids (Snell, 1986). He suggested that amino transfer between pyridoxal and pyridoxamine may be possible in enzymatic reactions. In other words, the cofactor was envisioned as an amino carrier between keto acids. This hypothesis was supported by a series of experiments involving partially purified enzymes such as aspartate aminotransferase, glutamate-oxaloacetic transaminase, tyrosine decarboxylase and glutamate-aspartate transaminase (Snell, 1986).

Although Gunsalus and coworkers demonstrated the requirement of phosphorylated pyridoxal for enzyme activity, they were unable to determine the position of phosphorylation in pyridoxal. In theory, phosphorylation could take place at the 3-hydroxyl, hemiacetal hydroxyl or 5-hydroxymethyl position. It was not until 1961 that the position of the phosphate moiety at the 5'-hydroxymethyl group of pyridoxal was finally confirmed by two separate research groups (Snell, 1994).

1.2. PLP-catalyzed reactions at α-carbon

The requirement for pyridoxal 5'-phosphate (PLP) in amino acid decarboxylation and transamination is well established from studies with *Streptococcus faecalis* and *Lactobacillus casei* that date back some fifty years ago. Since the early studies described above, enzymes other than aminotransferases and decarboxylases requiring PLP to function have been discovered. Although not an exhaustive list, these enzymes are

involved in deamination, racemization and transsulfuration of amino acids and in the metabolism of fats and carbohydrates (Dolphin et al., 1986). However, half of more than 100 PLP-dependent enzymatic reactions so far discovered are transamination type reactions (Sauberlich, 1985).

Reactions catalyzed by coenzyme PLP-requiring enzymes are categorized into three groups: The reaction could take place at α-, β- or γ-carbon. Decarboxylation, transamination and retroaldol cleavage require bond breaking at the α-carbon. Figure 2 depicts the general scheme of the three PLP-catalyzed reactions. The first step of all three reactions entails the internal Schiff base formation between PLP and ε-NH_2 of the lysine side chain. This is followed by substrate displacement of the ε-amino group of the lysine residue to form an external Schiff base or aldimine with the cofactor. Depending on the orientation of the substrate-PLP complex at the active site, one of the three bonds can be broken: C_α-COO in decarboxylation, C_α-H in transamination and C_α-R in retroaldol cleavage. A number of requisites have to be fulfilled for bond cleavage to take place.

One criterion for effective enzyme catalysis requires the coplanarity between the imine and π system. Dunathan (1966) proposed that the bond to be broken has to be oriented perpendicular to the plane of the pyridine ring and the imine double bond to maximize orbital overlap between the C_α-R bond and the conjugated π electron system (Figure 3). Once the C_α-R bond is broken, the electrons can be delocalized into the extended π system to stabilize the intermediate. In addition, the stability of the intermediate is enhanced by the protonated pyridinium nitrogen.

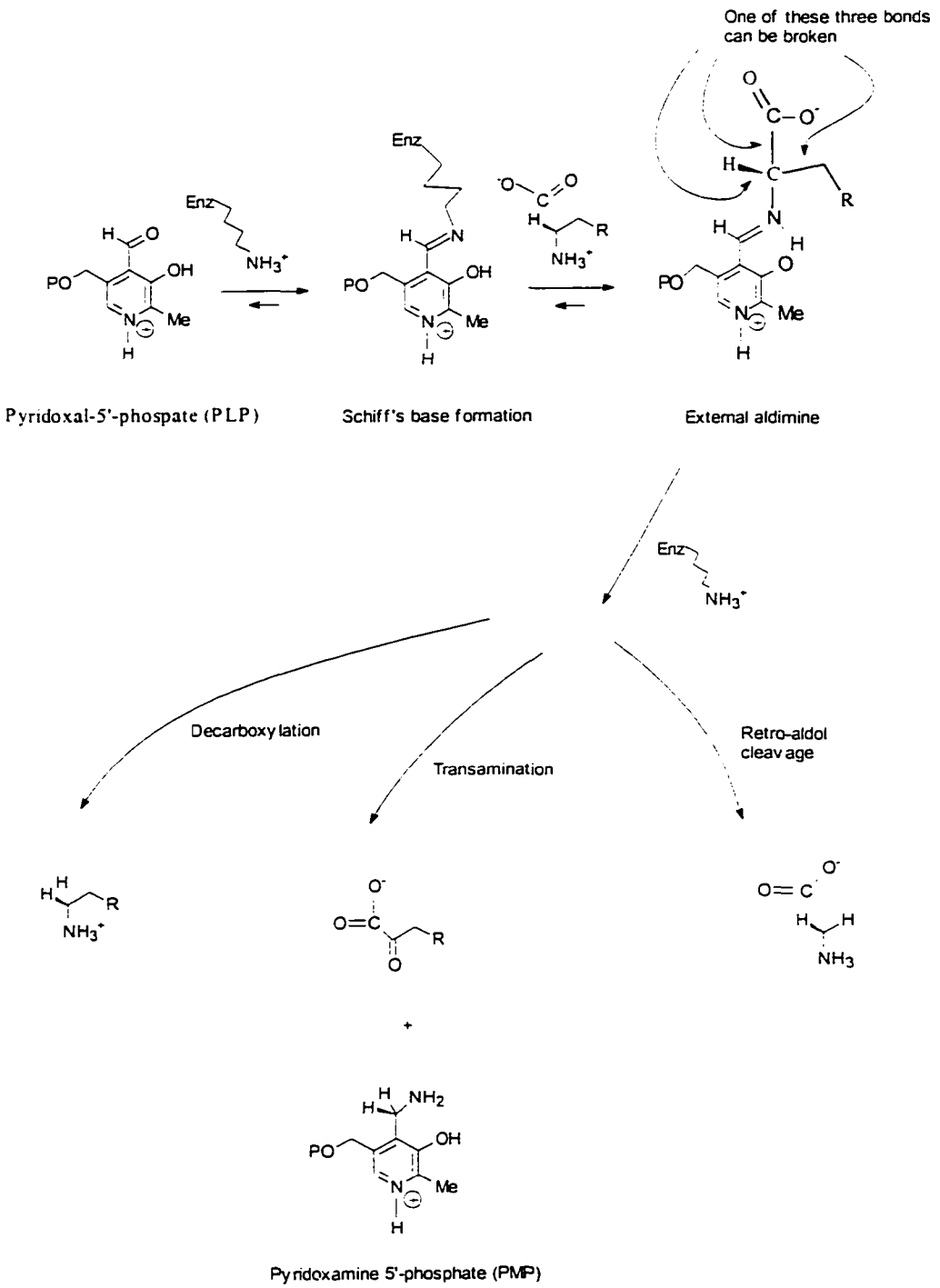

Figure 2. PLP-catalyzed decarboxylation, transamination and retrol cleavage (Gani, 1991).

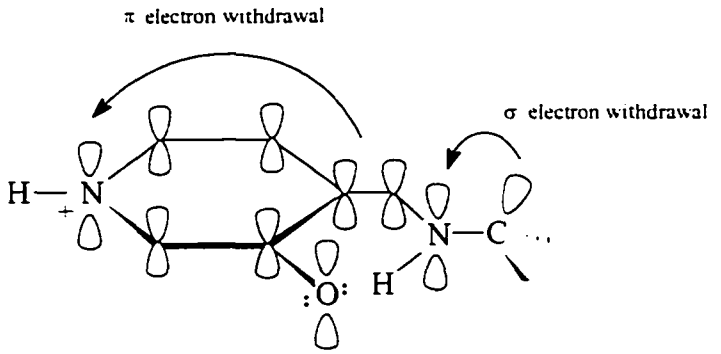

Figure 3. External aldimine C_α-R bond to be broken is parallel to π molecular orbital or perpendicular to ring.

In free solution, PLP complexed with an amine can catalyze the bond breaking process at a relatively slow rate when supplemented by metal cations such as Cu^{2+}, Zn^{2+} and Al^{3+} (Leussing, 1986). Because free rotation around the C_α-N bond can occur in solution, any of the three substituents on the α-carbon can be the leaving group. Hence chemical model reactions are inherently non-selective with several potential reaction courses and products. In biological systems, however, the enzyme active site geometry is rigidly defined. Only metabolically compatible amino acids are transformed at a substantial rate. The active site confers reaction specificity by bonding the PLP-substrate complex and orienting the substrate appropriately. By aligning a specific C_α-R bond of the substrate perpendicular to the cofactor ring, the enzyme can dictate the outcome of the reaction. Unlike chemical PLP reactions, metal cations are not involved in enzyme-catalyzed reactions.

In aminotransferases and decarboxylases, the PLP-substrate complex orientation can be accomplished by three attachment points at the enzyme active site. Aspartate aminotransferase from *E. coli* complexed with the inhibitor, 2-methyl-L-aspartate, (Okamoto et al., 1994) provides an example of how the complex is oriented at the active site. The first two attachment sites are common in PLP enzymes; protonated pyridinium nitrogen is held in place by negatively charged aspartate and the phosphate moiety lies in a polar pocket. The substrate binding site provides the third unique mold for maintaining a desired C_α-N conformation; side chains Arg292 and Arg386 form salt bridges with substrate α- and ω-carboxyl groups, respectively. The three-point attachment system orients the methyl group of 2-methyl-L-aspartate, which corresponds to the substrate α-proton, perpendicular to the ring. Two of the three attachment points at the active site of the ornithine decarboxylase from *Lactobacillus 30a* are similar to those of aminotransferases (Hackert et al., 1994; Momany et al., 1995). Likewise, Asp316 ion pairs with the N1 pyridinium ring of the cofactor and the PLP phosphate group lies in a site lined with polar residues. The third domain accountable for substrate specificity is tentatively assigned to Glu235, which lies within hydrogen bonding distance of the δ-amino group of L-ornithine.

Ivanov and Karpeisky (1969) proposed on thereotical grounds that PLP reorients during transimination. They postulated that transformation from internal to external Schiff base results in the exposure of opposite faces. The key stereochemical principle is that the reaction occurs on one face of the planar enzyme bound PLP-substrate complex;

the reactive face is exposed to solvent and accessible to substrate and external reagents whereas the opposite face remains shielded by protein. Two potential modes, rotation at C-5 to C-5' and rotation at C-4 to C-4', are shown in Figure 4.

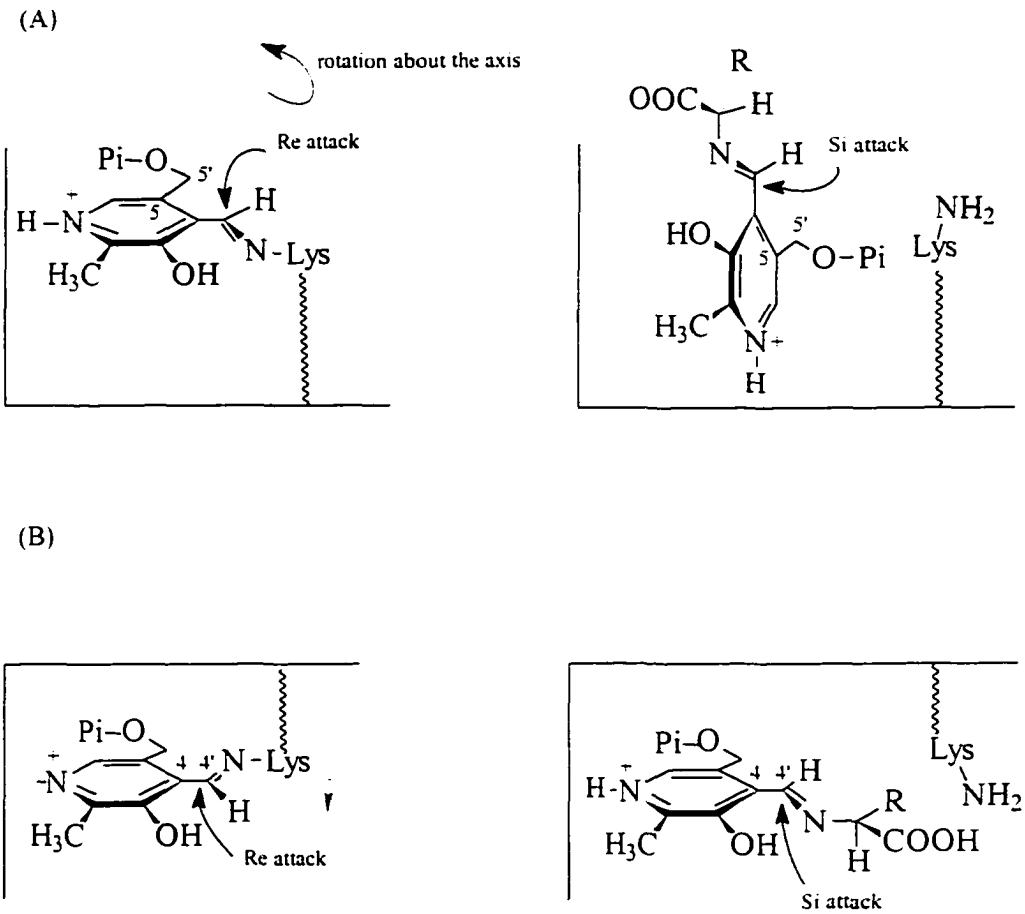

Figure 4. PLP reorientation during transimination: (A) C-5 to C-5' rotation and (B) C-4 to C-4' rotation.

Both transformations result in the exposed face *si* face relative to 4'-C in the PLP-substrate complex and *re* face in internal Schiff base. The exposed *si* face is prone to solvent attack while the *re* face is protected by the protein. Support for the postulate came from stereochemical studies with sodium borohydride reduction of internal and external Schiff base of PLP enzymes (Palcic and Floss, 1986 and references therein). Hydride attack took place at the *re* face of PLP-substrate complex in aspartate aminotransferase, tyrosine decarboxylase, tryptophan synthase, tryptophanase and tyrosine phenol-lyase. By contrast, PLP-substrate, PLP-product, or PLP-inhibitor complexes of PLP enzymes studied so far showed protonation at the *si* face. These enzymes include aspartate and alanine aminotransferases, tyrosine decarboxylase and tryptophan synthase.

The X-ray structure of aspartate aminotransferase reveals the *re* face of internal Schiff base is partially exposed to solvent, whereas the *si* face is shielded by the enzyme (Ford et al., 1980). Upon inhibitor methylaspartate binding, the PLP ring rotates 30° with C-5 to C-5' as a hinge. The motion is accompanied by the exposure of the *si* face to the solvent environment, where bond breaking and forming take place. On the contrary, the *re* face is protonated in D-amino acid aminotransferase (Sugio et al., 1995).

The next logical question to ask is why the ancestral enzyme selected one face of the cofactor and not the other to undergo catalysis? A theory was put forward by Dunathan and Voet (1974). They reasoned that the choice between *re* and *si* face is an early and completely random occurrence; neither choice is more efficient. The choice, once made, is difficult to reverse. Inversion of the PLP face requires a complete

rearrangement of active site residues and is energetically unfavorable. The progenitor protein, with its fixed cofactor binding, may have low substrate specificity. Through the course of evolution, the protein evolved into more sophisticated enzymes with the preservation of the original choice of PLP binding.

However, Christen et al. (1996) presented evidence that the preservation of the *si* face in L-amino acid aminotransferases (and *re* face in D-amino acid aminotransferases), which faces the catalytic base of the protein, is not coincidental. Model calculation of the L-amino acid/PLP complex showed that (1) the external aldimine must have the COO^- positioned far away from the phosphate group to attain conformation of minimum energy for maximum binding and (2) the C_α-H bond has to be positioned to undergo chemical reaction perpendicular to the π-system and towards the protein. To fulfill two such requirements, the *si* face of the 4'-C of the cofactor will be facing the protein and therefore towards the residue that catalyzes protonation. Meanwhile, the *re* side will be exposed to the solvent.

1.3. Properties of pyridoxine derivatives

Vitamin B_6 is a water-soluble vitamin. The three forms, pyridoxine, pyridoxal and pyridoxamine, are light sensitive in solution (Ang, 1979). The three forms are heat stable in acidic medium and heat labile in alkaline solution (Leklem, 1991).

The characteristic electron withdrawing property of the pyridine ring accounts for the diverse reactions PLP catalyzes (Leklem, 1991). Leussing (1986) listed several

structural features of PLP that makes the cofactor an ideal candidate for forming Schiff base and catalyzing enzymatic reactions. These include the 2-methyl group that brings the pK_a of the nitrogen ring proton closer to biological range; the phenoxide oxygen that stabilizes the immonium Schiff base, facilitates expulsion of nucleophiles at the 4'-C position and acts as a proton transfer intermediary; the phosphate moiety which anchors the coenzyme in a polar pocket; and the protonated N which neutralizes the negative charge acquired by imine as amino acid groups are activated and regulates the pK_a of the 3-hydroxyl group.

PLP dependent enzymes exhibit characteristic absorption peaks in the 300 to 500 nm region that arise from vitamin B_6-containing chromophore. These spectra tend to represent mixture of PLP and its related derivatives at the enzyme active site. Each species of the mixture can be described quantitatively by a lognormal distribution curve of uniquely specified position, height, width and skewness (Metzler and Metzler, 1987). Since width and skewness values are constant for similar compounds, it is possible to resolve overlapping spectral bands in complex equilibrium mixtures. Based on calculations from PLP spectra of aspartate aminotransferase and glutamate decarboxylase, Metzler and Metzler (1987) were able to determine the parameters describing distribution curves of potential pyridine derivatives at the active site.

Figure 5 depicts some PLP derivatives present at the active site. An absorption band with λ_{max} of about 430 nm is characteristic of a nitrogen-protonated Schiff base of the PLP. This ketoenamine form is covalently bound to the active site lysine. The

unprotonated Schiff-base linkage with an undissociated phenolic hydroxyl group absorbs at about 330 nm and is often called the enolimine form. These two absorption peaks represent tautomeric forms of PLP. PMP absorbs at approximately 325 nm. The spectrum of ketimine peaks at 327 nm and the shape of the absorption band is similar to that of PMP. A quinonoid intermediate, observed in some PLP enzymes reacted with quasisubstrates, exhibits an absorption peak at approximately 490 to 500 nm.

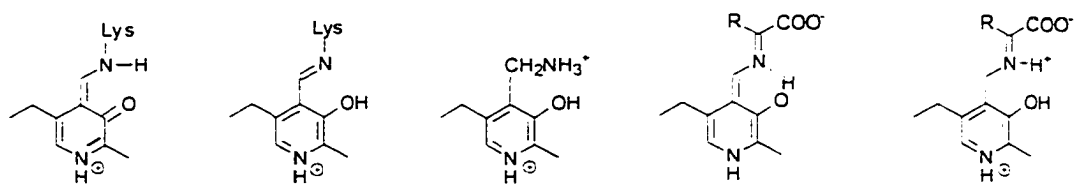

Figure 5. Different PLP forms present at enzyme active site have characteristic absorption peaks.

1.4. *Burkholderia cepacia* 2,2-dialkylglycine decarboxylase (DGD)

1.4.1. Introduction

2,2-dialkylglycine decarboxylase (DGD; EC 4.1.1.64) from the soil bacterium, *Burkholderia (Pseudomonas) cepacia*, was first reported by Aaslestad and Larson (1964). DGD is an unusual PLP-dependent enzyme because it catalyzes two distinct reactions, decarboxylation and transamination, at one active site. The decarboxylation-dependent

transamination reaction proceeds via a ping pong bi-bi mechanism. This double replacement mechanism proceeds as follows: the enzyme reacts with one substrate to give a covalently modified enzyme and releases one product, and then reacts with the second substrate to form a second product and regenerate the enzyme. Phosphoglycerate mutase, a phosphate-transferring enzyme, is one such example. The enzyme is phosphorylated by one substrate to form a phosphorylenzyme, which then transfers the phosphoryl group to a second substrate.

The two half reactions catalyzed by DGD are depicted in Figure 6. Reaction (1) involves PLP reacting irreversibly with either 2 methylalanine (2MA) or isovaline to produce carbon dioxide and ketone coupled with amino transfer to the cofactor to give PMP. Reaction (2) entails the amino transfer from PMP to pyruvate to yield L-alanine and regenerate PLP; this second step is reversible. The combined reaction of (1) and (2) is equivalent to the non-enzymatic reaction put forward by Kalyankar and Snell (1962).

The exact biological role of DGD remains unclear. Dempsey (1969) and Esaki et al. (1994) demonstrated that DGD is widespread in many soil bacterial and fungal species, implying that this enzyme probably plays an important ecological or physiological role within the soil community. DGD provides a soil dwelling microorganism defense against fungal dialkylglycine containing peptides, which are cytotoxic. The major constituents of these cytotoxic peptides are 2-methylalanine and isovaline (Bruckner and Pryzbylski, 1984). Both dialkylamino acids are substrates of

DGD. Keller et al. (1990) postulated that DGD may be involved in the degradation of fungal peptides to provide supplemental carbon and nitrogen sources for the hosts.

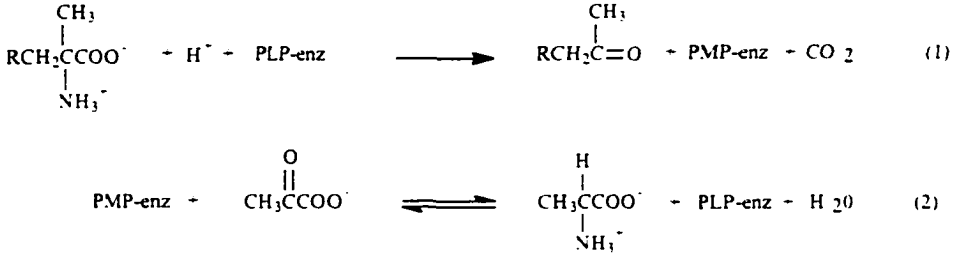

Reaction (1) and (2) gives the following net reaction:

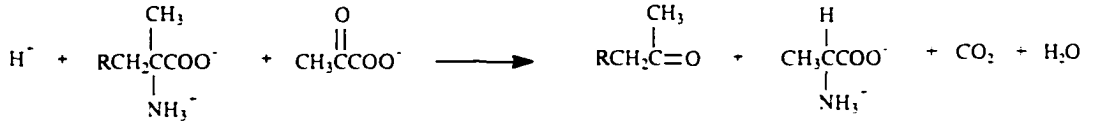

where R = H for 2MA and R = CH_3 for isovaline.

Figure 6. DGD decarboxylation-dependent transamination reaction.

Purified to homogeneity, DGD was first studied in some detail by several research labs (Bailey and Dempsey, 1967; Aaslestad et al., 1968; Lamartiniere et al., 1971). Based on experiments involving radioactive substrates and predicted stoichiometry of the reaction, Bailey and Dempsey (1967) demonstrated that DGD catalyzes a sequential decarboxylation and transamination reaction. The DGD subunit was shown to be 45 kDa by SDS gel electrophoresis and 47 kDa by sedimentation centrifugation in urea

(Lamartiniere et al., 1971). Since the native enzyme is estimated at 180 kDa (Lamartiniere et al., 1971; Sato et al., 1978), DGD is thus a tetrameric enzyme consisting of four identical subunits. Keller et al. (1990) reported the cloning, sequencing and expression of DGD in *E. coli*. The gene sequence encodes a subunit of 434 amino acids with the carboxyl end sharing substantial sequence similarity with aminotransferases but not decarboxylases. DGD can thus be best described as an aminotransferase, which through evolution has acquired decarboxylation activity, and not a decarboxylase that has evolved the ability to transaminate. The recombinant DGD expression in *E. coli* facilitates production of highly purified enzyme. Crystallization of the purified enzyme leads to the identification of the 3D protein structure. The 3D structure of DGD was eventually solved by Toney et al. (1995a), who provided intimate structural analysis of the enzyme and related how catalytic mechanisms could be achieved through precise organization within the enzyme.

1.4.2. Structural organization of DGD

The three dimensional structure of DGD was determined to 2.1 Å resolution by Toney et al. (1995a). The following is an account of the overall structural organization of the enzyme. In brief, a DGD monomer interacts tightly with another monomer to form a dimer. This is followed by a dimer associating loosely with another dimer to form a functional tetramer.

A DGD monomer is composed of 434 amino acids with a calculated molecular mass of 46,544 Da (Keller et al., 1990). Figure 7 depicts a ribbon presentation of the folded structure of the monomer. The secondary structural elements in the DGD subunit are presented in Figure 8. A DGD subunit is divided into three domains: a large PLP binding domain, a smaller C-terminal domain and an N-terminal segment. The large PLP binding domain is made up of seven-stranded β-sheet (*a, g, f, e, d, b, c*) of which six of the strands are parallel (+, -, +, +, +, +, +). This sheet is covered on both sides by eight helices of various lengths. Structures of all PLP-dependent enzymes discovered so far have the unique topology of the seven-stranded β-sheet at the large domain (Isupov et al., 1998). The interaction between the small domain with the large domain is mediated by the four-stranded antiparallel β-sheet (D, E, F and G). The three α-helices of the small domain pack against the β-sheets on the side opposite that of the large domain. The PLP binding site is located near the N-terminus of helix 4 and the C-termini of strands *e* and *f*. The monomer also contains two binding sites for alkaline metal ions. One is located near the active site and accounts for the dependence of activity on potassium ion. The other site binds sodium ion and is located at the carboxyl terminus of a α-helix.

Two monomers associate tightly to form the dimeric structure. The interaction surface between the monomers is large. There is 3770 $Å^2$ of a monomer surface area buried upon dimer formation. Close contacts between the two monomers in the dimer are made by the N-terminal helix and its associated loop. This substructure participates in

Figure 7. Stereoscopic presentation of a DGD monomer. α-helices and β-sheets are drawn as coils and arrows, respectively. The large PLP binding domain is at the bottom, the C-terminal domain is at the upper right. The N- and C-termini are marked (diagram from Toney et al., 1995a).

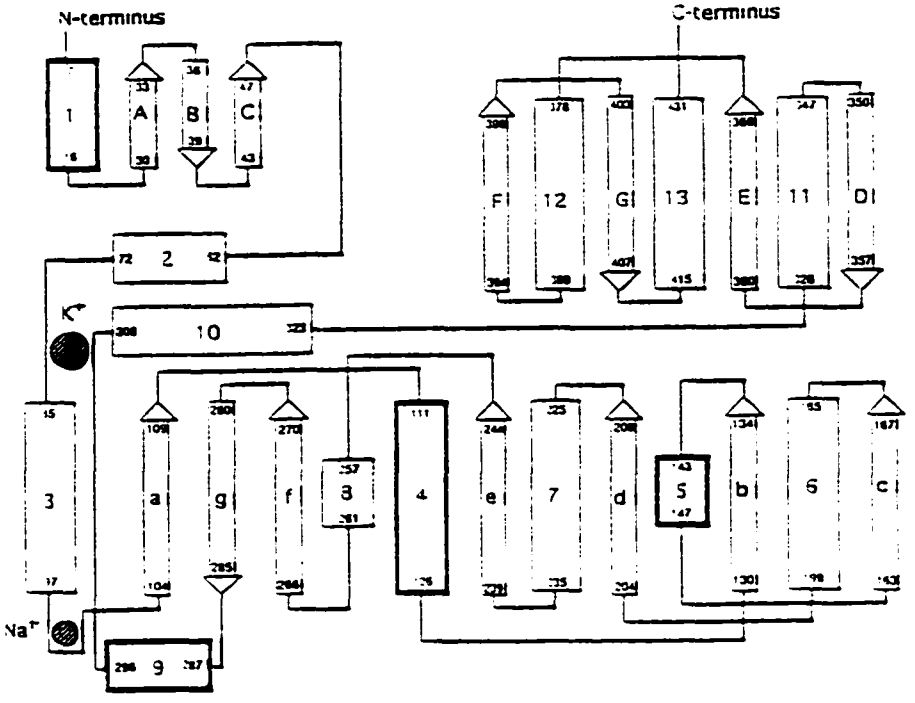

Figure 8. Secondary structural elements of a DGD monomer. Rectangular boxes in bold and thin outline represent α-helices above and below the β-sheets, respectively. β-strands are represented by boxes with arrows, which give the direction of the strands from amino to carboxy end. The residue range of each secondary structure is indicated. The approximate K^+ and Na^+ binding sites are shown (diagram from Toney et al., 1995a).

numerous hydrophobic and ionic interactions with the large domain of the other monomer.

The tetrameric structure has an overall dimension of 100 x 85 x 60 Å and is formed by the symmetric association of two dimers. The dimer-dimer interface is three times smaller than that of the monomer-monomer. This dimer-dimer interface is largely formed by the interactions between helix 6 and its N-terminal associated loop with their symmetry mates, and between this helix and strand *c* of the large domain β-sheet. About ten residues from each subunit are involved in the formation of the tetramer interface. Several hydrogen bonds and a water-mediated salt bridge also contribute to the interface.

Toney et al. (1995a) noted that the DGD monomer is similar in structure and overall folding to aspartate aminotransferase (AAT) monomer. The seven stranded pleated sheets and helices correspond closely in both monomers. Also, the shape and dimensions of DGD dimer are similar to AAT dimer. The DGD active site, however, is only moderately homologous to that of AAT. The only similarity is that the positions of the PLP pyridine nitrogen atom, the aspartate carboxylate group and the imidazole nitrogen atom of histidine are conserved in both AAT and DGD. Another notable feature is the tryptophan position in front of the PLP ring. The amino acid is parallel with the ring in AAT but perpendicular in DGD.

Four active sites are present in a DGD tetramer, which explain the four PLP binding sites per molecule of enzyme reported by Sato et al. (1978). Each active site is

formed from residues contributed by both monomers in the dimer formation. The DGD active site will be discussed in more detail in the next two sections.

1.4.3. Substrate and reaction specificity of DGD

DGD acts on various dialkyl-α-amino acids (Honma et al., 1972). The ability of DGD to decarboxylate or transaminate certain substrates depends on substrate orientation at the active site (Figure 9). The DGD active site consisting of three binding sites proposed by Toney et al. (1995a) is also included in Figure 9 to aid in explaining the results described below.

Bailey et al. (1970) proposed that the amino acid side chain, not the scissile bond, directs substrate-PLP conformation at the active site. They observed that DGD decarboxylates 2-methylalanine and L-alanine but transaminates D-alanine; hence they concluded that site-specific binding of the alkyl side chain at a common subsite anchors the substrate in such a way that permits decarboxylation or deprotonation at the scissile bond. Similarly, site-specific binding of an alkyl group could also explain why DGD metabolizes α-methyl-L-serine but not α-methyl-D-serine (Honma and Shimomura, 1976). The above observations indicated that site III can accommodate an alkyl group, but not a carboxyl group of D-ala or a carbinol group of α-methyl-D-serine.

In addition, the higher decarboxylation rate of L-isovaline compared to D-isovaline (Aaslestad et al., 1968; Honma et al., 1972) suggests that the α-methyl group

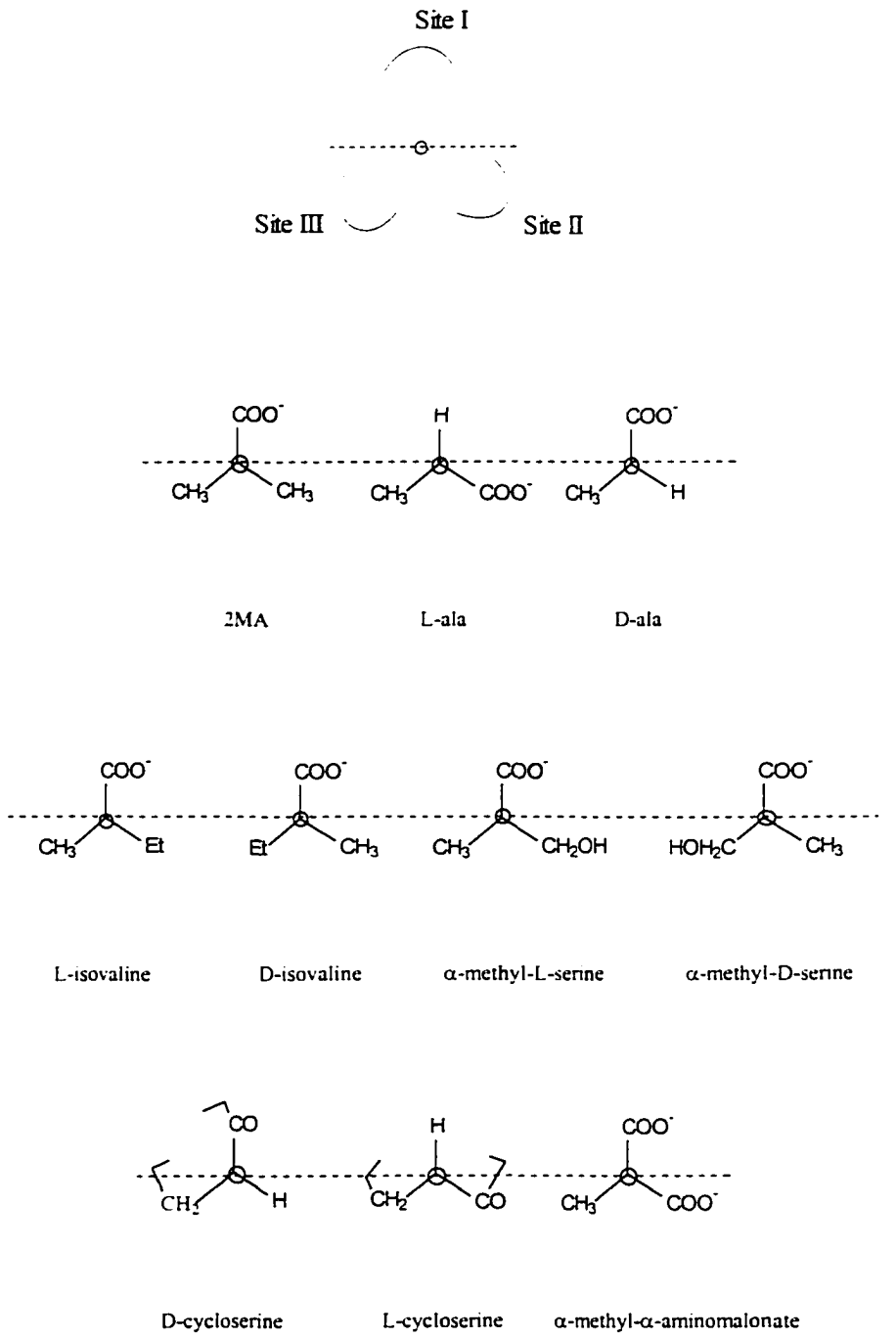

Figure 9. Position of various substrates at DGD active site. Amino side chain of substrates points away and perpendicular to paper. Dotted line represents plane of PLP ring in imine complex.

fits better at site III to permit efficient catalysis. The larger ethyl group of D-isovaline cannot be accommodated as well as a methyl group in site III, thus resulting in less effective decarboxylation. Inhibition study with D- and L-cycloserine further supports the concept that amino acid side chain, in particular a methyl group, orients substrate conformation (Bailey et al., 1970; Figures 9 and 10). The ring methylene positions the α-hydrogen of L-cycloserine for deprotonation. Such cleavage would result in a more stable inhibitor-cofactor complex, thus enhancing inhibition. However, the ring carbonyl would be directed towards scission in the D-isomer. Inhibition is less effective since the complex undergoes rearrangement and hydrolysis.

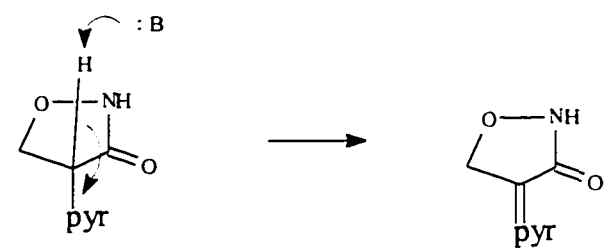

L-cycloserine

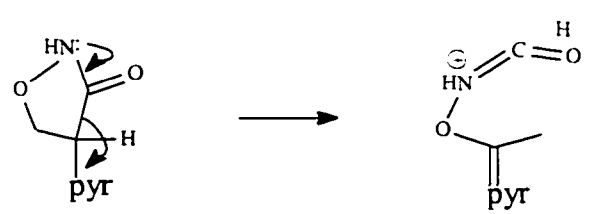

D-cycloserine

Figure 10. DGD inhibition by L- and D-cycloserine. pyr = pyridine.

In the proposed model by Toney et al. (1990a) (Figure 9), two of the three binding sites can accommodate a COO^- group. Gln52 and Lys272 are located at the first site while second site is occupied by Arg246. These residues could potentially form hydrogen bonds with the substrate COO^- groups. Supporting evidence for the three distinct binding sites comes from alternative substrates studies by Sun et al. (1998) [an example is α-methyl-α-aminomalonate in Figure 9]. They demonstrated that (a) site I accommodates the scissile bond from either a carboxylate or a hydrogen, (b) site II accepts an alkyl or a carboxylate group, and (c) site III accepts a methyl group but not a carboxylate or large alkyl group. The last inference agrees with the findings discussed in the previous paragraphs. In short, the dual nature of the binding sites is important in the ability of DGD to carry out decarboxylation and transamination.

1.4.4. Normal versus abortive decarboxylation

When the substrate enters the active site of PLP-dependent enzyme, transimination reaction between cofactor and amino terminal of amino acid results in external Schiff base formation. The imine is anchored at the active site by ionic and hydrogen bonding interactions with residues around the catalytic site. Breaking of the C_α-COO bond results in the formation of a carbanionic intermediate. This intermediate structure is stabilized by the conjugated π-electrons of the pyridine ring and also by its electron withdrawing capability. Decarboxylation reactions in all PLP decarboxylases are similar up to this point.

Protonation at C_α of the carbanionic intermediate allows most decarboxylases to form amine and PLP-lysine Schiff base. However, the carbanion of the DGD-catalyzed reaction follows a different route. Protonation at 4'-C permits DGD to generate a ketone and PMP. PMP then reacts with another keto acid in the second half reaction to form amino acid and regenerate PLP. One explanation for such selectivity may be related to the position of the general acid (Figure 11).

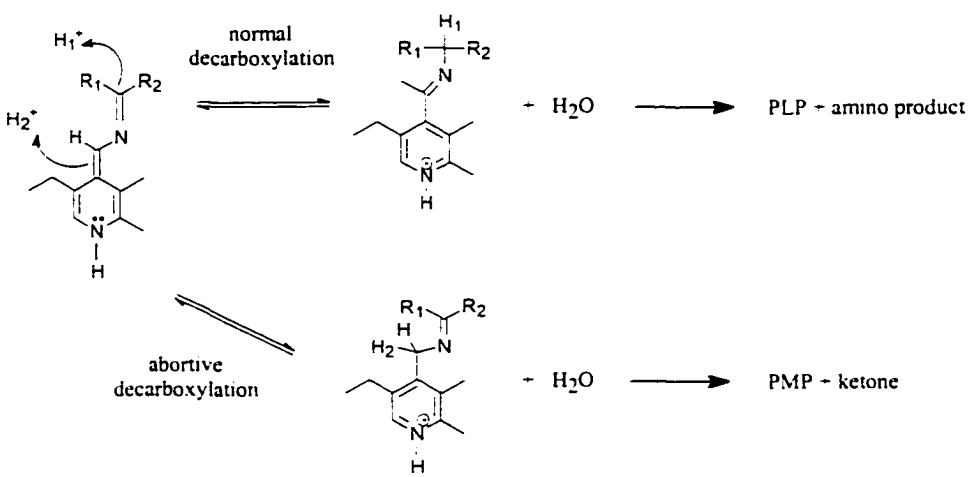

Figure 11. Regioselectivity of protonation of quinonoid intermediate leads to normal and abortive decarboxylation.

If the position of general acid is closer to C_α, normal decarboxylation occurs. If the general acid is located near the 4'-C, abortive decarboxylation takes place. Studies

with mono and dicarboxylic amino acids suggest that the presence or absence of a carboxylate group at site II could determine protonation at either C_α or 4'-C (Sun et al., 1998). Ionic interaction between Arg406 and substrate COO^- minimizes cofactor tilting so that either C_α or 4'-C is physically assessible to protonation by Lys272. Conversely, substrates lacking such ionic interaction would result in a larger cofactor tilt angle thus excluding protonation at C_α. The absence of carboxylate groups at site II leads in protonation at 4'-C in 2MA and D-ala (Figure 9). L-ala and α-methyl-α-aminomalonate can undergo protonation at C_α and 4'-C because of the ionic interaction between Arg406 and carboxylate group.

PLP-dependent decarboxylases catalyze protonation at 4'-C at a rate of once in 10^5 turnover (Tramonti et al., 1998 and references therein). It has been proposed that a histidine protonates at C_α whereas a lysine residue protonates at 4'-C in methionine and glutamate decarboxylases [Akhtar et al. (1990) and Tilley et al. (1994) cited in Tramonti et al. (1998)]. The absence of such a histidine in the active site vicinity may have determined the fate of DGD protonation at 4'-C position and not at C_α. A detailed analysis of the histidines, if any, at the DGD active site will provide clues if such theory is valid.

The protonation step of abortive decarboxylation is similar to the protonation step of transamination. In other words, DGD decarboxylation process is essentially a transamination with the exception that the leaving group is α-COO^-. During transamination, protonation takes place via the intramolecular 1,3-prototropic shift, which

involves the transfer of substrate α-H to 4'-C of the cofactor. Work done on some PLP enzymes suggests that the intramolecular proton shifting step could be mediated by a single base group at the active site in a suprafacial process (Palcic and Floss, 1986). Lysine may be the possible candidate for the role after it is released from the internal aldimine. The suprafacial process requires the general base to be located on the *si* face of the substrate-PLP complex for decarboxylation and protonation to be carried out.

Ultimately, protonation position of the quinonoid intermediate determines the course of reaction: protonation at C_α leads to normal (nonoxidative) decarboxylation while protonation at 4'-C results in abortive (oxidative) decarboxylation. Site directed mutagenesis of aminotransferases involving replacing active site lysine with other residues drastically reduced catalytic activities, thus supporting the role of lysine as a catalytic base (Toney and Kirsch, 1989; Nishimura et al., 1991). However, the active site lysine of aromatic L-amino acid decarboxylase may not function as a proton donor in the reprotonation step (Nishino et al., 1997).

1.5. Significance of conducting DGD research

DGD is structurally closely related to two medically important aminotransferases: ornithine aminotransferase (OrnAT) and γ-aminobutyrate aminotransferase (GabaAT) (Shen et al., 1998; Toney et al., 1995b). Gyrate atrophy, a hereditary disease that leads to progressive blindness and eventually blindness in humans, arises from dysfunctional OrnAT (Shen et al., 1998 and references therein). In mammals, GabaAT regulates γ-

aminobutyrate (GABA) concentration in the brain, where the molecule is a major inhibitory neurotransmitter (Toney et al., 1995b and references therein). The enzyme is also the target enzyme of an anti-epileptic drug, 4-aminohex-5-enoate, which is known as vinyl-GABA or Vigabatrin [Mumford and Cannon (1994) cited in Toney et al. (1995)].

So far, only the 3D structure of OrnAT has been published (Shen et al., 1998). The structure of GabaAT is still under X-ray crystallographic investigation but not yet available (Toney et al., 1995b). The significant sequence homology between DGD and GabaAT allowed the active site of GabaAT to be modeled from that of DGD (Toney et al., 1995b). From the computer-modeled GabaAT active site, Toney and coworkers were able to demonstrate how vinyl-GABA inactivates the enzyme. Shen et al. (1998) and Toney et al. (1995b) also noted that OrnAT and GabaAT share many similar features with DGD at the active site. The knowledge gained from understanding the mechanism of action of DGD can be applied to elucidate how OrnAT and GabaAT active sites function.

1.6. Project objectives

PLP-dependent aminotransferases are divided into four subgroups based on their degree of similarities in primary structure (Mehta et al., 1993). Protein sequence alignment showed that DGD is closely related to subgroup II (Mehta and Christen, 1994). However, DGD possesses the ability to catalyze decarboxylation not found among the subgroup II members. Furthermore, DGD catalyzes both decarboxylation and transamination reactions of amino acids at one active site. The sequential cleavage at α-

carboxyl and α-hydrogen at the active site is intriguing. Which amino acid(s) is(are) responsible for the unique ability of DGD to carry out decarboxylation in addition to transamination?

There are three main objectives in this thesis project:

(i) to determine which amino acid at the DGD active site enables the enzyme to catalyze decarboxylation in addition to transamination and how the amino acid promotes decarboxylation;

(ii) to determine if this amino acid influence the transamination ability of DGD;

(iii) to apply the knowledge of DGD active site to OrnAT and GabaAT active sites to elucidate how they function.

1.7. Hypothesis testing on how DGD catalyzes decarboxylation

Toney et al. (1995a) postulated that DGD-catalyzed decarboxylation may involve Gln52 and Tyr301*. These two amino acids reside at the top of the substrate binding site and have no similar counterparts in AAT. Toney and co-authors presented the following model for the role of Gln52 in decarboxylation. During protein crystallization, a MES molecule occupies the position where a substrate normally resides at the active site. Gln52 is within hydrogen bonding distance with the MES sulfonate group. It is therefore logical to hypothesize that Gln52 could be a hydrogen bond donor to the carboxylate group of a substrate in place of MES molecule. The onset of hydrogen bonding to

* denotes amino acid of the other monomer.

substrate carboxylate group is most likely required to orient the scissile bond perpendicular to the pyridine ring of PLP for promoting decarboxylation. The resulted quinonoid intermediate is then protonated at the 4'-C position. Subsequent transamination involves Lys272 serving as a proton acceptor and donor.

Current literature does not mention whether the decarboxylation and transamination reactions are separate events catalyzed by Gln52 and Lys272 respectively or are dependent on both residues for effective catalysis. However, in my opinion, the concept of decarboxylation and transamination as separate events catalyzed by Gln52 and Lys272 respectively is a much simpler model to visualize: Removal of Gln52 will abolish decarboxylation activity; removal of Lys272 will eliminate transamination activity.

The following hypothesis is formulated based on the above description at the DGD active site: Removal of Gln52 and hence the amide group will abolish decarboxylation activity but will not affect the transamination reaction. Replacement of Gln52 with amino acids capable of hydrogen bonding to substrate carboxylate group will retain decarboxylation activity. Alternatively, replacement of Gln52 with amino acids incapable of functioning as hydrogen bond donors will exhibit low or undetectable decarboxylation activity.

Several alternatives have been explored to test the above hypothesis. Plasmid DNAs encoding WT DGD were initially subjected to site-directed mutagenesis to mutate the codon coding for Gln52 into any other amino acids. Mutated plasmid DNA was then transformed into *E. coli*. Host bacteria carrying mutated plasmid DNA were induced to

express the recombinant protein. DGD mutant proteins were eventually purified by conventional chromatography methods and tested for the ability to decarboxylate 2-methylalanine and transaminate L-alanine separately. In addition, computerized protein sequence alignment has categorized DGD as a member of the PLP-enzyme family (Mehta and Christen, 1994). Sequence alignment of DGD with gene sequences of members from this enzyme family may help explain how Gln52 functions. Furthermore, 3D structures of some PLP-enzymes, in particular aminotransferases, have been solved and could provide additional information on how decarboxylation could be catalyzed at DGD active site.

1.8. Dissertation outline

This dissertation is divided into 5 parts. This chapter introduces the general concept of vitamin B_6 and the types of reactions catalyzed by PLP. Current literature relevant to DGD is also discussed in this chapter. Chapter 2 deals with the construction of Q52X DGD mutants, experiments conducted on the mutant enzymes and discussion on the experimental results. Chapter 3 describes comparative sequence alignment of DGD with moderately to highly homologous protein sequences downloaded from protein databanks on the World Wide Web. Amino acid alignment of Gln52 and certain histidine residues in DGD with similar proteins may yield clues on how DGD carries out decarboxylation. Active site comparisons of 3D structures of known PLP enzymes such as AAT, OrnAT and DGD are also discussed. Chapter 4 documents DGD purification

and spectrophotometric studies on WT and K272A DGDs. Lastly, in Chapter 5 are recommendations for the future direction of the project.

Chapter 2

Wild-type and mutant 2,2-dialkylglycine decarboxylases: Role of active site Gln52 investigated by site directed mutagenesis

2.1. Abstract

The ability of *Burkholderia (Pseudomonas) cepacia* 2,2-dialkylglycine decarboxylase (DGD) to catalyze sequential decarboxylation and transamination at a single active site depends on the dual nature of the subsite within the active site where α-COO^- and α-H bond cleavages take place. As observed in the crystal structure, the strategic position of Gln52 at the active site suggests a role in enhancing decarboxylation via formation of a hydrogen bond to the substrate carboxyl group. Ten Q52X mutants were constructed and their abilities to decarboxylate 2-methylalanine or transaminate L-alanine investigated. All mutants except Q52H exhibited decreased rates of decarboxylation compared to WT. Results of WT, Q52H and Q52N suggest that hydrogen bonding between the amide side chain of WT or τ-nitrogen on the imidazole ring of Q52H with substrate carboxyl group is required for decarboxylation. Mutants incapable of hydrogen bonding to substrate such as Q52A, Q52L and Q52W showed low decarboxylation activities, which are consistent with the proposed hypothesis.

Replacement of Gln52 resulted in increased transamination rates for some mutants and decreased transamination rates for others. These data suggest that Gln52 can influence the subsite environment that also catalyzes transamination. Furthermore, there is evidence demonstrating that the subsite environment of WT, Q52H and Q52E DGDs are different; the three DGD forms exhibited different chromophores at around λ_{max} of 500 nm when treated with either substrate in the presence of 3% glycerol. The concept of a catalytically isolated subsite within the DGD active site has important implications for OrnAT and GabaAT, two medically important aminotransferases that are closely related to DGD. Point mutations in the OrnAT subsite that catalyzes transamination could result in dysfunctional enzymes. Dysfunctional OrnAT has been associated to gyrate atrophy, a hereditary disorder that leads to blindness in humans. The amino acids at the GabaAT subsite could be alternative targets for drugs designed to inhibit GabaAT activity.

The concept of a catalytically isolated subsite within the DGD active site has important implications for OrnAT and GabaAT, two medically important aminotransferases that are closely related to DGD. Point mutations in the OrnAT subsite that catalyzes transamination could result in dysfunctional enzymes. Dysfunctional OrnAT has been associated to gyrate atrophy, a hereditary disorder that leads to blindness in humans. The amino acids at the GabaAT subsite could be alternative targets for drugs designed to inhibit GabaAT activity.

2.2. Introduction

2,2 dialkylglycine decarboxylase (DGD; EC 4.1.1.64) from the soil bacterium *Burkholderia (Pseudomonas) cepacia* was first reported by Aaslestad and Larson (1964) and studied in some detail by several research laboratories (Bailey and Dempsey, 1967; Aaslestad et al., 1968; Lamartiniere et al., 1971; Honma et al., 1972; Sato et al., 1978). The native enzyme exists as a tetramer and its molecular weight has been estimated at 180 kDa (Lamartiniere et al., 1971; Sato et al., 1978). The exact biological role of DGD remains obscure; its widespread presence in many soil bacterial and fungal species (Dempsey, 1969; Esaki et al., 1994) suggests this enzyme probably plays an ecological role in the soil community. The DGD substrates, 2MA and isovaline, are found predominantly in cytotoxic peptides produced by soil fungi (Bruckner and Pryzbylski, 1984). DGD may be involved in degradation of fungal peptides to provide supplemental carbon and nitrogen sources for host bacteria (Keller et al., 1990).

Keller et al. (1990) reported the cloning, sequencing and expression of DGD gene into *E. coli*. Comparison of the 434 amino acid sequence of DGD with other PLP-dependent enzymes revealed that DGD is more similar to aminotransferases, in particular the carboxyl terminal of rat ornithine aminotransferase where PLP-binding domain is located. No PLP-dependent decarboxylases showed significant homology with DGD. It has been suggested that DGD, being an aminotransferase, has acquired decarboxylation activity through evolution and not vice versa. Furthermore, Mehta and Christen (1994) designated DGD in one of the four major subfamilies of PLP

aminotransferases. Toney et al. (1995a) solved the 3D structure of DGD and provided detailed analysis on the structural and mechanistic aspects of the enzyme.

DGD is a unique PLP-dependent enzyme because it catalyzes two classical reactions, decarboxylation and transamination, at a single active site. Toney et al. (1995a) proposed that there are three binding sites within the DGD active site and the exceptional ability of DGD to catalyze both reactions depends on the nature of the binding sites. Toney et al. (1995a) also hypothesized that DGD decarboxylation could involve hydrogen bonding between the amide side chain of Gln52 and the substrate carboxyl group. Gln52 and Lys272 that catalyze decarboxylation and transamination respectively reside at one of the three binding sites (Toney et al., 1995a). It is unknown whether decarboxylation and transamination reactions are separate events catalyzed by Gln52 and Lys272 respectively or are dependent on both residues for effective catalysis. However, the first concept is a simpler model to visualize: Removal of Gln52 abolishes decarboxylation but does not affect transamination; removal of Lys272 abolishes transamination but does not affect decarboxylation.

To test the validity of the hypothesis which states that Gln52 promotes DGD decarboxylation, Q52X DGD mutants were constructed, the proteins purified to near homogeneity and their abilities to decarboxylate 2MA or transaminate L-ala investigated. Mutant DGDs incapable of hydrogen bonding to substrate at amino acid position 52 cannot decarboxylate 2MA while their abilities to transaminate L-ala will remain unaffected. Conversely, mutants able to form hydrogen bonds with substrate carboxyl

group will undergo a reduced rate of decarboxylation; it is probable that the decarboxylation level may be enhanced by the amino acid substitution at position 52.

2.3. Materials and Method

Bacterial strains and media. E. coli strains used were JM109 (*endA1, gyrA96, hsdR17(r_k^-, m_k^+), mcrB$^+$, recA1, relA1, Δ(lac-proAB), thi, supE44, F'[traD36, proAB, lac I^qZΔM15], λ^-*) and BHM 71-18 *mutS* (*supE, thi-1, Δ(lac-proAB), F'[proAB+,lac I^qZΔM15], mutS :: Tn10*). Competent cells were prepared according to the RbCl transformation procedure (New England Biolabs, 1994). Restriction enzymes were purchased from Promega. Bacterial media were M9/2MA (g/L: $Na_2HPO_4 \cdot 7H_2O$, 12.8; KH_2PO_4, 3; NaCl, 0.5; agar, 15; thiamine, 0.040; glucose, 0.4%; 2MA, 10 mM), LB (g/L: tryptone, 10; yeast extract, 5; NaCl, 10; agar, 15) and Terrific Broth (g/1.2 L: yeast extract, 28.8; tryptone, 14.4; glycerol, 4.8 mL; 120 mL 0.17 M KH_2PO_4, 0.72 M K_2HPO_4 solution). Other reagents at final concentration included ampicillin (80 μg/mL), tetracycline (50 μg/mL), IPTG (0.5 mM) and X-gal (20 μg/mL).

Construction of DGD expression vector pDGDA2 (5986 bp). The *dgdA* gene was amplified from pUC19C7/7b, a plasmid derived from pUC19C7 by exonuclease removal of about 1200 bp of non-coding DNA downstream of the *dgdA* gene (Keller et al, 1990). The amplification conditions were: 60 μL reaction volume containing 4 u *Taq* polymerase, 200 μM dNTPs, 1% formamide, 20 ng pUC19C7/7b template, 1 μM primers JK2-20 and JK13 (Table 1), 1x Taq buffer including 2.0 mM $MgCl_2$, and Milli-Q water

(> 10 megohms-cm), 25 cycles at 97 °C/1 min, 55°C/0.5 min and 73°C/2 min. The 1462 bp product was cut with *EcoR*I, the resulting 1396 bp *EcoR*I-*EcoR*I fragment was ligated to *EcoR*I-cut pBTac1 (4590 bp, Boehringer-Mannheim, Amann et al., 1983), and was transformed into competent *E. coli* JM109.

Construction of Q52X DGD expression vectors by site-directed mutagenesis. Mutagenic (JK71p, JK76p and JK77p) and selection (JK72p) primers were purchased from GIBCO BRL (Table 1). Template pDGDA2 was prepared with Wizard™ Minipreps DNA Purification System (Promega) and made up to 50 ng/μL.

Q52X DGD mutants were constructed as outlined in the Transformer™ site-directed mutagenesis kit (Clonetech) which utilizes mutagenic and selection primers to introduce specific base changes into a double stranded template. DNA template, selection and mutagenic primers (100 ng each) were added to a final volume of 20 μL in 1x annealing buffer. A control was started which contained (100 ng each): control plasmid pUC19M, control primer 1 (Trans Oligo Nde I/Nco I) and control primer 2 (reversion of the amber stop codon in the *lacZ* gene on pUC19M) were made up to 20 μL in 1x annealing buffer. The tubes were heated at 100°C for 3 min and chilled immediately in ice water bath for 5 min. 3 μL 10x synthesis buffer, 4 u T4 polymerase, 4 u ligase and 5 μL Milli-Q water were added. Reactions were kept at 37°C for 3.5 hrs and heated at 70°C for 10 min to inactivate the enzymes. Following primary restriction enzyme digestion, competent BMH 71-18 *mutS* cells were transformed with control and hybrid DNA.

Table 1. Primers used in construction of pDGDA2 and genetic engineering of Q52X DGD mutants. Bold letters indicate changes made to construct Q52X, Q52E and Q52N/Q52K respectively. All primers, except JK2-20 and JK13, were 5'-phosphorylated.

Primer	Purpose	Position on *dgdA* gene	Sequence (5'→ 3')
JK2-20 [a]			GCT GCA AGG CGA TTA ACT TG
JK13 [b]			CCA CAG AAT TCT ATG TCC CTG AAC GAC GAT
JK71p	mutagenic	+ strand, 150 to 180 nt	pCC GCG CTC ATN NNC CCC GAC GTG
JK72p [c]	selection	+ strand, 1410 to 1440 nt	pGC CAA AAC AGA ATC TAG ACT GCA GGT CG
JK76p	mutagenic	+ strand, 150 to 180 nt	pCC GCG CTC ATT **T**CC CCC GAC GTG
JK77p	mutagenic	+ strand, 150 to 180 nt	pCC GCG CTC ATN **T**TC CCC GAC GTG

[a] complementary to sequences outside an *EcoR*I restriction site in the adjacent pUC19 vector.
[b] contained the 5'-end of the *dgdA* gene (start codon double underlined), plus a new *EcoR*I site (underlined).
[c] underlined segment converted the only Hind III site on pDGDA2 to an equally unique Xba I site.

Table 2. Primers used in sequencing of WT and Q52X DGDs.

Primer	Plasmid location	Sequence (5' → 3')
JK5	20mer complementary to the first 20 nt of *dgdA* gene	ATG TCC CTG AAC GAC GAT GC
JK15	20mer complementary to *dgdA* coding strand 1106 to 1087 nt	CCT TGA CGA TCT CGA CGC CG
JK17	20mer of *lacZ* coding strand of pBTac1, located upstream of cloning site of pBTac	ATG TGT GGA ATT GTG AGC GG
JK25	25mer complementary to plasmid coding strand just outside vector-insert junction of pBTac1	GCT GAA AAT CTT CTC TCA TCC GCC A
JK41	20mer of *dgdA* coding strand 497 to 506 nt	TTC GCG ATT CCG GCG CCA TT
JK43	20mer of *dgdA* coding strand 902 to 921 nt	TTC TAT ACG ACG CAC GTG TC
JK46	20mer complementary to *dgdA* coding strand 595 to 566 nt	TCG AAC GCG TAG TCG AGT TC

Cells were grown overnight and plasmid DNA isolated the next day. Following secondary restriction enzyme digestion, plasmids were transformed into JM109. Control cells were plated on LB/X-gal/IPTG/amp plates to determine extent of the primary and secondary enzyme digest. JM109 clones transformed with hybrid DNA that grew on LB/amp plates were selected and screened for mutant DGD.

Screening for Q52X DGD mutants with selective growth medium. Screening JM109 colonies carrying functional DGD is simplified by the inability of *E. coli* to metabolize 2MA (Keller et al., 1990). Expression of WT DGD carried on a vector maintained under antibiotic selection enables the bacteria host to grow on minimal medium containing 2MA as sole nitrogen source. Bacteria expressing mutated forms of DGD will grow slowly or not at all on M9/2MA/amp plates. JM109 Q52X DGD colonies were restreaked on fresh LB/amp master plates. Colonies were then blotted onto M9/2MA/amp plates and incubated overnight at 37°C. Colonies that grew poorly or did not grow cannot metabolize 2MA and therefore may have mutated forms of DGD. These were selected from master plates and inoculated into 2 mL LB/amp tubes.

Automated DNA sequencing. Screening using automated DNA sequencing not only identifies mutants in targeted region, it also ensures that no extraneous mutations had occurred in other areas. Primers were prepared as 3 μM stocks (Table 2). Plasmid DNAs, purified using Wizard™ Minipreps, were sequenced with ABI Prism™ Dye Terminator Cycle Sequencing Ready Reaction Kit and AmpliTaq™ DNA polymerase FS.

Sequencing reaction consisted of 400 ng plasmid DNA, 3 μL Prism™ mix, 3 pmol primer and Milli-Q water to 15 μL. Cycle sequencing was carried out in 200 μL thin wall tubes on a Perkin-Elmer GeneAmp® PCR Systems 9600 thermal cycler (96°C/10 sec; 50°C/5 sec; 60°C/4 min; 25 cycles). Excess nucleotides were removed from the extension products by passing through Sephadex G-50 (Sigma) spin columns (Princeton Separations Centri-Sep™). Samples were analyzed on a 6.5% polyacrylamide gel by ABI 373 DNA Sequencer Stretch. Sequence data were examined with ABI DNA sequencing analysis, 1.2.1 and GenePro, 6.10 (Riverside Scientific Enterprises, 1993). Previous experience showed that automated DNA sequencing of these vectors typically produces readable sequences between 600 to 700 bp long of 70 to 95% accuracy.

WT and Q52X DGD Expression and Enzyme Purification. Protein purification was modified from a previous procedure (Keller et al., 1990). TB/amp/IPTG was inoculated with two 2 mL LB/amp starter culture grown overnight. Cells were grown to stationary phase at 37°C, cooled to 4°C and pelleted (5,000 rpm, 15 min, 4°C, GSA head). The pellet was resuspended in 160 mL sonication buffer (50 mM Tris, 5 mM KCl, 5 mM NaCl, 1 M $(NH_4)_2SO_4$, 2 mM NaPyr, 1 mM 2MA, 20 μM PLP at pH 7.9) and stirred magnetically for 30 min in ice/water bath. Sonication was carried out with a Sonication Ultrasonic Processor and Cell Disrupter (Heat Ultrasonics System, Model W225) for 10x at 1 min intervals (40% duty cycle at a power setting of 5) with cooling down periods to keep the suspension below 5°C. Protein concentration was determined with Bradford reagent (Bradford, 1976) at 596 nm after each sonication. Cell rupture was considered as

completed when protein concentration showed no significant increase. Bacterial debris were removed by centrifugation (11,000 rpm, 30 min, 4°C, GSA head) and supernatant decanted into a clean flask. Ammonium sulfate was added to a final concentration of 2.2 M. Protein precipitate was pelleted (11,000 rpm, 30 min, 4°C, GSA head), resuspended in 40 mL dialysis buffer (20 mM TEA, 5 mM KCl, 5 mM NaCl, 2 mM NaPyr, 1 mM 2MA, 20 μM PLP at pH 7.9), and dialyzed overnight in 2 L dialysis buffer at 4°C.

DEAE Toyopearl® 650M TSK-gel ion exchange matrix (Toyo Soda Mfg Co., Tokyo, Japan) was packed in a glass Bio-Rad chromatography column (30 cm x 3 cm) and pre-equilibrated with ion exchange buffer (20 mM TEA buffer, pH 7.9, 5 mM KCl, 5 mM NaCl). The dialysate was loaded onto the column. The column was washed with ion exchange buffer until the O.D. at 290 nm returned to baseline. Protein elution was carried out with a salt gradient of 5 mM KCl, 5 mM NaCl to 250 mM KCl, 250 mM NaCl (100 mL each). Fractions were collected and protein content determined with Bradford reagent. Fractions containing 5 to 10 μg protein were analyzed with SDS-PAGE (Bio-Rad Mini-PROTEAN® II Dual Slab Cell). SDS gels were scanned with IS-1000 Digital Imaging System (Alpha Innotech Corporation) to both locate fractions containing DGD and determine enzyme purity. Fractions of highest purity were pooled and desalted by eluting through a Bio-Rad Bio-Gel P-6DG gel column (50 cm x 1.5 cm, MW fractionation range of 1,000 to 6,000) pre-equilibrated with 15 mM phosphate buffer, 40 μM PLP, pH 6.75. Eluted fractions were again pooled and concentrated using Amicon® Centricon-30 (30,000 MW cut-off) in a SS34 head (5,000 rpm, 4°C). The retained sample was rinsed with 500 μL of 50 mM phosphate buffer, pH 7.5 and further concentrated to 1

mL final volume. Enzyme solutions, ranging from 20 to 30 mg/mL, were frozen in liquid nitrogen and kept in –70°C freezer as 50% glycerol stocks. Frozen enzymes were thawed on ice before use in the decarboxylation and transamination half reactions.

Decarboxylation and transamination half reactions. Control experiments indicated that the enzyme activity showed little change over time when frozen at -70°C (result not shown). The decarboxylation and transamination half reactions consisted of 3.9 μM DGD (in 50% glycerol), 35 mM phosphate buffer, pH 7.5, 16 μM PLP and 56 mM 2MA/L-ala at 22°C. Holoenzyme was prepared as follows: 300 μg protein was diluted into 25% glycerol solution to final volume of 50 μL, incubated with 80 μM PLP for 2 hrs and loaded onto CHROMA SPIN–10 columns (Clontech) and spun in a swinging bucket rotor at 1550 rpm for 4 min to remove unbound PLP. Reactions were carried out in 35 mM phosphate buffer, pH 7.5, 56 mM 2MA/L-ala and no PLP. The effect of glycerol on reaction rates was also examined. Glycerol could be removed from enzyme solution by binding the enzyme to a small DEAE column (5 mm x 23 mm), washing and eluting with appropriate buffers as outlined in the previous section. Protein solution was reconcentrated with Ultrafree-MC microcentrifuge filters (NMWL 30,000). Half reactions with non-glycerol enzyme preparation were carried out as with 50% glycerol enzyme stock and 16 μM PLP. The first order rate constants of the half reactions were determined by monitoring the disappearance of PLP peak and appearance of PMP peak with Hewlett-Packard 8452A diode array spectrophotometer and UV-Visible ChemStation Software.

2.4. Results

Construction of Q52X DGD expression vectors by site-directed mutagenesis. Ten plasmids expressing DGD mutants were isolated from recombinant JM109 (Table 3). Automated sequencing of these plasmids using primers JK5 or JK17 and JK46 confirmed the presence of mutated nucleotide(s) at amino acid position 52. *dgdA* gene sequences outside the mutated region were sequenced with the other four primers (Table 2). The data agreed with the sequencing results using the manual Sanger dideoxy method (Brayman, 1993) except for two discrepencies. Previous sequencing misread GCC as GCG at Ala312 and GTT as GTC at Val363. These degenerate third nucleotides do not alter identity of the amino acid they code for. Hence, the protein sequence remains the same. Misreading of the third nucleotide could be attributed to the difficulty in reading through a compressed GC rich region (United States Biochemical, 1993).

Table 3. Plasmids with mutated DNA bases at amino acid position 52 on pDGDA2.

Mutant	Plasmid	Mutated DNA sequence	Amino acid change
Q52A	pSW22	CAG → GCG	Gln → Ala
Q52D	pSW9	CAG → GAT	Gln → Asp
Q52E	pSW1	CAG → GAA	Gln → Glu
Q52G	pSW12	CAG → GGC	Gln → Gly
Q52H	pSW306	CAG → CAC	Gln → His
Q52K	pSW19	CAG → AAG	Gln → Lys
Q52L	pSW150	CAG → CTA	Gln → Leu
Q52N	pSW59	CAG → AAT	Gln → Asn
Q52R	pSW276	CAG → CGA	Gln → Arg
Q52W	pSW121	CAG → TGG	Gln → Trp

WT and Q52X DGD Expression and Enzyme Purification. Bacterial pellets weighing 15 to 20 g were harvested from 1.2 L of TB medium. The purified WT and mutant DGDs were homogenous as indicated by a single band on SDS-PAGE. The mutant protein bands migrated the same distance as the WT enzyme. Scanning SDS gels with the IS-1000 Digital Imaging System determined enzyme purity at 90%. Ion exchange chromatography and P-6DG gel filtration elution profiles of mutant DGDs were similar to WT DGD.

Decarboxylation and transamination half reactions. A control experiment containing PLP and either 2MA or L-ala was set up to determine cofactor and substrate stability over time. The initial PLP shift from 390 to 400 nm is due to the formation of external aldimine between free PLP and amino acid; no further reaction could be detected. 2MA decarboxylation and L-ala transamination rates of WT and mutant DGDs were shown in Table 4 and Figure 12. All reactions in Table 4 (enzyme concentration at 3.9 μM), except the last three, were carried out in excess PLP (16 μM). The last three reactions were conducted with holoenzyme preparations (i.e. PLP-bound enzymes) with no PLP added to the reaction. The rate of PLP disappearance is complemented by the rate of PMP appearance during both half reactions in all DGDs examined. The synchronous disappearance of the PLP peak and appearance of the PMP peak are indicative that the Q52X DGD mutants are able to carry out decarboxylation or transamination, although to some lesser extent than WT DGD.

Table 4. Mutant DGD were tested for ability to decarboxylate 2MA and transaminate L-ala [a].

DGD	k ($-CO_2$) [b]	k ($-NH_3$) [b]	Faster reaction	($-NH_3$)/ ($-CO_2$) [c]	Notes
WT	38	44	($-NH_3$)	1.2	peak at 500 nm, shoulder at 530 nm
Q52A	1.9	3.9	($-NH_3$)	2.0	
Q52D	12	67	($-NH_3$)	5.8	
Q52E	2.9	120	($-NH_3$)	43	peak at 520 nm
Q52G	14	13	($-NH_3$) = ($-CO_2$)	1.0	
Q52K	- [d]	-	-	-	no peak shift
Q52H	58	1.2	($-CO_2$)	≈ 0	peak at 500 nm
Q52L	<1.0	1.6	($-NH_3$)	>1.6	
Q52N	6.4	80	($-NH_3$)	12	
Q52R	<1.0	32	($-NH_3$)	>32	
Q52W	<1.0	3.0	($-NH_3$)	>3.0	
Q52D [e]	11	61	($-NH_3$)	5.8	
Q52H [e]	50	25	($-CO_2$)	0.5	peak at 500 nm
Q52R [e]	5.8	29	($-NH_3$)	5.0	

[a] reaction consisted of 3.9 μM mutant DGD, 16 μM PLP, 56 mM 2MA/L-ala in 35 mM phosphate buffer, pH 7.5, carried out at 22°C. All reactions were carried out at least twice. Margin of error was about 5%. Final glycerol concentration was 3% v/v.

[b] ($-CO_2$) = decarboxylation, ($-NH_3$) = transamination. k (x 10^{-4} s^{-1}) is based on first order reaction where k_{obs} = 0.693 / $t_{1/2}$, and $t_{1/2}$ is time required (in seconds) to reduce half of total A.U. of PLP (or increase half of total PMP).

[c] Ratio of transamination rate versus decarboxylation rate.

[d] no reaction was detected.

[e] mutant was incubated with excess PLP and eluted through Chromaspin columns, reaction conditions similar to [a] with no added PLP.

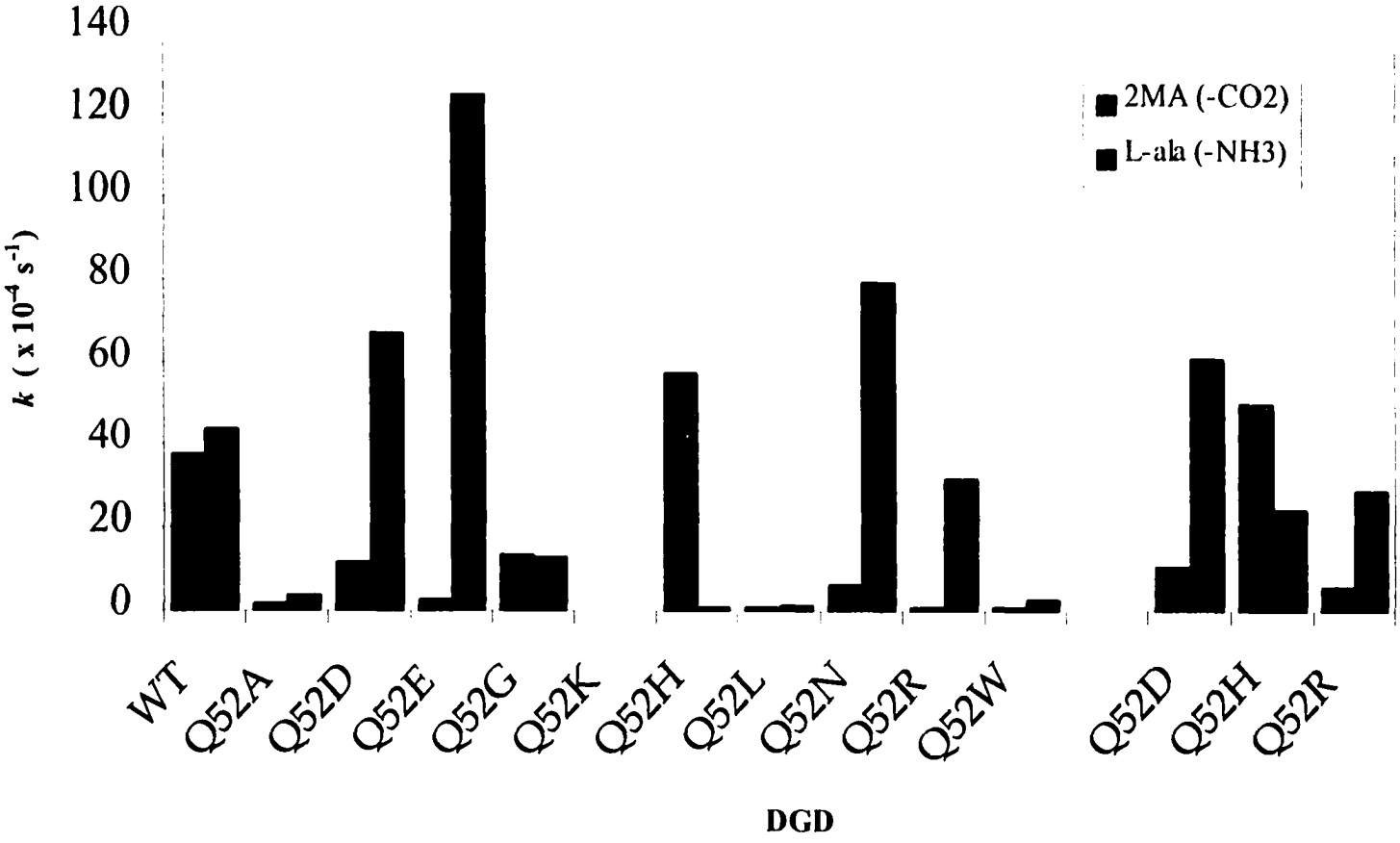

Figure 12. 2MA decarboxylation and L-ala transamination rates of WT and mutant DGDs. The last three reactions on the right were conducted with mutant DGD holoenzymes in the absence of free PLP.

WT DGD exhibited decarboxylation and transamination rates of 3.8 x 10^{-3} s^{-1} and 4.4 x 10^{-3} s^{-1} respectively. Upon site-directed mutagenesis, DGD mutants exhibited an array of 2MA and L-ala reaction rates. All mutant DGDs, except Q52G and Q52H, catalyze transamination faster than respective decarboxylation; transamination rates range from 1.6 to 43 times higher than decarboxylation rates. More interestingly, Q52D, Q52N and Q52E catalyze transamination approximately 6, 12 and 43 times faster than respective decarboxylation. Under similar experimental conditions, Q52E was found incapable of decarboxylating D-ala (Figure 13).

If the transamination rates of all DGD forms were then compared to that of WT, Q52E, Q52N and Q52D transaminate L-ala 2.8, 1.8 and 1.5 fold faster than WT respectively. In contrast, the relative decarboxylation rates of the four DGD forms are reversed of transamination rates. Decarboxylation rate of WT is the highest, followed by Q52D, Q52N and Q52E. Among the mutants engineered, Q52H is the only mutant showing significant level of decarboxylation. In fact it is 50% more efficient in decarboxylating 2MA than WT. However, Q52H transamination rate is almost undetectable.

Q52G decarboxylates 2MA and transaminates L-ala at similar rates. The reaction rates are also considerably lower than that of WT. Q52K lacked any detectable activity. While Q52A, Q52L and Q52W showed residual decarboxylating and transaminating activities, Q52R exhibited insignificant decarboxylation rate but a significant level of transamination. The arginine mutant transaminates L-ala at appreciable rate, about 0.7 times that of WT.

Since it is possible that some of the low reaction rates were due to the inability of the mutants to catalyze more than one round of substrate turnovers. Holoenzyme forms of Q52D, Q52H and Q52R were prepared and assessed for their abilities to catalyze one round of substrate turnover (Table 4). Q52D and Q52R holoenzymes showed comparable half reaction rates to those preformed with 16 μM PLP. However, transamination rate of Q52H holoenzyme was 20-fold higher than that conducted with 16 μM PLP whereas the decarboxylation rate stayed relatively the same.

Figures 13 to 20 depict the decarboxylation and transamination reactions of selected mutant DGDs with various substrates. 2MA decarboxylation and L-ala transamination of WT DGD showed the concurrent decrease and increase in PMP and PLP peaks respectively (Figure 21).

Effect of glycerol on quinonoid formation and reaction rates. Addition of 3% v/v glycerol promoted absorption bands at roughly 500 nm in both half reactions of WT, Q52E and Q52H (Table 4). The appearance of the peak was accompanied by a pinkish color development in the reaction solution. The absorption peak at 500 nm has been designated as the quinonoid intermediate (Jenkins, 1964; Morino and Snell, 1967). WT exhibited λ_{max} at 500 nm and a shoulder at 530 nm (Figure 21). The quinonoid intermediate of Q52H and Q52E showed λ_{max} at 500 nm and 520 nm respectively (Figures 14, 15, 16 and 17). Removal of glycerol from the Q52H decarboxylation reaction showed no quinonoid peak as depicted in Figure 18. Q52N, the second fastest transaminase, showed no quinonoid peak in 3% v/v glycerol (Figures 19 and 20).

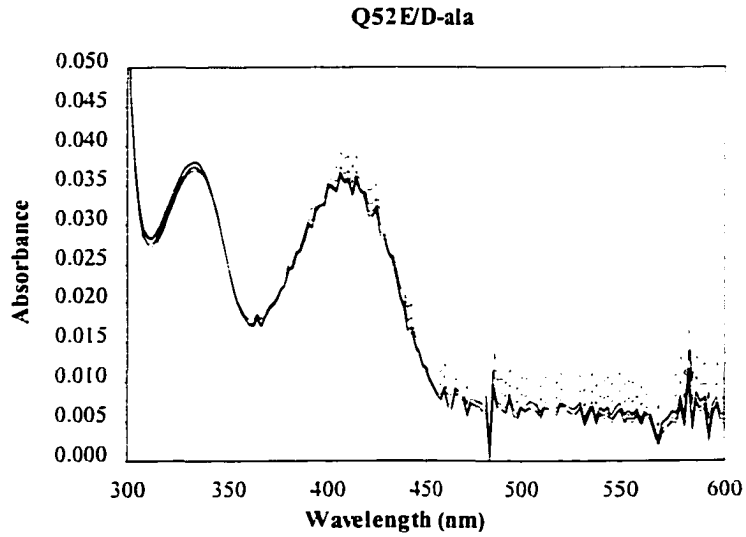

Figure 13. Q52E/D-ala decarboxylation half reaction. Reaction conditions similar to those with other substrates. Scans were taken every 10 min. No activity was detected in 1 hr; the result is consistent with the hypothesis that the carboxyl group of D-ala was oriented towards Glu52 and not decarboxylated.

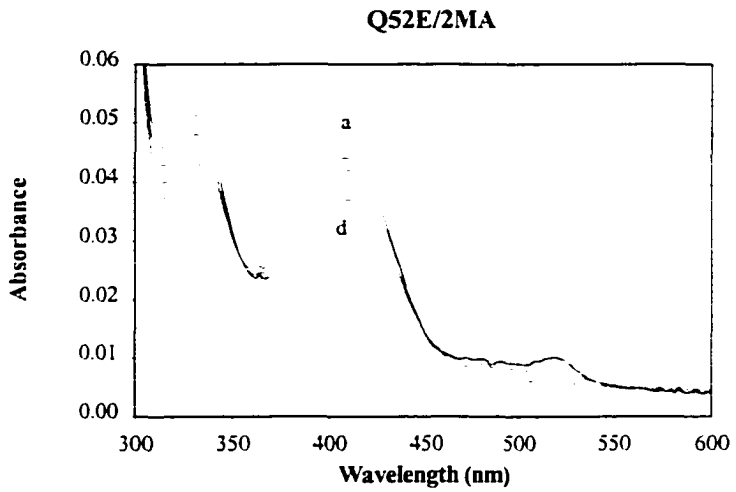

Figure 14. Q52E/2MA decarboxylation half reaction. Reaction: 3.9 μM holoenzyme, 56 mM 2MA in 35mM phosphate buffer, pH 7.5 at 22°C. Scans were taken at 0, 10, 30 and 60 min after protein addition (a – d). The 520 nm peak appeared immediately after protein was added.

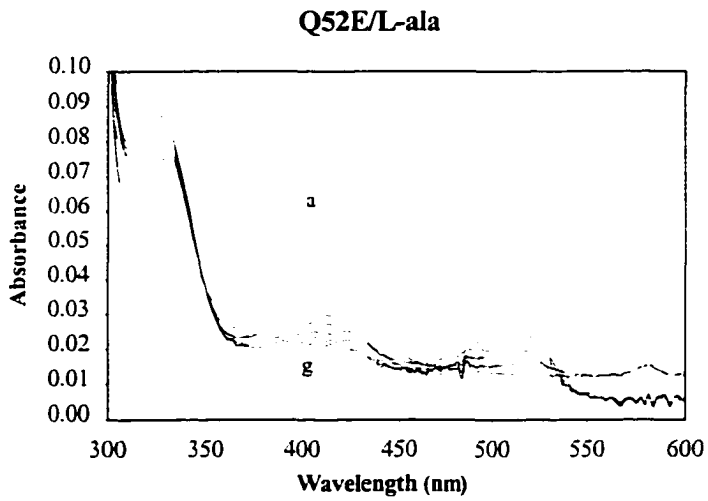

Figure 15. Q52E/L-ala transamination half reaction. Reaction: 3.9 μM holoenzyme, 56 mM L-ala in 35mM phosphate buffer, pH 7.5 at 22 °C. Scans were taken at 0, 1, 5, 10, 20, 30 and 40 min after protein was added (a – g). A peak absorbing maximumly at 520 nm was noted.

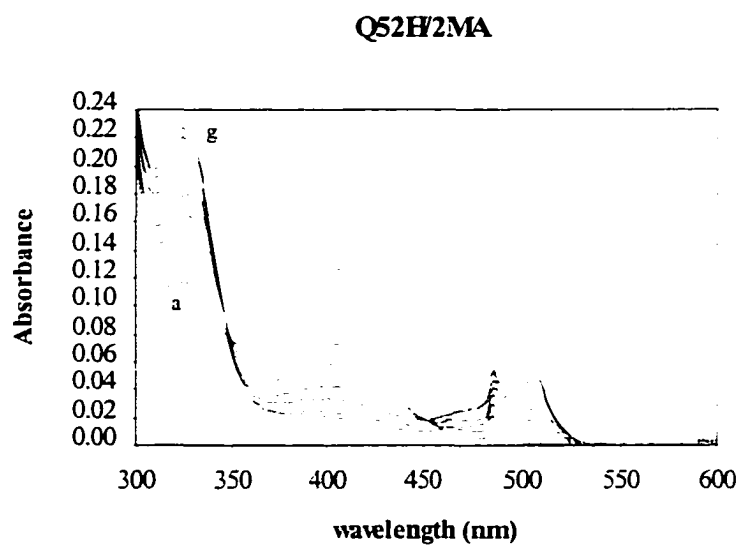

Figure 16. Q52H/2MA decarboxylation half reaction. Reaction: 3.9 μM holoenzyme, 16 μM PLP, 56 mM 2MA in 35 mM phosphate buffer, pH 7.5 at 22°C. Scans from 300 to 600 nm were taken at 0, 5, 10, 20, 30, 60 and 100 min after addition of protein (a – g). Appearance of an absorption peak at 500 nm was noted.

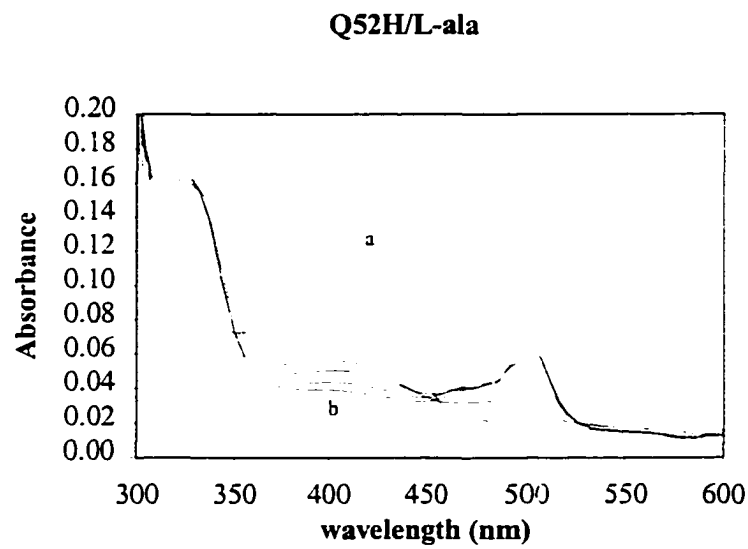

Figure 17. Q52H/L-ala transamination half reaction. Reaction: 3.9 μM holoenzyme, 56 mM L-ala in 35mM phosphate buffer, pH 7.5 at 22 °C. Scans from 300 to 600 nm were taken before adding the enzyme (a); 0, 5, 15, 25 and 30 min after protein was added (b). The 500 nm peak appeared immediately after protein was added and reached maximum absorption after 5 min.

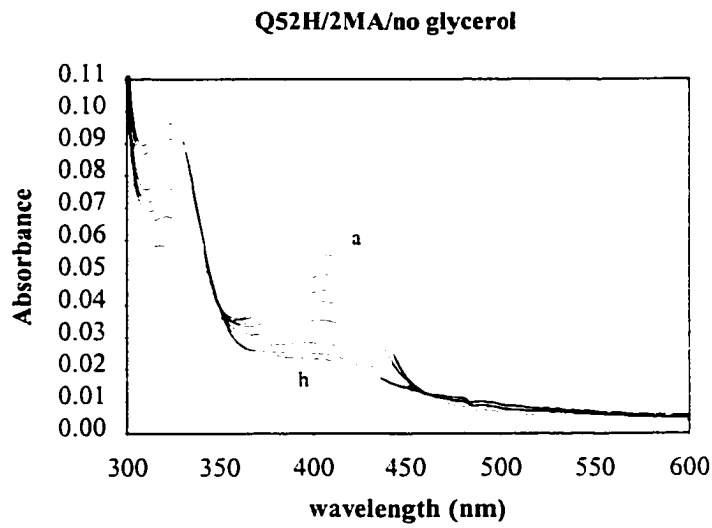

Figure 18. Q52H/2MA decarboxylation half reaction without glycerol. Reaction conditions similar to that using protein with added glycerol. Scans were taken at 0, 1, 2, 3, 5, 10, 15 and 20 min after addition of Q52H (a – h). Note the absence of absorption band at 500 nm.

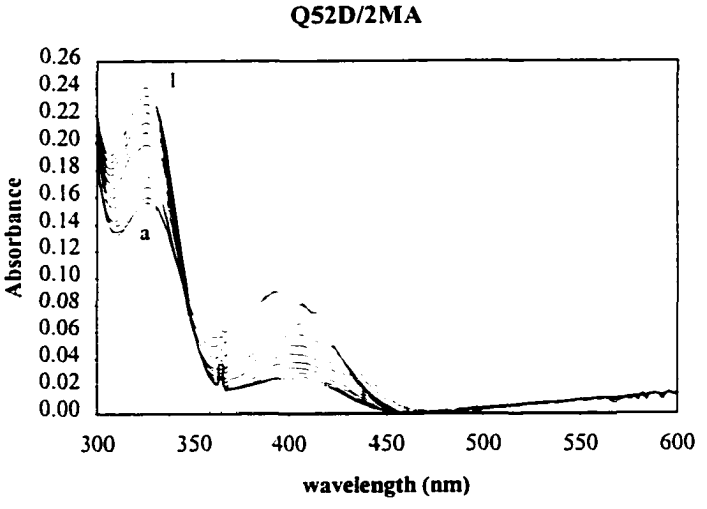

Figure 19. Q52D/2MA decarboxylation half reaction. Conditions similar to those in Figures 13 and 16. Scans were taken at 0, 0.5, 1 to 10 hrs (a - l). Note the absence of the 500 nm absorbing peak.

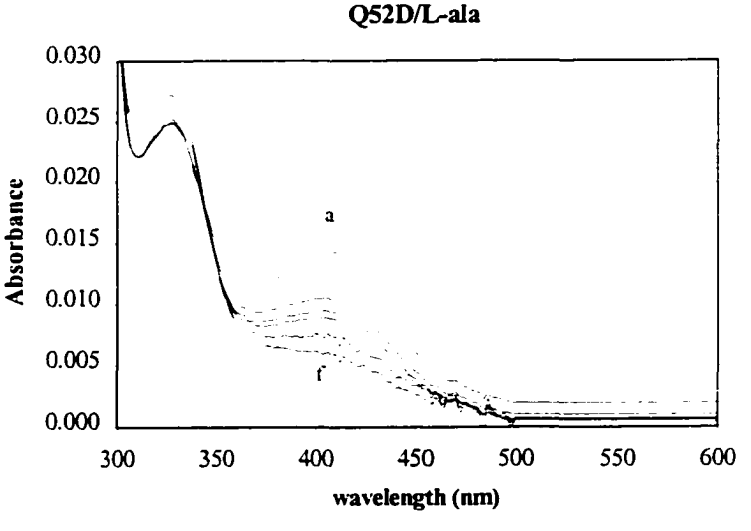

Figure 20. Q52D/L-ala transamination half reaction. Conditions similar to those in Figures 14 and 17. Scans were taken at 0, 0.25, 0.5, 1, 2, and 3 hrs after protein was added (a – f).

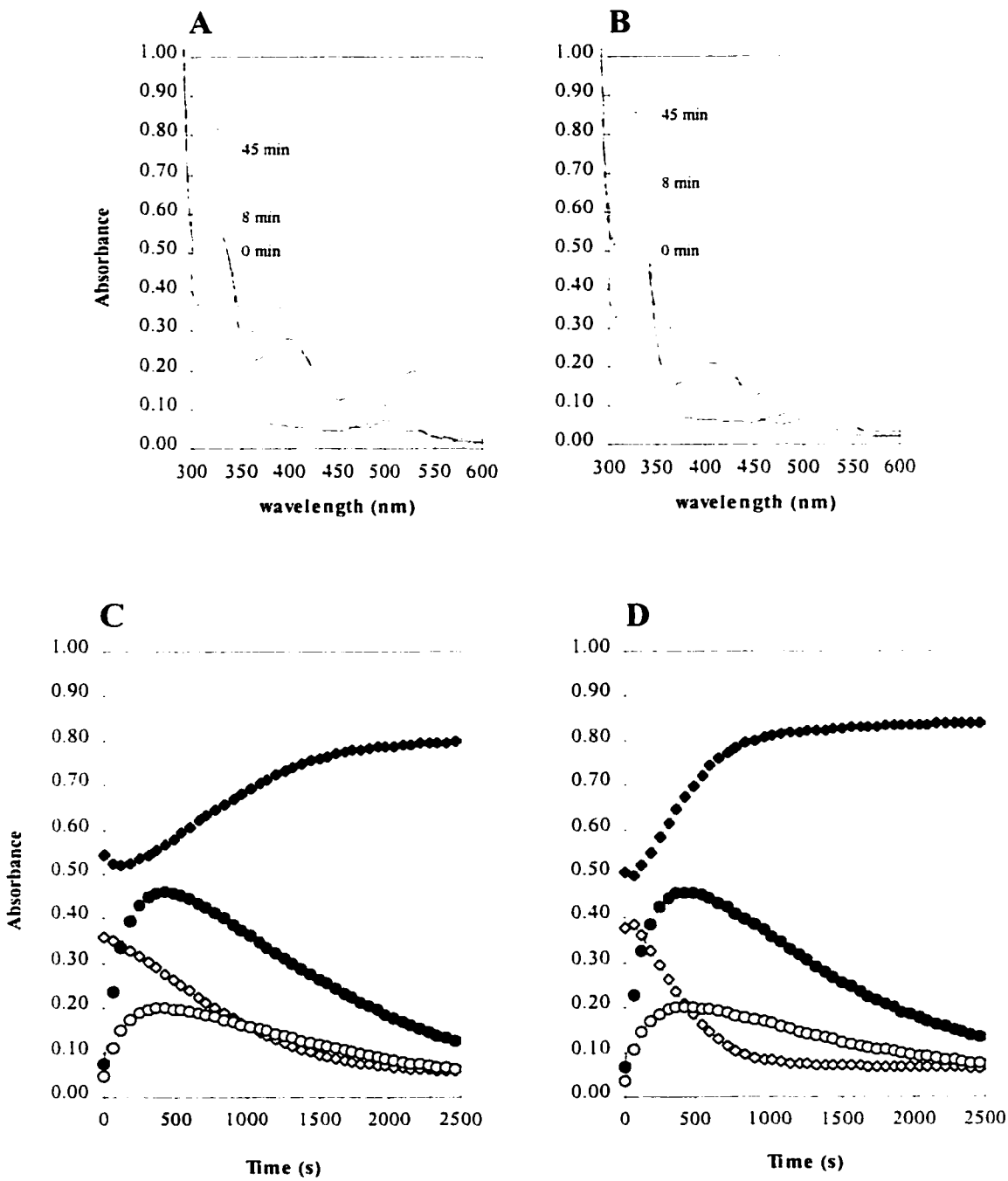

Figure 21. WT/2MA decarboxylation half reaction and WT/L-ala transamination half reaction. 12.5 μM WT DGD pre-incubated with 85 μM PLP in 50 mM phosphate buffer, pH 7.5 at 22°C for 1 hour. 50 mM 2MA (A and C) or L-ala (B and D) were then added. C and D: reactions were monitored at 300 nm (◆), 390 nm or 400 nm (✧), 500 nm (●) and 530 nm (O). λ_{max} of PLP-enzyme complex in (C) and (D) are 390 nm and 400 nm respectively. Final glycerol concentration was 3% v/v.

Presence of glycerol did not alter reaction rates of selected DGD forms (Table 5). The only pronounced difference is the absence of a quinonoid peak in reactions with no added glycerol. Figures 21C and D indicated that, at least in the WT DGD reaction, the quinonoid formation and decay over time is dependent on the presence of glycerol and not 2MA or L-ala.

Table 5. Effects of glycerol [a] and without glycerol [b] on WT and mutant DGD decarboxylation and transamination reaction rates. Reactions described in method section, similar to those in Table 4. [c] ($-CO_2$) = decarboxylation of 2MA, ($-NH_3$) = transamination of L-ala.

PLP	DGD	k ($-CO_2$)[c]	k ($-NH_3$)[c]
16 μM	WT [a]	37.7	43.8
	WT [b]	33.5	49.8
16 μM	Q52E [a]	2.89	125
	Q52E [b]	<1.00	107
16 μM	Q52N [a]	6.42	79.5
	Q52N [b]	5.50	77.0
Enzyme bound	Q52H [a]	50.2	24.6
	Q52H [b]	52.5	19.3

2.5. Discussion

WT and Q52X DGD Expression and Enzyme Purification. Q52X DGD mutants exhibited similar migrating distance compared to WT DGD in SDS gels, implying the Q52X subunits have similar molecular weights as that of the native enzyme. The comparable elution volume in the P-6DG size exclusion chromatograms suggested that the mutants, like the WT enzyme, exist as tetrameric structures. The ion exchange chromatography elution profiles of mutant DGDs were similar to WT DGD. This implies that the total charges on protein surface and therefore the nature of protein interaction of mutant DGD

with DEAE matrix was similar to WT DGD. Conceivably, base changes in amino acid position 52 posed no significant structural changes in these proteins.

The codons chosen at the mutated region could effect the level of expression of mutant DGDs in *E. coli*. Two observations could be made from the *E. coli* codon usage database compiled from CUTG (Codon Usage Tabulated from Genbank, release 102; Appendix 1): (1) strongly expressed codons such as CAG, GAT and GAA (code for WT, Q52D and Q52E respectively) yield higher levels of recombinant protein production of almost 4 mg/g wet cells; (2) weakly expressed codons such as CTA and CGA (code for Q52L and Q52R respectively) show mutant protein production of about 2.4 mg/g wet cells. The 2-fold increase in level of expression warrants the use of strongly expressed codons when overproducing mutant DGD in *E. coli* JM109 (refer to Appendix 2 for protein production of mutant DGDs).

Decarboxylation and transamination half reactions of WT and Q52X DGDs. Replacement of Gln52 with other residues affected both decarboxylation and transamination to different extent. In most instances, decarboxylation rates exhibited marked decreases. On the other hand, transamination rates of some mutants increased while others decreased. The experimental results support the hypothesis that hydrogen bonding promotes decarboxylation. Since hydrogen bond formation may be the requisite for release of substrate COO^-, Q52X mutants able to bond with substrate α-group perpendicular to the π-pyridine ring were considered. Mutants Q52D, Q52E, Q52N and Q52H fall under this category. These mutants were then arranged in the order of

increasing decarboxylation and transamination rates with accordance to results in Table 4 and Figure 12.

Rate of decarboxylation	Q52H > WT > Q52D > Q52N > Q52E
Rate of transamination	Q52E > Q52N > Q52D > WT > Q52H

Among the five forms of DGD, Q52H is the fastest 'decarboxylating' mutant and also the slowest in transaminating L-ala. However, Q52E is the opposite of Q52H; it is most apt at transaminating L-ala but decarboxylates 2MA poorly. Although Q52E and Q52H showed impressive potential to transaminate and decarboxylate substrates respectively, they were likely ruled out through the course of evolution because of their inefficiencies in catalyzing the other half reaction. The most surprising finding is that WT is not the most perfect enzymatic form to perform decarboxylation or transamination; glutamine is the preferred residue because both reactions could be carried out at the best possible rate.

Histidine (H), glutamine (Q) and asparagine (N) at strategic position in proteins provide clues into how enzymatic activity could be influenced by potential hydrogen bonding between the amino acid side chain and substrate (Lowe et al., 1985; Vaalar and Snell, 1989). According to Lowe et al. (1985), the τ-N and π-N of histidine could be superimposed by side chain amide groups of glutamine and asparagine respectively (Figure 22).

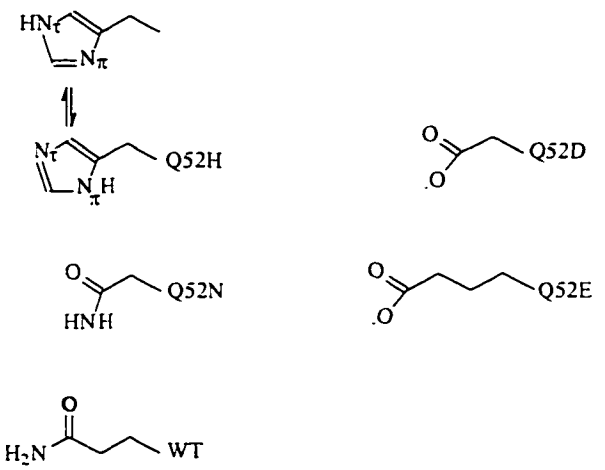

Figure 22. Amino acid side chain at position 52 capable of hydrogen bonding.

WT decarboxylation rate is 0.7 and 6 fold of Q52H and Q52N respectively, whereas the transamination rate is 1.7 and 0.6 times of Q52H and Q52N respectively. DGD decarboxylation is more affected by the replacement of Gln52 while transamination capability is less critical of the mutated residues. τ-N of histidine compensates glutamine amide side chain and also partially enhances the decarboxylation step. On the other hand, π-N of histidine does not participate in hydrogen bonding as evident by the lack of Q52N decarboxylation. Hence, the glutamine amide side chain and histidine τ-N are important for hydrogen bonding in facilitating decarboxylation. Furthermore, slow reaction rates of Q52L and Q52W, which are not potential hydrogen bond donors, supported the concept of hydrogen bonding between Gln52 and substrate.

The Q52H decarboxylation rate is the highest of all the mutants studied and is 1.5 times faster than WT. Under physiological conditions, histidine can act as a general

acid/base catalyst or as a hydrogen bond donor to substrate. The following reasoning is provided to explain hydrogen bonding between the protonated imidazole ring and 2MA. Keller et al. (1997) reasoned that pK_a of Gln52 has to match that of substrate carboxylate group for productive hydrogen bonding that enhances decarboxylation. Since the pK_a of glutamine is higher than histidine under normal conditions (i.e. out of the active site), the microenvironment at the active site needs to lower the pK_a of Gln52. Histidine with pK_a of 7 is better at enhancing 2MA carboxylation.

Q52G could be regarded as a reference point for other mutants. Lacking a polar, charged or hydrophobic side chain, Q52G typifies an environment in the active site pocket where no amino acid occupies position 52. Nevertheless, under the influence of other active site residues (e.g. Tyr301) and/or the active site microenvironment, 2MA decarboxylation and L-ala transamination rates are 1/3 those of WT. The reaction rates of Q52A, Q52L and Q52W DGDs could be considered negligible because they lagged behind those of Q52G. An important inference can be made from these mutants: A hydrogen bond (or ionic interaction) between the substrate and the active site residue is important in DGD-catalyzed decarboxylation and transamination reactions. Toney et al. (1990a) predicted DGD decarboxylation is enhanced by the presence of Gln52 but did not expect transamination activity to be influenced by Gln52. Keller et al. (1997) proposed that the DGD active site is more hydrophobic compared to other aminotransferases. Hydrophobic environment has been attributed to accelerate decarboxylation rate (Marlier and O'Leary, 1986). This hydrophobicity requirement is

fulfilled by the aromatic rings of Tyr301* and Phe79* surrounding Gln52. However, in a hydrophobic active site, DGD-catalyzed transamination may require additional interactions between the substrate and the active site residues, such as hydrogen bonds, for the reaction to be carried out effectively.

The inactive enzyme form Q52K could be attributed to the close proximity of Lys52 to Lys272; Lys52 may interfere with substrate binding or prohibit the substrate from forming external Schiff base, a prerequisite for PLP-dependent catalysis. Arginine forms strong bifurcated hydrogen bonds with the carboxyl group of 2-methyl-L-aspartate in two of the binding sites in AAT (Okamoto et al., 1994). Similar observation was noted in Q52R. The carboxyl group of 2MA was held in place by Arg52 but no reaction took place, resulting in undetectable decarboxylation rate.

Effect of side chain length on decarboxylation and transamination. The carboxyl ends of Q52D and Q52E increase transamination but depress decarboxylation. In fact, decarboxylation rates of both mutants are slower than Q52G (control) and comparable to those of Q52L and Q52W (bulky R groups). One possible explanation is that electrostatic repulsion between side chain and substrate carboxyl groups prevents 2MA from being oriented properly at the active site. In Q52E, the negligible D-ala reaction rate agreed with that of 2MA. Both substrates are oriented at the active site for decarboxylation. However, the carboxyl side chain of Q52E repels the substrate carboxyl group, thus resulting in non-productive reaction.

---

* denotes amino acid of the other monomer in the dimeric structure

Q52E transaminates faster than Q52D. It is possible that Glu52, and not Lys272, catalyzes proton abstraction. This suggestion arises from van Poelji et al. (1990) who investigated the catalytic role of Glu214 of pyruvoyl-dependent histidine decarboxylase from *Clostridium perfringens*. They proposed that by recycling between the ionized and unionized forms, Glu214 protonates the quinonoid intermediate after the decarboxylation step. By similar reasoning, the ionized Glu52 could abstract a proton from L-ala. Again, Glu52 is more effective in deprotonating L-ala since the abstracted proton is within reach by the longer carboxyl side chain of Q52E. Another possible explanation is that Asp52 and Glu52 enhances the basicity of Lys272, thus increasing the rate of proton abstraction (Figure 23).

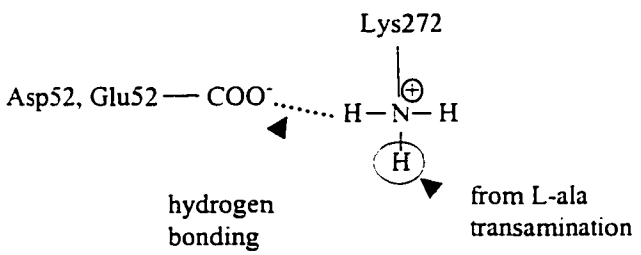

Figure 23. Enhanced basicity of Lys272 by Asp52 and Glu52.

Multiple substrate turnovers in Q52D, Q52H and Q52R DGDs. Judging from the reaction rates of holoenzymes with those in excess PLP, Q52D and Q52R can catalyze multiple substrate turnovers. Q52H transamination exhibited negligible multiple substrate turnover rates. PLP or 2MA (or both) intake into the Q52H active sites may be somewhat limited

after the first substrate turnover. At present, explanation of the results awaits more in-depth experiments.

Quinonoid formation in WT, Q52E and Q52H DGDs. Appearance of an absorption band near 500 nm in PLP-dependent enzymes is fairly common under certain conditions. Substrate analogs (Zakomirdina et al., 1989; Ben-Kasus et al., 1996; Philips et al., 1997), addition of organic solvent (Faleev et al., 1994; Ahmed et al., 1996) and site-directed mutagenesis of active site lysine to arginine (Philips et al., 1991; Toney et al., 1991) are some of the methods employed to induce quinonoid intermediate. This report demonstrated addition of glycerol and normal substrates induce quinonoid formation in WT and certain mutant DGDs. The absorption band, representing the quinonoid intermediate, is observed in both half reactions with glycerol; the band disappears as reaction progresses. This red peak formation can be eliminated when glycerol is removed from the enzyme preparation. Glycerol does not alter reaction rates since the three forms of DGDs tested showed similar decarboxylation and transamination rates with and without glycerol. It is unclear how glycerol induces formation of the quinonoid intermediate. Faleev et al. (1994) proposed water-organic solvent could distort or interfere with proper orientation of the basic catalytic group within enzyme active site. In this case, the decreased ability of Lys272 to reprotonate the quinonoid intermediate could account for the appearance of transient peak in WT, Q52E and Q52H. Isupov et al. (1998) cited that their preliminary data on a quinonoid complex of tryptophanase suggest that the serine residue in the active site Ser-X-X-Lys motif could hydrogen bond to

Lys266 in the external aldimine and/or quinonoid steps of the reaction. Similarly, Thr269 could hydrogen bond to Lys272 during the quinonoid step in DGD. The increasingly hydrophobic environment may have slowed down the release of Lys272 from Thr269, thus impeding the reprotonation step of the quinonoid intermediate. Nevertheless, further speculation on this scenerio is not attempted with the limited information provided by Isupov et al. (1998). Alternatively, a yet-to-be determined active site residue could be catalyzing the reprotonation step and is affected differently by the more hydrophobic environment.

Decarboxylation or deprotonation of the external aldimine produces quinonoid intermediate absorbing maximally at different wavelengths in Q52E, Q52H and WT DGDs. Q52E and Q52H showed singular λ_{max} at 520 nm and 500 nm respectively whereas WT showed dual peaks at 500 and 530 nm. So far, the possibility that the quinonoid complex (Figure 24) could account for the difference in λ_{max} is eliminated since the transient species exhibited similar λ_{max} in both 2MA and L-ala half reactions. The only deviating factors among the three DGD forms are the leaving group of the PLP/substrate complexes and the replacement of amino acid at position 52. The leaving groups of the PLP/substrate complexes were similar in the three DGD forms and therefore could not have affected the λ_{max}. The final possibility is that the replacement of Gln52 with histidine and glutamate changed the subsite environment substantially enough to shift λ_{max} of the intermediates. The subsite is catalytically, if not physically, isolated from the rest of the DGD active site. Any amino acid mutation within the subsite will affect the microenvironment within that subsite.

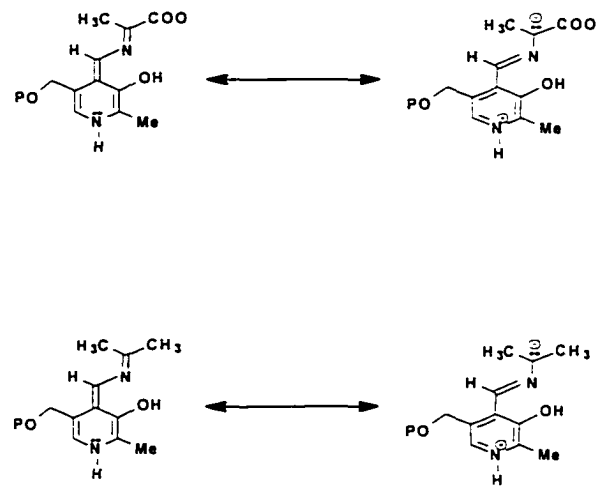

Figure 24. Quinonoid intermediates in L-ala-PLP and 2MA-PLP complexes.

OrnAT and GabaAT active sites. The concept of a catalytically isolated subsite within the DGD active site has important implications for OrnAT and GabaAT, two medically important aminotransferases that are closely related to DGD. Gyrate atrophy, a hereditary disorder that leads to blindness in humans, can be traced to dysfunctional OrnAT (Shen et al., 1998 and references therein). Point mutations in the OrnAT genes are detected in patients suffering from gyrate atrophy. The rational that an enzyme lacking a catalytically or structurally important residue can result in a dysfunctional enzyme is applicable to OrnAT. Since OrnAT is structurally related to DGD, both active sites may share similar features. DGD catalytic ability was compromised when one of the active site residues was mutated. Similarly, the catalytic ability of OrnAT could alter if the point mutations code for an amino acid is located at the subsite.

Presently, the anti-epileptic drug, vinyl-GABA, inactivates GabaAT by forming an α,β-unsaturated ketimine, then an enamine that tautomerizes (Toney et al., 1995b). The amino acids at the GabaAT subsite could be alternative targets for drugs designed to inhibit GabaAT activity.

2.6. Conclusion

Experimental results supported the hypothesis that hydrogen bonding to the substrate carboxyl group is crucial for the ability of DGD to carry out decarboxylation. However, transamination rates of the Q52X DGD mutants were affected; transamination rates for some mutants increased while others decreased. In the DGD-catalyzed transamination, hydrogen bonding (or ionic interaction) between substrate and active site residues becomes an important factor in ensuring reaction takes place in a hydrophobic active site environment. Decarboxylation and transamination reactions are not mutually exclusive events as previously perceived; replacement of Gln52, which is proposed to catalyze decarboxylation, has a profound effect on the DGD transamination ability.

WT DGD is not the optimal enzyme form for catalyzing decarboxylation or transamination. Nevertheless, glutamine is the preferred residue because it catalyzes both half reactions at reasonable rates.

Addition of 3% v/v glycerol did not affect decarboxylation and transamination rates in WT, Q52E and Q52H DGDs but induced the formation of long-wavelength absorbing intermediates in the three DGD forms. These absorption peaks are generally attributed to the accumulation of quinonoid intermediates. The different λ_{max} of the quinonoid

intermediates in the three DGD forms suggest that the subsite is catalytically, if not physically, isolated from the rest of the DGD active site. Any amino acid mutation within the subsite will affect the microenvironment within that subsite.

The concept of a catalytically isolated subsite within the DGD active site has important implications for OrnAT and GabaAT, two medically important aminotransferases that are closely related to DGD. Point mutations in the OrnAT subsite that catalyzes transamination could result in dysfunctional enzymes. Dysfunctional OrnAT has been associated to gyrate atrophy, a hereditary disorder that leads to blindness in humans. The amino acids at the GabaAT subsite could be alternative targets for drugs designed to inhibit GabaAT activity.

Chapter 3

Evolutionary relationships between 2,2-dialkylglycine decarboxylase (DGD) and PLP-dependent enzymes: Investigations into amino acids responsible for DGD decarboxylation

3.1. Abstract

Protein sequence alignment revealed that 2,2-dialkylglycine decarboxylase (DGD) is closely related to PLP-dependent aminotransferases (Mehta and Christen, 1994). However, DGD possesses the ability to decarboxylate amino acids not found within the family. More intensive protein sequence comparison and computer protein modeling were undertaken to investigate this unique ability of DGD. All four invariant residues of structural and functional importance found in all PLP aminotransferases were verified in DGD [Gly216 (314AT[2]), Asp243 (340AT), Lys272 (385AT) and Arg406 (562AT)].

Gln52 and one of the histidines near the active site are thought to contribute to DGD decarboxylation activity. Even though DGD decarboxylation depends on Gln52 and therefore probably the amino terminus, no known decarboxylases share substantial similarity with the amino end of DGD. Aminotransferase subgroup I and II members, except ornithine aminotransferase (OrnAT), lack residues at position 52 capable

[2] refers to the numbering system of amino acid applicable to aminotransferases (AT) in general (Mehta et al., 1993).

of hydrogen bonding with substrate carboxyl group. Even then, Tyr85 OrnAT, which corresponds to Gln52 DGD, does not hydrogen bond with analog carboxyl group but participates in enzyme inhibition via ring to ring interaction. More importantly, the protein backbone dictates the exact position of Gln52 for optimal interaction with the substrate carboxyl group. This is evident by the position of the corresponding Val39 of aspartate aminotransferase (AAT), which faces away from substrate due to a slight turn of the protein main chain.

Two out of the seven histidines could be partly responsible for DGD decarboxylation. His77 and 304 are part of a network that coordinates the potassium ion and are in close proximity to Gln52. The potassium ion requirement in DGD transamination or decarboxylation or both reactions is unknown. His77 and 304 mutations in wild-type DGD, Gln52 to His52 mutant (catalyzing decarboxylation only) and Gln52 to Glu52 mutant (catalyzing transamination only) may provide clues to solve the mystery.

3.2. Introduction

PLP-dependent enzymes are divided into a number of families that catalyze distinctive reactions; the largest family by far is the α family (Christen et al., 1994). The α family enzymes, with few exceptions, carry out reactions at the substrate α carbon. Among the members are most aminotransferases, which catalyze the reversible amino transfer of amino acids and oxo acids. Analysis by multiple protein sequence alignment revealed that aminotransferases belong to a single family of homologous proteins (Mehta

et al., 1993). Although these enzymes are grouped into one family, they exhibit an array of substrate specificity. Mehta and co-authors further divided the aminotransferases into 4 subgroups, based on their degree of similarities in primary structure. Conceivably, the earliest enzymes were reaction specific and evolved divergently to become substrate specific (Christen et al., 1994). In contrast, PLP decarboxylases are classified in at least four evolutionary unrelated groups (Christen et al., 1994). Decarboxylases exhibiting the same substrate specificity can be unrelated at the amino acid sequence level. Likewise, decarboxylases within the same organism, e.g. arginine decarboxylases in *E. coli*, can be of different lineages. PLP decarboxylases thus represent an example of convergent evolution in B_6 enzymes.

Keller et al. (1990) showed that the overall DGD sequence is most similar to ornithine aminotransferases (OrnAT), in particular rat OrnAT. Both DGD and rat OrnAT shared 56% homology at the carboxyl termini where the PLP-binding domain is located. They also addressed the question of whether DGD, being an aminotransferase, has acquired decarboxylation activity through evolution or vice versa. Based on sequence and structural similarities, DGD is most related to subgroup II (Mehta and Christen, 1994), one of the four major subfamilies of PLP aminotransferases (Mehta et al., 1993). While most members within subgroup II only transaminate substrates, DGD carries out sequential decarboxylation and transamination. Apparently, DGD has evolved from the aminotransferases only after the enzymes had specialized into subgroups.

Toney et al. (1995a) postulated that the ability of DGD to catalyze decarboxylation in addition to transamination could be explained by the strategic

presence of Gln52 at the enzyme active site. The singular presence of Gln52 in DGD, and not in other PLP enzymes, can promote decarboxylation by first forming a hydrogen bond with the substrate carboxyl group. In addition, Sato et al. (1978) presented evidence of an important histidine residue in DGD decarboxylation activity. Chemical inactivation of a histidyl residue inhibited decarboxylation selectively and converted DGD into a simple aminotransferase. The DGD primary sequence showed that the enzyme lacks the typical histidine-lysine pair at the active site of decarboxylases. Nevertheless, Keller et al. (1990) speculated a histidine, not adjacent to lysine but present elsewhere at the active site, may still be required for the decarboxylation half reaction. It is probable both Gln52 and one of the seven histidines in DGD are required for decarboxylation. Primary sequence alignment of subgroup II members and DGD may provide insight into how Gln52 as well as which histidine allow DGD to catalyze decarboxylation. In other words, residues of other enzymes at positions equivalent to DGD Gln52 and histidines could explain the roles these amino acids play in DGD decarboxylation.

Since Gln52 is located at the amino end, it is hypothesized that the N-terminus of DGD could be responsible for catalyzing decarboxylation. Is DGD more homologous to decarboxylases at its amino end but retains its aminotransferase characteristics at its carboxyl end? It may be possible to locate within protein databases sequences homologous to DGD amino end and coincidentally a decarboxylase. The objective of the following study was to use protein sequence comparison to elucidate the relationships of DGD with aminotransferases and decarboxylases, as well as gain an understanding of which specific residues contribute to DGD decarboxylation.

3.3. Method

Using the BLAST (Basic Local Alignment Search Tool, Altschul et al., 1990), 140 amino acids from the DGD N-terminus were compared to known amino acid sequences from Genbank (release103), Brookhaven Protein Data Bank (release 82), Swiss-Prot (release 34) and NBRF-PIR (release 54). Protein sequences of positive hits from the search were compiled in a databank. Multiple sequence alignments were carried out using Omiga 1.0.1 Clustal W algorithm with default parameters (Oxford Molecular Group, 1997). Protein sequence homology was scored with GenePro 6.10 (Riverside Scientific Enterprise, 1994). 3D enzyme structures were downloaded from Brookhaven Protein Data Bank (release 82) and visualized with Sybyl 6.2 (Tripos, 1995) or RasMol 2.6 (R. Sayle, 1995).

3.4. Results

Mehta et al. (1993) located four invariant residues of structural and functional importance in 51 sequences of PLP aminotransferases. Mehta and Christen (1994) found DGD only fulfils two such requirements; Lys272 forms a Schiff base with cofactor and Asp243 pairs with pyridine N of coenzyme. By using the Omiga 1.0.1 multiple alignment algorithm and 3D structural information, two additional residues were located that allow DGD to be categorized as an aminotransferase. The following four residues in DGD are involved in the designated functions described previously (Mehta et al., 1993). (1) Gly216 (314AT) participates in type I β-turn sandwiched between the large PLP binding domain and the smaller C-terminal domain; (2) Asp243 (340AT) forms a salt

bridge/hydrogen bond to N1 of pyridoxal 5'-phosphate; (3) Schiff base formation takes place at Lys272 (385AT) and (4) α-carboxylate group of substrate is oriented by Arg406 (562AT).

Protein sequence comparison of Gln52 DGD to aminotransferase subgroups I and II. Alignment of Gly42 to Ser54 DGD with AAT, a member of subgroup I, is shown in Table 6. DGD is less related to AAT as evident by homology scores of 13 to 15% with prokaryotic, cytosolic and mitochondrial AATs. AAT valine or alanine occupies the position corresponding to Gln52 of DGD; these residues are incapable of hydrogen bonding.

The BLAST algorithm search showed that only PLP aminotransferases subgroup II share significant amino terminal homology with DGD. Search results also indicated that although DGD decarboxylation depends on Gln52, no known decarboxylases share substantial similarity with amino end of DGD. The six aminotransferases showing significant homology at the amino termini are acetylornithine (AcornAT), alanine-glyoxylate (AGAT), 4-aminobutyrate (GabaAT), ω-amino acid-pyruvate (omega-APAT), ornithine (OrnAT) and 7,8-diamino-pelargonate (DapaAT) aminotransferases. Two PLP aminotransferases from *Caenorhabditis elegans* and *Bacillus firmus* whose functions have yet to be determined were also listed as positive hits. DGD not only shares significant homology with subgroup II members in terms of overall sequences (Mehta and Christen, 1994) but also N-terminal sequences.

Table 6. Gly42 to Ser54 DGD compared to AAT, member of PLP aminotransferase subgroup I.

Enzyme	Source	% homology to DGD													References
DGD	*Burkholderia cepecia*		G	R	A	I	L	D	F	T	S	G	**Q**	M	S	Toney et al. (1995)
AAT	*Escherichia coli*	13	P	G	K	-	I	N	L	G	I	G	V	Y	K	Okamoto et al. (1994)
AAT	pig cytosolic	13	P	R	K	-	V	N	L	G	V	G	A	Y	R	Arnone et al. (1985)
AAT	chicken cytosolic	14	S	R	K	-	V	N	L	G	V	G	A	Y	R	Borisov et al. (1985)
AAT	chicken mitochondria	15	S	K	K	-	M	N	L	G	V	G	A	Y	R	McPhalen et al. (1992)
Concensus												G	*			

* denotes Q52 DGD aligned with V or A of subgroup I aminotransferases

Seventeen subgroup II aminotransferases from different sources were tabulated and their sequences compared to DGD (Table 7). Homology scores between DGD and subgroup II members range from 32 to 19%. *B. firmus* aminotransferase shares the most sequence similarity with DGD; 32% of DGD 433 amino acids aligned with 445 residues of *B. firmus* aminotransferase. *M. tuberculosis* 4-aminobutyrate aminotransferase scores 30% homology with DGD.

Glycine and proline residues occupy similar positions in primary sequences of subgroup I and II enzymes (Tables 6, 7 and 8). Both amino acids are conserved for structural purposes; these residues allow specific main chain conformations in proteins unattainable with other amino acids. Within the DGD structure, residues Gly42, Gly51 and Pro308 participate in β turns between helixes (Toney et al., 1995a). Conservation of glycines and prolines in primary sequences is usually an indication that the proteins are folded into similar shapes and hence belong to the same enzyme family (Branden and Tooze, 1991). Additionally, the similarity of the 3D structures of AAT, OrnAT, DGD and tryptophanase attest to the fact that these enzymes are homologous.

Gly42 to Ser54 of DGD alignment with subgroup II yielded one other consensus residue: aspartate is most likely conserved for functional purposes since the residue can form hydrogen bond (Table 7). Asp47 of DGD is located at the carboxyl end of the three stranded antiparallel β-sheets in the N-terminal segment (see pp. 18) and participates in type I β-turn (Toney et al., 1995a). It is very likely that aspartate at the corresponding positions in other members take part in similar bonding. The most noteworthy finding is that Gln52 DGD aligned with isoleucine (AcornAT, AGAT and GabaAT), leucine

Table 7. Gly42 to Ser54 DGD compared to PLP aminotransferases subgroup II.

Enzyme	Source	% homology to DGD													References
												↓			
DGD	*Burkholderia cepecia*		G	R	A	I	L	D	F	T	S	G	**Q**	M	S	Keller et al. (1990)
AcornATag	*Alnus glutinosa*	27	G	R	E	Y	L	D	L	S	A	G	I	A	V	Guan et al. (1996)
AcornATec	*Escherichia coli*	22	G	K	E	Y	V	D	F	A	G	G	I	A	V	Heimberg et al. (1990)
AcornATkl	*Kluyveromyces lactis*	23	N	K	E	Y	I	D	F	T	A	G	I	A	V	Janssen et al. (1997)
AcornATs	*Synechocystis* PCC6803	28	G	K	S	Y	L	D	F	V	A	G	I	A	T	Kaneko et al. (1996)
AcornATy	yeast	22	G	K	E	Y	I	D	F	T	A	G	I	A	V	Heimberg et al. (1990)
AGATrn	mouse	25	G	N	R	Y	L	D	F	F	S	G	I	V	T	Lee et al. (1995)
ATbf	*Bacillus firmus*	32	G	V	K	Y	L	D	F	T	S	G	I	A	V	Quirk and Krulwich (1991)
ATce	*Caenorhabditis elegans*	22	G	K	K	Y	L	D	F	F	G	G	I	V	T	Wilson et al. (1994)
GabaATan	*Aspergillus nidulans*	20	G	N	M	L	L	D	V	Y	A	Q	I	A	S	Richardson et al. (1989)
GabaATmt	*Mycobacterium tuberculosis*	30	G	N	R	L	I	D	L	G	S	G	I	A	V	Conner et al. (1996)
GabaATy	yeast	19	G	N	T	Y	L	D	L	Y	A	Q	I	S	S	Andre and Jauniaux (1990)
omega-APATpp	*Pseudomonas putida*	24	G	R	K	V	Y	D	S	L	S	G	L	W	T	Yohana et al. (1992)
OrnAThu	human	24	G	R	K	Y	F	D	F	L	S	S	Y	S	A	Inana et al. (1986)
OrnATrn	mouse	23	G	R	Q	Y	F	D	F	L	S	A	Y	G	A	Mueckler and Pitot (1985)
OrnATy [1]	yeast	22	G	K	L	Y	L	D	F	L	S	A	Y	S	A	Degols (1987)
DapaATbs	*Bacillus sphaericus*	24	N	Q	R	Y	L	D	A	V	S	S	W	W	V	Gloeckler at al. (1990)
DapaATec	*Escherichia coli*	21	G	R	R	L	V	D	G	M	S	S	W	W	A	Otsuka et al. (1988)
Concensus			G					D				G	*			

[1] partial sequence ends at A54

* denotes Q52 DGD aligned with I, L, Y or W of subgroup II aminotransferases

Table 8. Tyr301 to Pro400 DGD compared to PLP aminotransferases subgroup II.

Enzyme	Source	↓			↓						
DGD	*Burkholderia cepecia*	Y	T	T	H	V	S	D	P	L	P
AcornATag	*Alnus glutinosa*	G	T	T	F	A	G	G	P	L	V
AcornATec	*Escherichia coli*	G	S	T	Y	G	G	N	P	L	A
AcornATkl	*Kluyveromyces lactis*	G	T	T	Y	G	G	N	P	L	G
AcornATs	*Synechocystis* PCC6803	A	S	T	F	G	G	N	P	L	A
AcornATy	yeast	G	T	T	Y	G	G	N	P	L	A
AGATrn	mouse	F	S	T	F	G	G	S	P	L	A
ATbf	*Bacillus firmus*	G	T	T	F	G	G	N	P	I	A
ATce	*Caenorhabditis elegans*	N	-	T	Y	G	G	N	P	L	A
GabaATan	*Aspergillus nidulans*	F	N	T	W	M	G	D	P	S	R
GabaATmt	*Mycobacterium tuberculosis*	G	G	T	F	G	G	N	P	V	A
GabaATy	yeast	F	N	T	W	C	G	E	P	A	R
omega-APATpp	*Pseudomonas putida*	G	Y	T	Y	S	A	H	P	V	A
OrnAThu	human	G	S	T	Y	G	G	N	P	L	G
OrnATrn	mouse	G	S	T	Y	G	G	N	P	L	G
DapaATbs	*Bacillus sphaericus*	S	H	S	Y	T	G	N	T	L	A
DapaATec	*Escherichia coli*	G	P	T	F	M	G	N	P	L	A
Concensus		*		T	$		G		P		

* denotes Y301 DGD aligned with mostly G of subgroup II aminotransferases

$ denotes H304 DGD aligned with F, W or Y of subgroup II aminotransferases

(omega-APAT), tyrosine (OrnAT) and tryptophan (DapaAT) of other subgroup II enzymes. All residues, except tyrosine, cannot hydrogen bond with respective substrates.

Investigations into the role of histidines in DGD. Using the Omiga 1.0.1. multiple sequence alignment function, the residues of subgroup II members at positions corresponding to the seven histidyl residues of DGD were tabulated in Table 9. Only some histidines within subgroup II are conserved. His16, 139 and 294 DGD share no significant homology at corresponding positions of subgroup II members; in fact, the amino acids seem random. His59 is found in all except GabaATs and DapaATec. His61 is present in some AcornATs, AGATrn, a few OrnAT, DapaATec but not in GabaAT, omega-APATpp and DapaATbs. All AcornATs and AGATm have histidyl residues at positions corresponding to DGD His77. In fact, His59, 61 and 77 are the most highly conserved histidines among the members. These histidines form either part of the DGD active site or maintain monomer-monomer interaction. The singular presence of His304 in DGD is a surprise; other enzymes have bulky groups such as tryptophan, phenylalanine and tyrosine at corresponding positions. Of the three amino acids, only tyrosine is capable of donating a hydrogen bond.

The absence of His304 DGD at corresponding positions among other subgroup II members is intriguing and hence warrants further analysis. Table 8 shows alignment of Tyr301 to Pro400 DGD with other subgroup II enzymes. Threonine is conserved in all but one enzyme. Thr303 has important structural and functional implications in DGD catalysis (Toney et al., 1995a). It hydrogen bonds with potassium ion near the active site

Table 9. Alignment of DGD histidines with PLP aminotransferases subgroup II.

Enzyme	Source	Position in DGD						
		16	59	61	77	139	294	304
DGD	*Burkholderia cepecia*	H	H	H	H	H	H	H
AcornATag	*Alnus glutinosa*	R	H	D	H	Q	I	F
AcornATec	*Escherichia coli*	E	H	H	H	P	H	Y
AcornATkl	*Kluyveromyces lactis*	Y	H	N	H	P	L	Y
AcornATs	*Synechocystis* PCC6803	T	H	H	H	L	P	F
AcornATy	yeast	F	H	N	H	P	L	Y
AGATm	mouse	P	H	H	H	S	A	F
ATbf	*Bacillus firmus*	P	H	H	G	H	W	F
ATce	*Caenorhabditis elegans*	K	H	H	H	S	N	Y
GabaATan	*Aspergillus nidulans*	E	Y	N	I	T	P	W
GabaATmt	*Mycobacterium tuberculosis*	A	N	S	T	H	H	F
GabaATy	yeast	E	Y	N	V	S	P	W
omega-APATpp	*Pseudomonas putida*	Y	H	R	S	A	M	Y
OrnAThu	human	Y	H	H	L	K	I	Y
OrnATm	mouse	Y	H	H	L	K	I	Y
DapaATbs	*Bacillus sphaericus*	S	H	N	T	T	Y	Y
DapaATec	*Escherichia coli*	T	Y	H	V	E	S	F
Number of histidines		1	13	9	8	3	3	1

and also N-pyridines of His77 and His304. Furthermore, the amide bond and hydroxyl groups of Thr303 donate hydrogen bonds to the oxygen atoms of the PLP phosphate ester. However, the threonine in other members cannot hydrogen bond to residues such as phenylalanine and tryptophan at positions corresponding to His77 DGD. Thr303 DGD, Thr322 OrnAT and the structural equivalents in other enzyme members are indispensable for providing additional hydrogen bonds to phosphate oxygens of the cofactor. However, one cannot speculate the role of threonine in coordinating metal ions in other subgroup II members. OrnAT, the only other subgroup II member of known structure, shows no metal ions dependency (Shen et al., 1998); the structurally equivalent residue is positioned unfavorably to form ligands to a potassium ion. Metal ions requirement of other subgroup members has been somewhat studied. Echetebu et al. (1987) that found tyrosine aminotransferase is inhibited by metal ions Ca^{2+}, Mn^{2+}, Zn^{2+}, Hg^{2+} and Ag^{2+}, but was unaffected by chelating agents and other divalent cations. The 3D structure of tyrosine aminotransferase is presently unavailable. Mayer et al. (1994) reported that glutamate-1-semialdehyde aminotransferase exhibits no metal ion dependency for activity. No discussion on such topic was provided in the 3D structure of glutamate-1-semialdehyde aminotransferase published by Hening et al. (1997).

In addition to Gln52, Tyr301 has been speculated to be involved in DGD decarboxylation (Toney et al., 1995a). Residues at equivalent positions with Tyr301 DGD are mostly glycines and phenylalanines (Table 8). The hydroxyl group of Tyr301 has been postulated to hydrogen bond with Gln52.

DGD and AAT active sites visualization with Sybyl 6.2. Sequence comparison analysis gives only a one dimensional view of the functionality of select residues. DGD and AAT active sites visualized with Sybyl molecular modeling software offer an added advantage to our analysis (Fig. 25A and B). Val39 AAT from *E. coli* (Okamoto et al., 1994) aligns with Gln52 DGD (Table 6) and is part of a region known to undergo significant main-chain conformational change upon substrate analog binding. Segment movement shields the active site from the solvent environment. This is followed by protein backbone N atom of Gly38 hydrogen bonding to substrate α-carboxylate. Gln52 of DGD and Val39 of AAT differ in their spatial orientation within the active site despite their alignment in the primary sequences. Gln52 amide side chain is positioned towards, and thus hydrogen bonded to substrate α-carboxylate (Figure 25A). Conversely, Val39 side chain faces away from the substrate (Figure 25B). It is evident that protein backbone twisting dictates the orientation of these residues. Hence, the ability of an amino acid hydrogen bonding with substrate cannot be determined solely by primary sequence alignment.

In an attempt to convert AAT into an enzyme capable of catalyzing decarboxylation, V39 and α-CH_3 were replaced with glutamine and α-carboxylate respectively. Following energy minimization, the mutated residue glutamine was at relatively similar position as before; the amide side chain was still directed away from the active site. It is concluded that mutation Val39 to Gln39 is unlikely to adapt AAT into a decarboxylating enzyme.

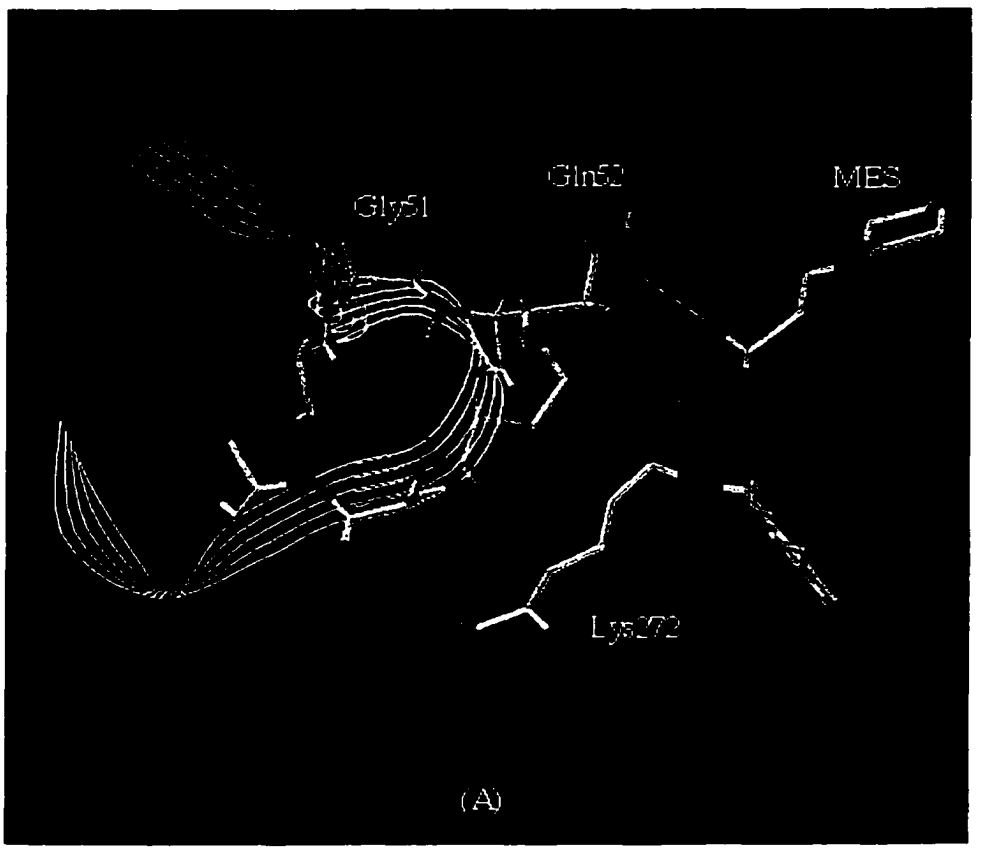

Figure 25 A. DGD active site residues. Gln52 hydrogen bonds to OS1 of MES sulfonate group.

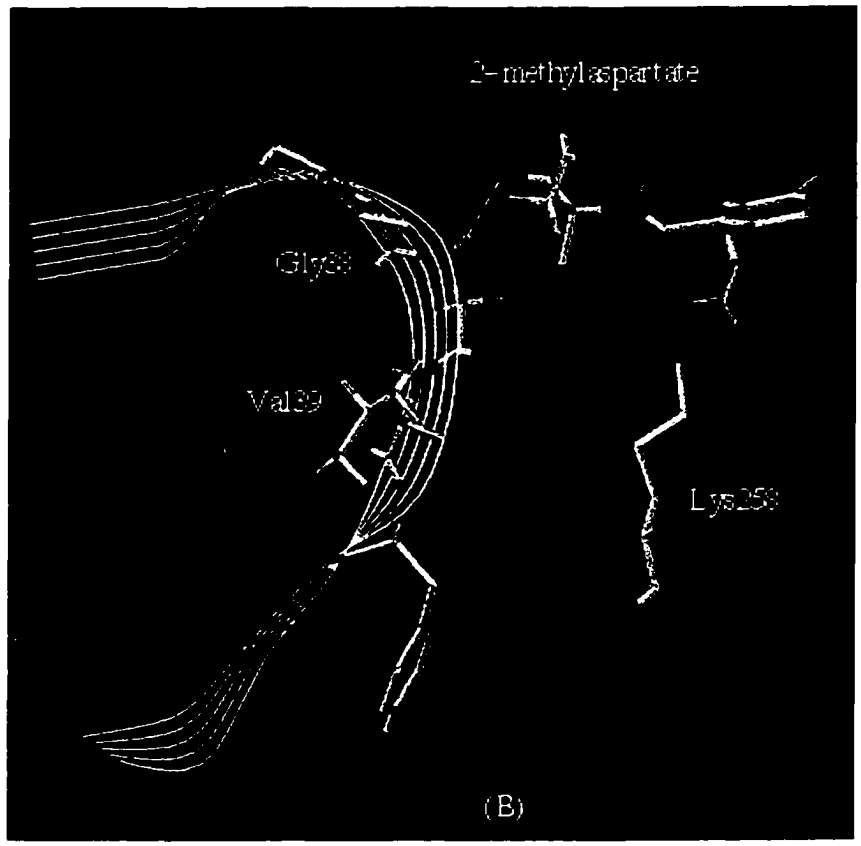

Figure 25 B. AAT active site residues. Gly38 main chain N hydrogen bonds with α–carboxyl group of substrate. AAT x-ray crystal structure reveals that a rotation of helix brings the Gly38 nitrogen into a position to hydrogen bond with α-carboxyl of the substrate, 2-methyl-L-aspartate (Okamoto et al., 1994).

3.5. Discussion

DGD shares similar protein structure with OrnAT and GabaAT, members of subgroup II aminotransferases (Toney et al., 1995b). While overall protein scaffolding among the enzymes may be similar, substrate specificity is not. The ability of DGD to decarboxylate and transaminate at one active site probably arises from strategic residue alteration within that locality. Attempts to locate decarboxylases sharing sequence similarity with DGD amino end proved unsuccessful. DGD is more homologous to aminotransferases, despite its ability to catalyze decarboxylation. Additionally, DGD fulfills all the requirements as an aminotransferase outlined by Mehta et al. (1993).

Comparison of active site amino acid composition of other subgroup II aminotransferases with DGD may aid in the dissection of how specific amino acids contribute to DGD decarboxylation. DGD and OrnAT are the only two subgroup II enzymes of known 3D structures (Toney et al., 1995a; Shen et al., 1998). Watanabe et al. (1989) gave a brief structural description of omega-APAT. An active site model for GabaAT, based on DGD structure, was presented by Toney et al. (1995b).

Protein sequence comparison of Gln52 DGD to aminotransferase subgroup I and II. It is hypothesized that Gln52 DGD enhances decarboxylation via formation of hydrogen bond to substrate carboxyl group (Toney et al, 1995a). Primary sequence comparison concluded that this hydrogen bonding feature is not shared among most subgroup I and II enzymes (except OrnAT). Although the possibility of the main polypeptide chain hydrogen bonding to substrate cannot be ruled out, bulky residues such as isoleucine,

leucine and tryptophan prevent such bonding unless the side chains are positioned away from the active sites. Ultimately, hydrogen bonding to substrate carboxyl cannot guarantee decarboxylation as evident by analysis of OrnAT active site residues as described below. More importantly, the scissile bond must be perpendicular to the PLP π system for effective decarboxylation. Shah et al. (1997) presented the crystalline structure of human OrnAT complexed with inhibitors L-canaline and gabaculine. Tyr85 OrnAT, which aligned with Gln52 DGD, does not hydrogen bond to analog carboxyl group. Instead, this residue contributes to the stability of inhibitor-enzyme complex via ring to ring interaction that permanently inactivates the enzyme (Shah et al., 1997). Tyr55 and Arg180 hydrogen bond to analog carboxyl in order to position ornithine for transamination at δ position; alteration of these residues results in unproductive substrate turnover. In fact, these two specific tyrosine and arginine residues are present in all AcornATs, OrnATs as well as DGD at similar location by alignment with Omiga 1.0.1. and slight manual adjustments. OrnAT active site accommodates an elongated substrate that is absent in DGD probably explains why Tyr20 and Arg153 DGD are distant from the MES molecule and do not take part in catalysis.

Role of histidines in DGD. Sato et al. (1978) demonstrated chemical labeling of one of the seven histidyl residue converted DGD into an aminotransferase and suggested a modified histidine may participate in decarboxylation. Only three out of the seven histidines are located near the active site. His77 and His304 are near the potassium ion binding site. At present, the absolute requirement for potassium ions is unknown for

DGD transamination or decarboxylation or both reactions. However, due to the close proximity of the potassium ion of a monomer to Gln52 (which was shown to promote decarboxylation) of the other monomer, it is reasonable to propose that potassium ion, His77 and 304 are required for decarboxylation (Figure 26). To test the hypothesis, site directed His77 and 304 mutants of wild type DGD, glutamine 52 → histidine mutant (catalyzing decarboxylation only) and glutamine 52 → glutamate mutant (catalyzing transamination only) could provide clues to the puzzle.

His139, Asp243 and pyridine nitrogen of PLP (Figure 27) could be as important to DGD as the equivalent trio is to the mechanism of AAT (Yano et al., 1993) and most likely in GabaAT (Table 9). In AAT, the histidine-aspartate-N(1) of PLP trio forms a charge relay system that assists the electron flow from the labile bond towards the pyridine ring. Out of the fifteen sequences analyzed, His59, 61 and 77 DGD are the most conserved histidines among the members. Coincidentally, these residues lie in regions either bordering the active site or participating in dimer formation.

Histidines have been shown to be important in coordinating metal ions in some enzymes. DGD has been shown to be dependent on potassium ions for activity and stability (Aaslestad et al., 1968). Wragg et al. (1997) demonstrated by selectively labeling histidines of ppGaNTase with DEPC possibly inactivate the enzyme by interfering with the manganese binding site. Similarly, two strictly conserved histidines in 2-oxoglutarate-dependent dioxygenases and related enzymes are part of the putative iron-binding site (Lukacin and Britsch, 1997). The absolute conservation of threonine in DGD (at position

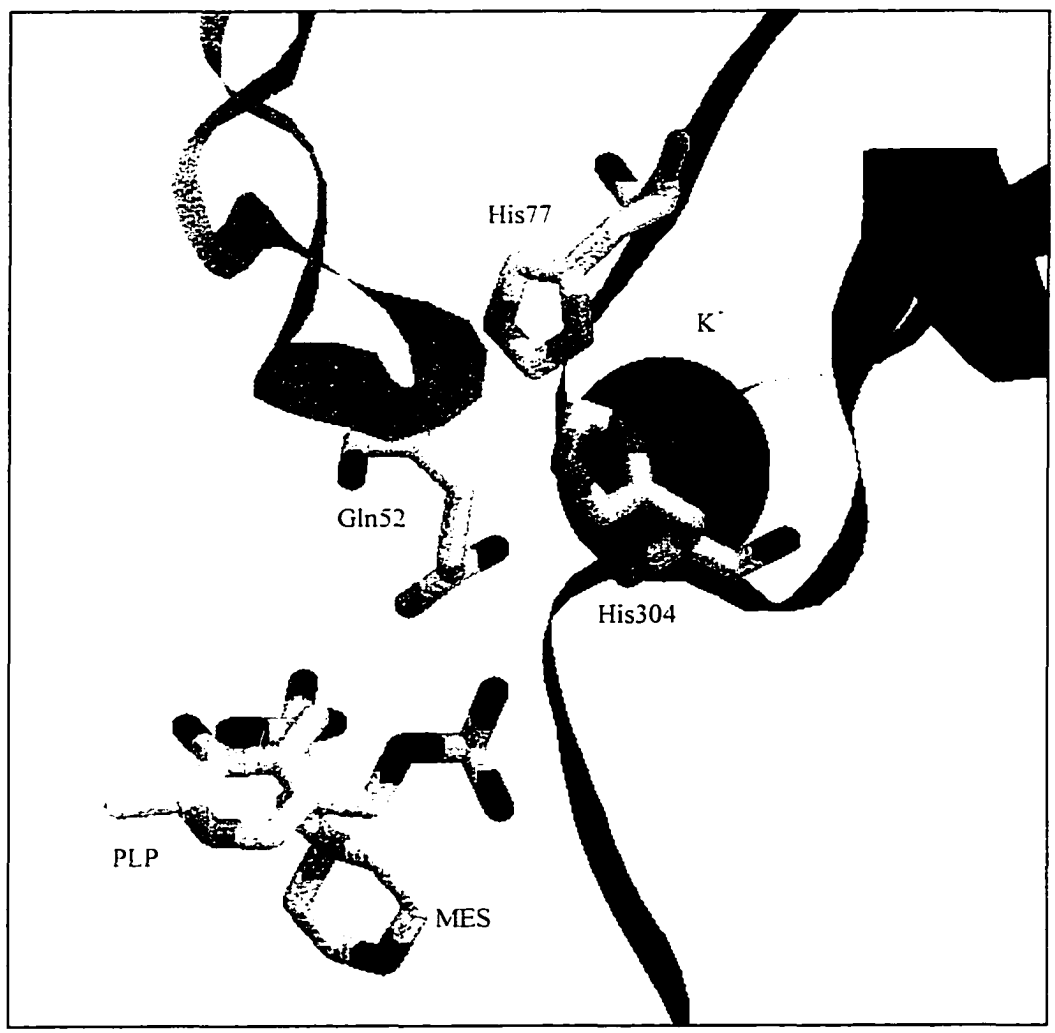

Figure 26. The positions of His77 and His304 relative to DGD active site. In this diagram, PLP and MES reside at the active site of the other monomer.

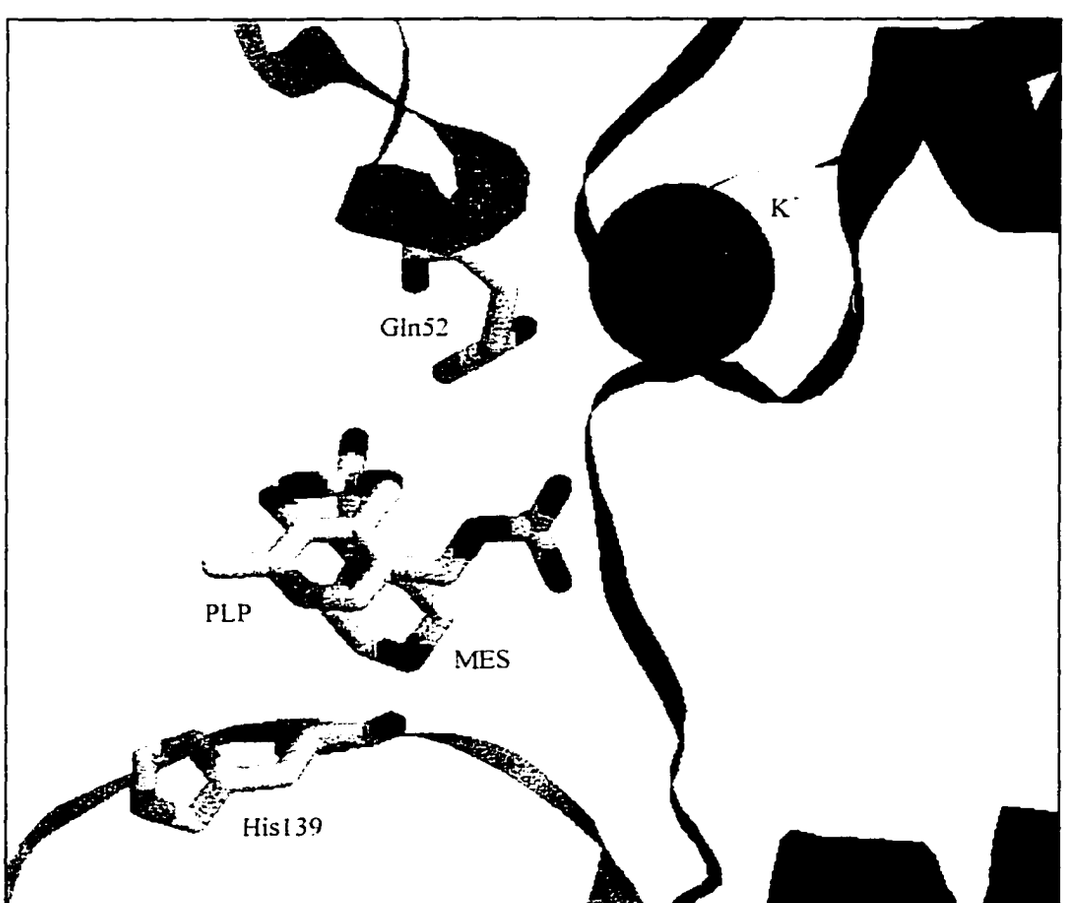

Figure 27. The position of His139 relative to the DGD active site (where PLP and MES are located).

303) and associated enzyme members prompts the suggestion that the activities of some, if not most, subgroup II enzymes are dependent on metal ions.

Comparison of DGD and AAT active sites. Primary sequences comparison aligned Gln52 DGD with Val39. Gln52 DGD faces towards substrate while Val39 AAT faces away from substrates. A differential twist of the respective enzyme protein backbone determine whether the aligned residue can hydrogen bond with the substrate. Three of the four invariant residues conserved in all aminotransferases (Mehta et al., 1993) are found in the 2D representations of DGD and AAT active sites (Figure 28). Lysines of both enzymes are positioned on the *si* face for proton abstraction. Asp243 DGD and Asp222 AAT stabilize the protonated N(1) of PLP via salt bridge formation. It accelerates the abstraction of α-group from the amino acid substrate and stabilizes the transition state (Yano et al., 1993). Equivalent aspartate residues are also found in crystal structures of tryptophanase (Isupov et al., 1998) and OrnAT (Shen et al., 1998). Arg406 DGD, Arg292 and Arg386 AAT provide positive charge to form ionic bond with substrate carboxyl group. This conserved feature is also shared among other enzymes catalyzing reactions involving mono/dicarboxylic acids as substrates. Examples include serine hydroxymethyltransferase (SHMT; EC 2.1.2.1), a PLP dependent enzyme catalyzing C_α-C_β cleavage (Jagath et al., 1997), and flavanone 3β–hydroxylase (EC 1.14.11.9), a non-heme iron enzyme involved in the biosynthesis of flavanols, anthocyanidins and catechins in plants (Lukacin and Britsch, 1997).

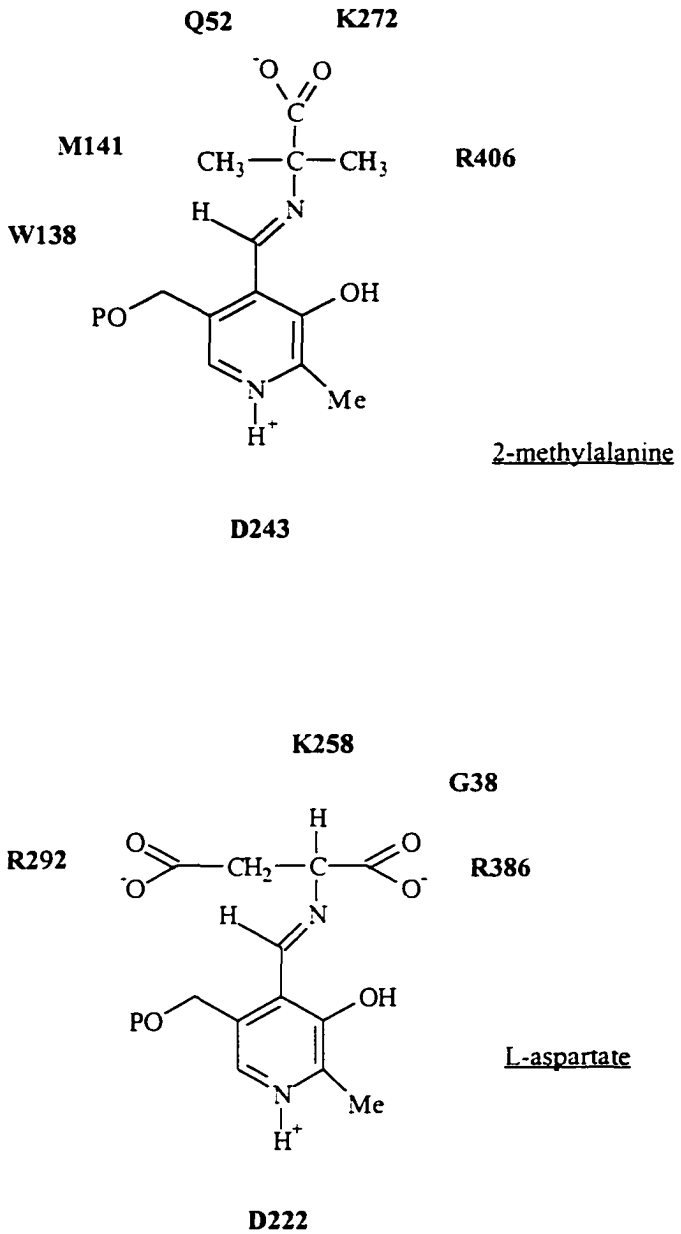

Figure 28. 2D representation of *Burkholderia cepacia* DGD and *Escherichia coli* AAT active site residues. Top: *Burkholderia cepacia* DGD active site residues and 2MA/PLP substrate complex (Toney et al., 1995a). Bottom: *Escherichia coli* AAT closed form active site residues and L-aspartate/PLP complex (Okamoto et al., 1994).

3.6. Conclusion

Further evidence was provided to show that DGD is an aminotransferase that has acquired decarboxylation activity through evolution. The four invariant residues in all PLP aminotransferases proposed by Mehta et al. (1993) were determined in DGD. The N-terminal protein sequence is more homologous to that of aminotransferases even though Gln52 and hence the N-terminus were postulated to promote decarboxylation.

If DGD is more related to aminotransferases, how does it catalyze decarboxylation? Gln52 and one of the histidines at the active site have been suggested to enhance DGD decarboxylation activity. The potential of Gln52 DGD to form hydrogen bond with substrate carboxyl is an exception among the aminotransferases. However, the histidine that could be responsible for decarboxylation is less obvious; His77 and 304 that form part of network that coordinates the potassium ion are likely candidates since the metal ion requirement in DGD transamination or decarboxylation or both reactions has yet to be determined.

Chapter 4

Protein purification and spectrophotometric studies of wild-type 2,2-dialkylglycine decarboxylase and the Lysine 272 to Alanine mutant

4.1. Abstract

The active site Lysine 272 to Alanine mutant of 2,2-dialkylglycine decarboxylase (DGD) was used to determine the catalytic function of the residue during decarboxylation and transamination. The mutation seriously compromised the mutant's ability to catalyze both decarboxylation and transamination reactions. The decarboxylation rate was 6.9 x 10^{-5} that of wild-type while the transamination rate was undetectable. The results also indicated that Lys272 is important in catalyzing α-proton abstraction in L-ala, but not the departure of the carboxyl group in 2MA. However, effective and efficient catalysis of both substrates requires the transaldimination reaction that transfers the cofactor from Lys272 to substrate in order to 'activate' the substrate.

Wild-type DGD forms an absorption peak at 500 nm in the presence of 3% glycerol. Accumulation of the quinonoid intermediate could be attributed to the decreased rate of 4'-C protonation compared to the C_α-COO^- and C_α-H bond cleavages. A more hydrophobic environment could affect the rate of protonation at the substrate level. Different active site residues maybe involved in decarboxylation/deprotonation and

protonation of the PLP-substrate complex. Due to insignificant level of enzyme activity, K272A DGD does not form such an absorption peak.

4.2. Introduction

Lys272 has been shown to be indispensable in catalyzing the α-proton abstraction step in aspartate aminotransferase (Toney and Kirsh, 1989), D-amino acid aminotransferase (Nishimura et al., 1991), glutamate-1-semialdehyde (Grimm et al., 1992) and tryptophan synthase (Lu et al., 1993). A lysine-to-alanine active site mutant of DGD was genetically engineered to allow investigation into the catalytic role of Lys272 (Brayman, 1993). Replacement of active site lysine residue to alanine proved disastrous to enzyme activity. Brayman's results showed that the mutant was unable to catalyze decarboxylation and transamination. He then concluded that Lys272 is critical in both half reactions. The active site lysine acts as general acid during decarboxylation and as general base during transamination. Attempts to restore catalytic activity of the mutant using exogenous amines to mimic the lost lysine side chain were unsuccessful (Brayman, 1993). Based on the results, Keller et al. (1997) suggested that the DGD active site environment is more hydrophobic than most aminotransferases since it precludes buffer and solvent molecules. It was later discovered that K123N mutation was unintentionally introduced during the construction of the expression vector of K272A DGD. The mutation was excised and a gene region containing the correct codon was inserted (J. W. Keller, personal communication). Although mutation K123N is located on the protein

surface and is unlikely to take part in catalyzing any reactions, K272A DGD activity was re-examined and the results compared to the K123N, K272A double mutant.

Addition information on WT DGD protein purification was presented in this chapter. Several spectrophotometric studies on WT and K272A DGDs were conducted. In particular, it was demonstrated that the K272A mutation has a more significant effect on transamination compared to decarboxylation.

4.3. Materials and Method

4.3.1. WT and K272A DGDs protein purification

DGD purification protocol has been outlined in Chapter 2. Briefly, the purification procedure entails sonication, ammonium sulfate precipitation, DEAE ion exchange chromatography and finally P-6DG gel filtration. Purified proteins were stored as 50% glycerol stock at –70°C.

4.3.2. WT and K272A DGDs spectrophotometric studies

WT and K272A DGDs holoenzyme preparations. Holoenzyme was prepared as follows. One hundred and eighty μg of purified protein (in 50% glycerol) was incubated with 50 mM 2MA, 5 mM NaPyr and 50 μM PLP in a 50 mM phosphate buffer, pH 7.5 at room temperature for 10 min. The 50 μL solution was then loaded on CHROMA SPIN-10 columns (Clontech) to remove unbound PLP, products and unreacted substrates.

Reagents. Reaction rates were determined by monitoring the disappearance of pyruvate at 220 nm over time. The ideal substrate concentration range is between 0.5 and 5 K_m of substrate. This places 2MA and pyr concentrations in the range of 5 to 50 mM and 0.2 to 2 mM respectively. Stock solutions included 62.5 mM phosphate buffer, pH 7.5, 1 mM PLP, 1000 mM 2MA and 40 mM sodium pyruvate. 2MA solution series were prepared to final concentrations of 5, 10, 20 and 50 mM when delivered in 150 μL aliquots. Pyruvate solution series were prepared to give 0.2, 0.4, 1 and 2 mM final concentrations when delivered in 20 μL aliquots.

Assay protocol. In a 0.5 cm path length quartz cuvet, incubate the following reagents for 5 min at 22°C: 800 μL phosphate buffer, 25 μL PLP and 10 μg protein. The Hewlett Packard 8452A diode array spectrophotometer was then rezeroed from 200 to 400 nm. 150 μL 2MA and 20 μL NaPyr were mixed throughly and then added to the cuvet. The decrease in pyruvate concentration was monitored by continuously scanning at 222 nm at every sec for 3 min. In a final reaction volume of 1 mL, the enzyme concentration was measured at 0.1 mg/mL. Sixteen reactions were carried out at 22°C in a single experiment.

pH dependence of molar absorptivity of WT and K272A DGDs. The pH dependence of the enzymes was investigated according to protocol similar to Brayman (1993). The spectra of WT and K272A DGDs were taken in the range of 300 to 500 nm over a pH

range from 5.5 to 11.0 in increments of 0.5 22°C. The following buffers at 100 mM were used: 2-(N-morpholino) ethanesulfonic acid (MES), pH 5.5, 6.0, 6.5; morpholinopropane-sulfonic acid (MOPS), pH 7.0; N-(2-hydroxyethyl)piperazine-N'-2-ethanesulfonic acid (HEPES), pH 7.5; triethanolamine (TEA), pH 8.0; N-tris(hydroxymethyl)methyl-3-aminopropanesulfonic acid (TAPS), pH 8.5; 2-(N-cyclohexylamino)ethanesulfonic acid (CHES), pH 9.0, 9.5; 3-(cyclohexylamino)-propanesulfonic acid (CAPS), pH 10.0, 10.5 and 11.0. Buffer pH was adjusted with 4 M NaOH or HCl. 2.5 μM WT protein in 300 μL buffer and 5.5 μM K272A in 500 μL buffer were added in quartz spectrophotometer cuvets and the spectra recorded. A ratio increase or decrease within the pH range could indicate enzyme active site is pH dependent.

K272A DGD decarboxylation and transamination half reactions. K272A holoenzyme was prepared accordingly and tested for its ability to decarboxylate 2MA or transaminate L-ala. The reaction consisted of 2.75 μM protein, 40 mM 2MA/L-ala in 15 mM phosphate buffer, pH 6.75 at 22°C.

4.4. Results

4.4.1. WT and K272A DGDs protein purification

Samples from each WT DGD purification step were run on a SDS-PAGE minigel (Figure 29). The purified enzyme was homogeneous as judged by the presence of a single

45 kDa protein band corresponding to the DGD monomer. DGD percentages relative to total protein in each purification step were tabulated in Table 10. DGD purity is generally between 85 and 90%. Table 11 showed the total protein yield and specific activity of WT DGD at each purification stage. One hundred and forty units of WT DGD were purified from approximately 40 g of bacterial pellet; specific activity (U/mg) of WT DGD increased 18-fold after the DEAE step.

4.4.2. WT and K272A DGDs spectrophotometric studies

WT DGD rate profile. The K_{2MA} and K_{pyr} were determined at 9.47±1.47 mM and 0.52±0.06 mM respectively from the double reciprocal plot of pyruvate consumption rate versus concentration of 2MA (Figure 30).

Formation of WT DGD quinonoid intermediate. The sharp isobestic point between the 330 nm and 400 nm peaks at 350 nm is consistent with the transformation of one PLP complex species into the PMP form (Figure 31). Presence of glycerol in WT DGD reactions induced the formation of a chromophore absorbing maximally at 500 nm with a shoulder at 530 nm (Figure 32). The chromophore is generally attributed to the accumulation of quinonoid intermediates. A decrease in the PLP peak, an increase in the 'red' peak and a somewhat constant PMP peak were observed. The peak is associated with the enzyme, as evident by the filtrate from protein concentration using Amicon® Centricon–30 (30,000 NW cut-off) showed no peak at 500 nm.

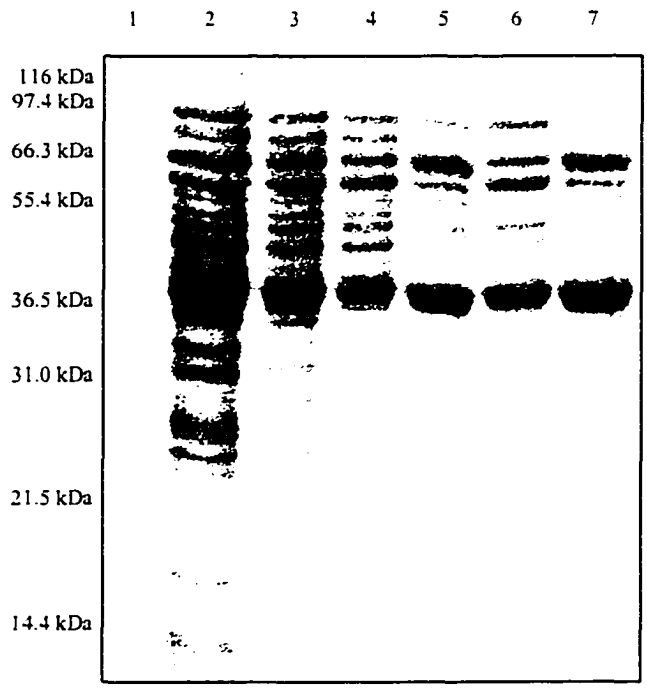

Fig. 29. Densitometric analysis of a SDS-PAGE gel containing purified WT DGD. 20 μg protein in sonication and 5 μg protein in other samples were loaded and separated on 12% SDS-PAGE gel. Lane 1, MW markers [4]; lane 2, sonication; lane 3, A.S. pption; lane 4, dialysate; lane 5, pooled DEAE (highest protein conc.), lane 6, pooled DEAE_2 (high protein conc.). lane 7, pooled P-6DG (from lane 5). DGD band in a typical P-6DG sample scan would be 80 to 90% pure.

[4] Novex Mark12™ wide-range protein standards: β-galactosidase (116 kDa), phosphorylase b (97.4 kDa), bovine serum albumin (66.3 kDa), glutamic dehydrogenase (55.4 kDa), lactate dehydrogenase (36.5 kDa), carbonic anhydrase (31.0 kDa) trypsin inhibitor (21.5 kDa) and lysozyme (14.4 kDa).

Table 10. Densitometric analysis of purified WT DGD in SDS-PAGE minigel.

Purification step	% of total
Sonication	10
Ammonium sulphate precipitate	20
DEAE	75
PDG6	85 -90

Densitometric measurements and data analysis were done with the IS-1000 Digital Imaging System, software version 1.97, Alpha Innotech Corporation.

Table 11. Yield of WT DGD per purification step.

Purification step	Total mg	mg/ml	U/mg	Total U[a]	% protein retained
Sonication	565	4.3	/[b]	/[b]	100
A.S. precipitation[c]	221	11.0	/[b]	/[b]	50
Dialysate	229	6.4	0.3	59.6	53
DEAE_1[d]	34	2.6	5.1	176.4	8
P-6DG_1[d]	26	2.2	5.4	140.6	6

[a] one unit of enzyme activity represents the amount of enzyme consuming 1 µmol of pyruvate in 50 mM phosphate buffer, pH 7.9, 150 mM 2MA, 1 mM pyruvate and 25 µM PLP per minute at 22°C

[b] specific activities are too low to be measured accurately

[c] A.S. = ammonium sulphate

[d] protein pool of highest specific activity

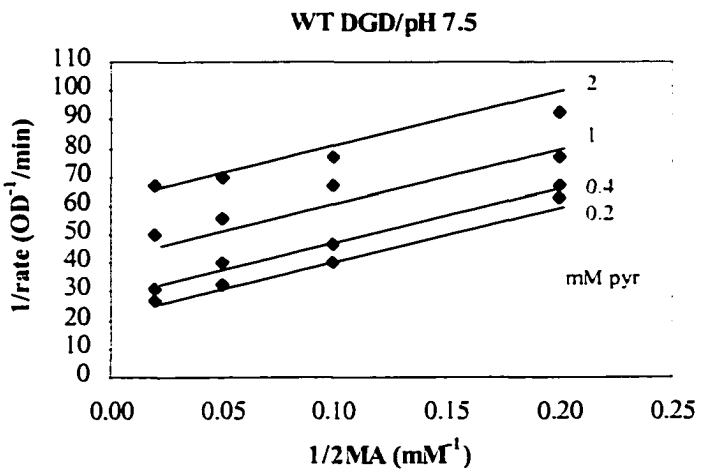

Figure 30. Double-reciprocal plot of the initial velocity of the reaction catalyzed by WT DGD. 2MA final concentrations were 5, 10, 20 and 50 mM. Pyruvate final concentrations were 0.2, 0.4, 1 and 2 mM. The data were based on 3 sets of 16 enzyme assays.

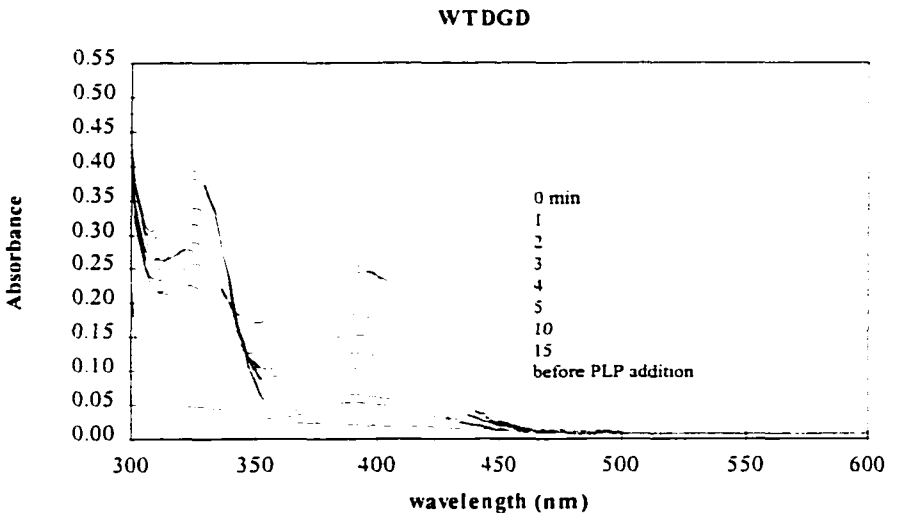

Figure 31. Spectrophotometric changes in WT DGD after 2MA and pyr addition. 700 μg protein, 50 mM 2MA, 5 mM pyr and 80 μM PLP in 50 mM phosphate buffer, pH 7.5.

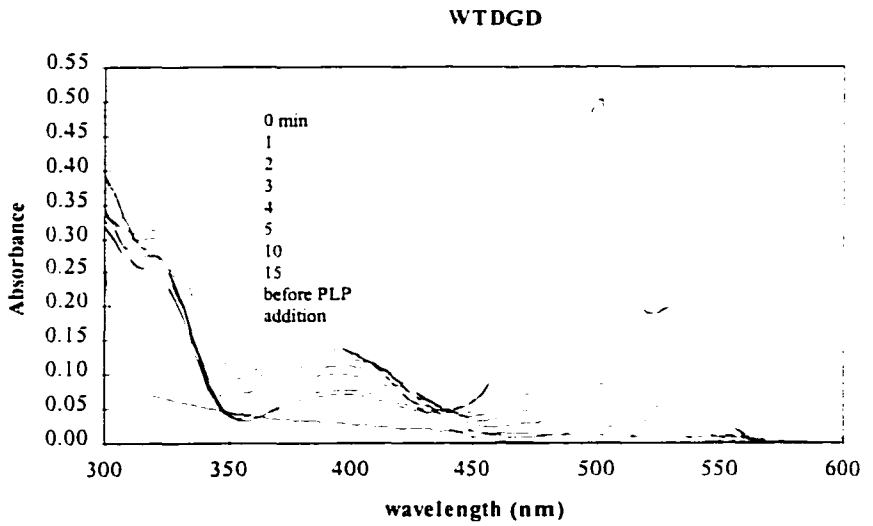

Figure 32. Spectrophotometric changes in WT DGD (glycerol) after 2MA and pyr addition. 10 μM protein (50% glycerol stock), 50 mM 2MA, 5 mM pyr and 80 μM PLP in 50 mM phosphate buffer, pH 7.5. Final glycerol concentration was 4 % v/v. Note the appearance of a 500 nm absorption peak.

pH dependence of molar absorptivity of WT and K272A DGDs. All spectra showed two peaks with λ_{max} of 326 and 400 nm, representing PLP and PMP form of the enzymes respectively. The PLP/PMP ratio of both proteins remained constant in the range of pH tested (results not shown). The lack of pH dependence of WT and K272A is consistent with Brayman (1993); the pK_a at the internal aldimine nitrogen did not change from pH 5.5 to 11.0.

K272A DGD decarboxylation and transamination rates. 2MA decarboxylation and L-ala transamination reactions of K272A holoenzyme took place to differing extent (Figure 33). The holoenzyme exhibited two peaks with λ_{max} of 330 and 400 nm, representing the enolimine (PMP) and ketoenamine (PLP) forms of the cofactor residing at the active site. Addition of substrates in both half reactions shifted λ_{max} from 400 to 416 nm. Beyond this step, K272A DGD decarboxylates 2MA to some extent but does not catalyze L-ala transamination. An extended K272A decarboxylation reaction consisting of 5.5 μM K272A holoenzyme and 40 mM 2MA in a 15 mM phosphate buffer, pH 6.75, determined first order reaction rate at 5.5×10^{-5} s^{-1} (Figure 34). K272A decarboxylation rate is 6.9×10^{-5} that of WT DGD.

4.5. Discussion

WT DGD rate profile. The K_{2MA} and K_{pyr} of purified *Burkhodaria (Pseudomonas) cepacia* DGD were 9.47±1.47 mM and 0.52±0.06 mM respectively. These values are in close

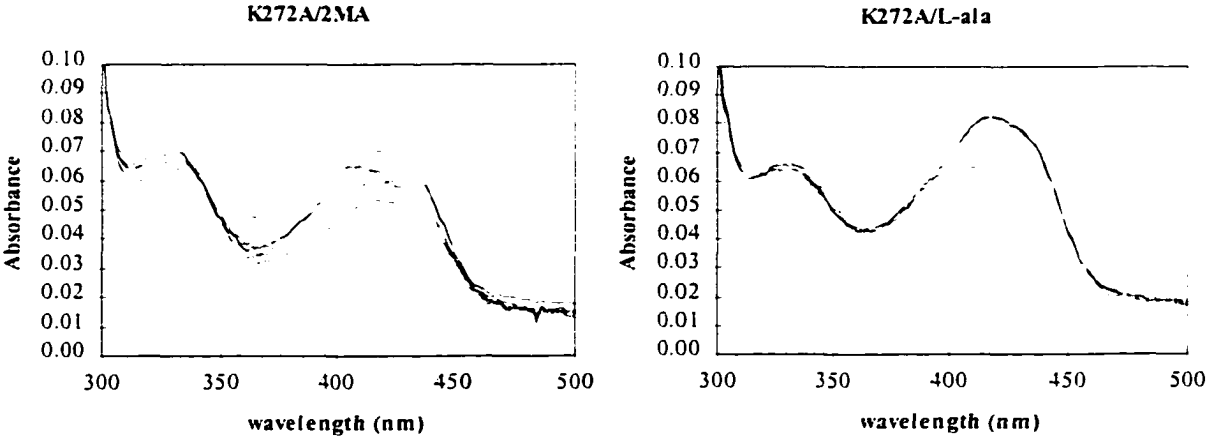

Figure 33. K272A DGD decarboxylation and transamination half reactions. K272A/2MA: spectra recorded at 0, 0.5, 1, 1.5, 2 and 3.5 hr after adding 2MA. K272A/L-ala: scans recorded at 0, 0.5, 1, 1.5 and 2 hr after adding L-ala. Reaction conditions: 2.75 μM protein and 40 mM 2MA/L-ala in 15 mM phosphate buffer, pH 6.75.

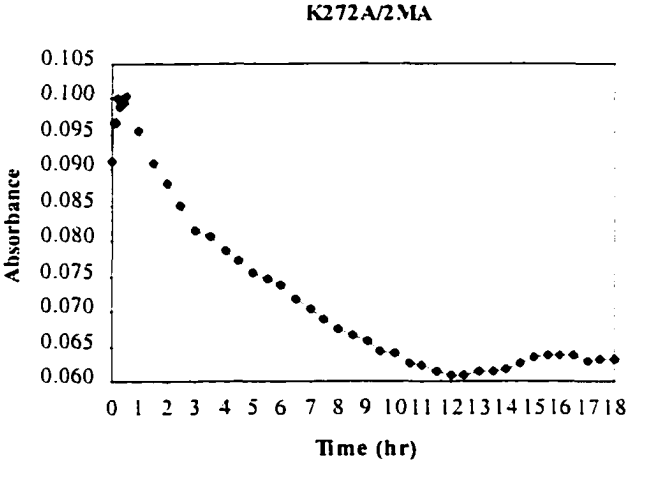

Figure 34. K272A DGD 18 hrs decarboxylation half reaction profile. Reaction conditions: 5.5 μM K272A, 40 mM 2MA in 15 mM phosphate buffer, pH 6.75. Time required to reduce half of total PLP was 3.5 hrs.

range with those obtained from Bailey and Dempsey (1967), Aaslestad et al. (1968) and Lamartiniere et al. (1971) (Table 12). The eukaryotic DGD from *Fusarium solani* shared many characteristics with bacterial DGD, in terms of structural organization, physical properties and substrate specificity (Esaki et al., 1994). The affinity towards 2MA is almost 3 times that of the bacterial DGD. Reaction rates at 2 mM pyruvate were slower than expected. This finding collaborates with Honma and Shimomura (1973) who reported concentration higher than 2 mM pyruvate inhibits DGD activity.

Table 12. K_{2MA} and K_{pyr} values of bacterial and eukaryotic DGDs.

Source	K_{2MA} (mM)	K_{pyr} (mM)	References
Pseudomonad Ps-1	8	2	Bailey and Dempsey (1967)
Pseudomonad sp.	4.5	2.5	Aaslestad et al. (1968)
B. cepacia	8.7	1.7	Lamartiniere et al. (1971)
F. solani	28	[a]	Esaki et al. (1994)

[a] not determined. K_m α-ketobutyrate = 0.3 mM.

Formation of WT DGD quinonoid intermediate. Bond cleavage of the external aldimine results in the transient formation of an intermediate, which absorbs at approximately 500 nm. The ascribed carbanionic species is usually referred to as the quinonoid intermediate (Jenkins, 1964; Morino and Snell, 1967). Many PLP-dependent enzymes exhibit similar bands with quasisubstrates or inhibitors.

Addition of glycerol induces the formation of a transient species absorbing at 500 nm in WT DGD. The accumulation of the quinonoid intermediate indicates that the 4'-C

protonation is slower than the C_α-COO^- and C_α-H bond cleavage. The solvent environment could have decreased the rate of protonation. Alternatively, the reaction at α- and 4'-C may be catalyzed by two different active site residues. A comparable example where two active site residues catalyze one reaction came from the mutagenesis studies of D-amino acid transaminase reported by Yoshimura et al. (1992), who showed that although exogenous amines could not substitute for Lys145 to abstract α-proton, K145N mutant was capable of performing transamination to a certain extent. They argued that an amino acid common to WT and K145N enzymes, e.g. Lys267, probably plays a role of being a less efficient base in the mutant, most likely as an auxillary catalyst. Similar, a DGD active site residue other than Lys272 acts as a general base to abstract proton and a residue yet to be determined is responsible for protonation at 4'-C (see pages 62 to 64 for more discussion).

K272A DGD lacked the '500 nm' chromophore found in WT DGD in the presence of 3% glycerol, probably due to insignificant level of decarboxylation or transamination. One possible interpretation could be the reprotonation of the transient species is faster than the rate of decarboxylation in active site lysine mutant. This scenario may be possible only if another residue, and not Lys272, functions as the proton donor in the 4'-C protonation step.

pH dependence of molar absorptivity of WT and K272A DGDs. The lack of spectral changes as pH varies from 5.5 to 11.0 in both WT and K272A DGDs indicates that there

is no change in the pK_a at the internal aldimine nitrogen of PLP residing at the active sites (Brayman, 1993; this work). Spectral data obtained from WT and K303A aromatic L-amino acid decarboxylase (Nishino et al., 1997) showed similar observation; the two enzyme forms showed no apparent pH dependency. On the contrary, spectra of tryptophanase (Zakomirdina et al., 1989), aspartate aminotransferase (Inoue et al., 1991) and aromatic amino acid aminotransferase (Hayashi et al., 1993) change with pH due to protonation of PLP-lysine aldimine at the active site. It is likely that DGD active site environment resembles that of decarboxylases more than those of aminotransferases and tryptophanase. The decarboxylation process is thought to depend on the hydrophobic environment that removes the water molecules and ions that might otherwise stabilize the carboxylate moiety (Marlier and O'Leary, 1986).

K272A DGD decarboxylation and transamination half reactions. The PLP molecule bound at the K272A active site is optically active as determined by the CD spectrum of the mutant (Brayman, 1993). Since Schiff's base formation is impossible, the cofactor is anchored in place via non-covalent bonds such as ionic interaction and hydrogen bonding.

Active site lysine to alanine mutation cripples the ability of K272A DGD to transaminate L-ala. The inability of K272A DGD to catalyze transamination is consistent with PLP enzymes involving C_α-H cleavage where replacement of lysine residue with other amino acids resulted in drastic decrease in catalytic rate. Mutagenesis studies of

aspartate aminotransferase (Toney and Kirsh, 1989) and D-amino acid aminotransferase (Nishimura et al., 1991) showed that the lysine-to-alanine mutants lacked any significant level of transamination but partial restoration of activity could be accomplished by using exogenous amines as auxillary catalysts. Brayman (1993) reported that attempts to use exogenous amines to revive the catalytic ability of K272A mutant were unsuccessful. The exogenous amines could only act as base to abstract α-proton in active site K272A mutant provided the amines can enter the active site. However, the speculated hydrophobic active site environment of DGD may prevent the entry of such auxillary catalysts.

K272A mutation affects 2MA decarboxylation to a lesser extent, which is in agreement with the conclusion of Nishino et al. (1997) who demonstrated that Lys303 of aromatic L-amino acid decarboxylase is not essential for the decarboxylation step. Since there is no amino group at the position 303 in the mutant, substrate forms external aldimine with PLP via dehydration. Product release must then proceed via hydrolysis.

A number of inferences emerge from the study. Firstly, Lys272 is critical for the α-proton abstraction step found commonly in reactions catalyzed by aminotransferases. It is anticipated that ε-amino group of lysine, when liberated upon substrate-PLP external aldimine formation, acts as a general base catalyst for C_α proton abstraction. However, the decarboxylation step is not dependent on this lysyl residue since the mutant can catalyze the reaction at a very slow rate. The marked decrease in decarboxylation rate could be explained: The active site lysine is indispensable for the increase of the

reactivity of 4'-aldehyde group of PLP by forming the Schiff base. Although the non-covalent bound PLP could form external aldimine with substrates and thus, in theory, reaction would proceed, the lack of enzyme activity in the mutants implies the importance of transformation from internal to external aldimine in promoting reactions of substantial rates.

4.6. Conclusion

In summary, Lys272 is important in catalyzing the α-proton abstraction in L-ala transamination and is not required for 2MA decarboxylation. The K272A DGD mutagenesis study is consistent with the current opinion that transamination involves C_α-H bond cleavage and the general base catalyst Lys272, whereas decarboxylation requires only bond breaking at C_α-COO^-. However, Lys272 is necessary to 'activate' the substrate/PLP complex so that both decarboxylation and transamination reactions could be catalyzed at reasonable rates.

Chapter 5

Recommendations for future research

Recommendation 1: Combine chemical modification by DEPC and site-directed mutagenesis to elucidate the function of histidines in DGD.

This method was employed by Wragg et al. (1997). The role of histidine residues in ppGaNTase was evaluated by mutagenesis of each hisitidine to an alanine residue. They proposed that the critical residues could be important in either coordinating the manganese ion, an essential factor for activity or maintaining structural integrity. The method could be modified to determine which histidine residues in DGD are critical for decarboxylation or transamination or both. Time dependent inactivation of the wild-type DGD and the histidine to alanine constructs is initiated with the addition of DEPC and terminated with L-histidine. The inactivated wild-type and mutant DGDs could be tested for decarboxylation and transamination activities. In theory, wild-type DGD will exhibit a gradual decrease in activity as DEPC inactivation duration progresses. The mutants with non-critical histidine mutated to alanine will also follow similar inactivation curves as the wild-type DGD. However, mutants with histidine residues critical to either reaction mutated to alanine residues will show negligible activity from the start of DEPC inactivation.

The PLP moiety in DGD is distant from the potassium ion (Figure 25, page 81), thus excluding direct involvement of the monovalent cation in catalysis. However, as pointed out by Isupov et al. (1998), the potassium ion in tryptophanase may maintain the relative position of certain domain or segment of the enzyme for effective catalysis. Likewise, mutation of His77 and His 304 to alanine residues may disrupt decarboxylation and/or transamination.

Recommendation 2: Mutagenesis of Tyr301 to glycine and phenylalanine to elucidate the function of Tyr301.

Residues at equivalent positions with Tyr301 DGD are mostly glycines and phenylalanines (Table 8, page 76). The dual functionality of this residue in DGD is unique among the aminotransferases. Firstly, the hydroxyl group of Tyr301 is postulated to hydrogen bond with Gln52, which has been shown to be critical for the decarboxylation step. Secondly, Tyr301 is thought to contribute to the hydrophobicity of the active site environment which enhances decarboxylation. The tyrosine to glycine mutant abolishes both functions while the phenylalanine mutant retains its hydrophobic character but no hydrogen bonding to Gln52.

Recommendation 3: Use rapid-scanning stopped-flow spectrophotometry in conjunction with circular dichroism to study coenzyme/analog spectra.

Using rapid-scanning stopped-flow spectrophotometry, Philip et al. (1997) reported that tyrosine phenol-lyase and tryptophanase form absorbance peaks at 500 nm

when reacted with fluorine-substituted analogs. The electron-withdrawing property of the fluorine could enhance or retard reaction rates of intermediate formation in a normal catalytic cycle. Also, fluorinated analogs could potentially disrupt critical hydrogen bonding between enzyme and substrate. Combination of WT, Q52H, Q52E DGDs and fluorinated analogs would be useful in interpreting the mechanism of the DGD catalytic cycle, especially the quinonoid formation in the three DGD forms.

Ben-Kasus et al. (1996) studied CD spectra of tryptophanase and its mutants with quasisubstrates, which are competitive inhibitors of the enzyme. They reasoned that the reorientation of either a tryptophan or tyrosine residue near the active site is thought to induce CD peak formation at 290 nm (Ben-Kasus et al., 1996). Once the covalent bond is formed between PLP and substrate, the residue shifts to its new position. It would be interesting to see if DGD exhibits this peak because Trp138 is located within the active site.

REFERENCES

Aaslestad, H. G. & Larson, A. D. (1964). Bacterial metabolism of 2-methylalanine. *J. Bacteriol.* **88**, 1296-1303.

Aaslestad, H. G., Bouis, P. J., Jr., Philips, A. T. & Larson, A. D. (1968). Characterization of a decarboxylation-dependent transaminase. In *Pyridoxal Catalysis: Enzyme Model Systems* (Snell, E. E., Braunstein, A. E., Severin, E. S. & Torchinsky, Y. M., eds), pp. 479-490, Wiley Interscience, New York.

Ahmed, S. A., McPhie, P. & Miles, E. W. (1996). Mechanism of activation of the tryptophan synthase alpha2beta2 complex. Solvent effects of the co-substrate beta-mercaptoethanol. *J. Biol. Chem.* **271**, 29100-29106.

Akhtar, M., Stevenson, D. E. & Gani, D. (1990). Fern L-methionine decarboxylase: kinetics and mechanism of decarboxylation and abortive transamination. *Biochemistry* **29**, 7648-7660.

Altschul, S. F., Gish, W., Miller, W., Myers, E. W. & Lipman, D. J. (1990). Basic local alignment search tool. *J. Mol. Biol.* **215**, 403-10.

Amann, E., Brosius, J. & Ptashne, M. (1983). Vectors bearing a hybrid trp-lac promoter useful for regulated expression of cloned genes in *Escherichia coli*. *Gene* **25**, 167-178.

Andre, B. & Jauniaux, J. C. (1990). Nucleotide sequence of the DURM gene coding for a positive regulator of allophanate-inducible genes in *Saccharomyces cerevisiae*. *Nucleic Acids Res.* **18**, 7136.

Ang, C. Y. W. (1979). Stability of three forms of vitamin B6 to laboratory light conditions. *J. Assoc. Off. Anal. Chem.* **62**, 1170-1173.

Arnone, A., Rogers, P. H., Hyde, C. C., Briley, P. D., Metzler, C. M. & Metzler, D. E. (1985). Pig cytosolic aspartate aminotransferase: The structures of the internal aldimine,

external aldimine, and ketimine and of the β subform. In *Transaminases* (Christen, P. & Metzler, D. E., eds), pp. 138-155, Wiley and Sons, New York.

Bailey, G. B. & Dempsey, W. B. (1967). Purification and properties of an α-dialkyl amino acid transaminase. *Biochemistry* **6**, 1526-1533.

Bailey, G. B., Chotamangsa, O. & Vuttivej, K. (1970). Control of pyridoxal phosphate enzyme reaction specificity studied with α-dialkylamino aid transaminase. *Biochemistry* **9**, 3243-3248.

Ben-Kasus, T., Markel, A., Gdalevsky, G. Y., Torchinsky, Y. M., Philips, R. S. & Parola, A. H. (1996). Interactions of *Escherichia coli* tryptophanase with quasisubstrates and monovalent cations studied by the circular dichroism and fluorescence methods. *Biochim. et Biophys. Acta* **1294**, 147-152.

Borisov, V. V., Borisova, S. N., Kachalova, G. S., Sosfenov, N. I. & Vainshtein, B. K. (1985). X-ray studies of chicken cytosolic aspartate aminotransferase. In *Transaminases* (Christen, P. & Metzler, D. E., eds), pp. 155-164, Wiley and Sons, New York.

Bradford, M. M. (1976). A rapid and sensitive method for the quantitation of microgram quantities of protein utilizing the principle of protein-dye binding. *Anal. Biochem.* **72,** 248-254.

Brandon, C. & Tooze, J. (1991). *Introduction to Protein Structure*, Garland Publishing, New York.

Brayman, T. G. (1993). Construction and characterization of an active site mutant of 2,2-dialkylglycine decarboxylase. M.S. dissertation, University of Alaska Fairbanks.

Bruckner, H. & Pryzbylski, M. (1984). Isolation and structural chracterization of polypeptide antibiotics of the peptaibol class by high-performance liquid chromatography with field desorption and fast atom bombardment mass spectrometry. *J. Chromatog.* **296**, 263-275.

Christen, P., Mehta, P. K. & Sandmeier, E. (1994). Molecular evolution of pyridoxal-5'-phopshate-dependent enzymes. In *Biochemistry of Vitamin B6 and PQQ* (Marino, G., Sannia, G. & Bossa, F., eds), pp. 9-13, Birkhauser Verlag, Switzerland.

Christen, P., Kasper, P., Gehring, H. & Sterk, M. (1996). Stereochemical constraint in the evolution of pyridoxal-5'-phosphate-dependent enzymes. A hypothesis. *FEBS letters* **389**, 12-14.

Conner, R., Churcher, C. M., Barrell, B. G., Rajandream, M. A. & Walsh, S. V. (1996). Sequence submitted to DDBJ/EMBL/GenBank databases.

Degols, G., Jauniaux, J. C. & Wiame, J.M. (1987). Molecular characterization of transposable-element-associated mutations that lead to constitutive L-ornithine aminotransferase expression in *Saccharomyces cerevisiae*. *Eur. J. Biochem.* **165**, 289-296.

Dempsey, W. B. (1969). Metabolism of α–aminoisobutyric acid by soil bacteria. *J. Bacteriol.* **97**, 182-185.

Dolphin, D., Poulson, R. & Avramovic, O. (1986). Editors of *Coenzymes and Cofactors, vol 1*, Wiley & Sons, New York.

Dunathan, H. C. (1966). Conformation and reaction specificity in pyridoxal phosphate enzymes. Proc. *Natl. Acad. Sci. USA* **55**, 712-716.

Dunathan, H. C. & Voet, J. G. (1974). Stereochemical evidence for the evolution of pyridoxal-phosphate enzymes of various function from a common ancestor. *Proc. Nat. Acad. Sci. USA* **71**, 3888-3891.

Echetebu, C. O., Ifem, F. M. & Echetebu, Z. O. (1987). Hepatic tyrosine aminotransferase from the rainbow lizard *Agama agama*: purification and some properties. *Biochimie* **69**, 223-230.

Esaki, N., Watanabe, M., Kurihara, T. & Soda, K. (1994) Fungal thermostable α-dialkylamino acid aminotransferase: occurrence, purification and characterization. *Arch. Microbiol.* **161**, 110-115.

Faleev, N. G., Dementieva, I. S., Zakomirdina, L. N., Gogoleva, O. I. & Belikov, V. M. (1994). Tryptophanase from *Escherichia coli*: catalytic and spectral properties in water-organic solvents. *Biochem. Mol. Biol. Int.* **34**, 209-216.

Ford, G. C., Eichele, G. & Jansonius, J. N. (1980). Three-dimensional structure of a pyridoxal-phosphate-dependent enzyme, mitochondrial aspartate aminotransferase. *Proc. Natl. Acad. Sci. USA* **77**, 2559-2563.

Gale, E. F. (1946). The bacterial amino acid decarboxylases. *Advan. Enzymol.* **6**, 1-32.

Gani, D. (1991). A structural and mechanistic comparison of pyridoxal 5'-phopshate dependent decarboxylase and transaminase enzymes. *Phil. Trans. R. Soc. Lond. B* **322**, 131-139.

Gloeckler, R., Ohsawa, I., Speck, D., Ledoux, C., Bernard, S., Zinsius, M., Villeval, D., Kisou, T., Kamogawa, K. & Lemoine, Y. (1990). Cloning and characterization of the *Bacillus sphaericus* genes controlling the bioconversion of pimelate into dethiobiotin. *Gene* **87**, 63-70.

Grimm, B., Smith, M. A. & von Wettstein, D. (1992). The role of Lys272 in the pyridoxal 5-phosphate active site of *Synechococcus* glutamate-1-semialdehyde aminotransferase. *Eur. J. Biochem.* **206**, 579-585.

Guan, C., Ribeiro, A., Akkermans, A. D., Jing, Y., van Kammen, A., Bisseling, T. & Pawlowski, K. (1996). Nitrogen metabolism in actinorhizal nodules of *Alnus glutinosa*: expression of glutamine synthetase and acetylornithine transaminase. *Plant Mol. Biol.* **32**, 1177-1184.

Gunsalus, I. C., Bellamy, W.D., Umbreit, W.W. (1944). A phosphorylated derivative of pyridoxal as the coenzyme of tyrosine decarboxylase. *J. Biol. Chem.* **155**, 685-686.

Hackert, M. L., Carroll, D. W., Davidson, L., Kim, S.-O., Momany, C., Vaaler, G. L. & Zhang, L. (1994). Sequence of ornithine decarboxylase from *Lactobacillus* sp. strain 30a. *J. Bacteriol.* **176**, 7391-7394.

Harris, S. A., Heyl, D. & Folkers, D. (1944). The structure and synthesis of pyridoxamine and pyridoxal. *J. Biol. Chem.* **154**, 315-316.

Hayashi, H., Inoue, K., Nagata, T., Kuramitsu, S. & Kagamiyama, H. (1993). *Escherichia coli* aromatic amino acid aminotransferase: characterization and comparison with aspartate aminotransferase. *Biochemistry* **32**, 12229-12239.

Heimberg, H., Boyen, A. H., Crabeel, M. & Glansdorff, N. (1990). *Escherichia coli* and *Saccharomyces cerevisiae* acetylornithine aminotransferases: evolutionary relationship with ornithine aminotransferases. *Gene* **90**, 69-78.

Hennig, M., Grimm, B., Contestabile, R., John, R. A. & Jansonius, J. N. (1997). Crystal structure of glutamate-1-semialdehyde aminomutase: an alpha2-dimeric vitamin B_6-dependent enzyme with asymmetry in structure and active site reactivity. *Proc. Natl. Acad. Sci. USA* **13**, 4866-4871.

Honma, M., Ikeda, M. & Shimomura, T. (1972). Aminotransferase activity of α-aminoisobutyric acid decomposing enzyme. *Agr. Biol. Chem.* **36**, 1661-1666.

Honma, M. & Shimomura, T. (1973). Kinetic studies on α-aminoisobutyrate decomposing enzyme. *Agr. Biol. Chem.* **38**, 953-958.

Honma, M. & Shimomura, T. (1976). α-Aminoisobutyrate decomposing enzyme in α-methylserine metabolism. *Agr. Biol. Chem.* **40**, 2105-2106.

Inana, G., Totsuka, S., Redmond, M., Dougherty, T., Nagle, J., Shiono, T., Ohura, T., Kominami, E. & Katunuma, N. (1986). Molecular cloning of human ornithine aminotransferase mRNA. *Proc. Natl. Acad. Sci. U.S.A.* **83**, 1203-1207.

Inoue, K., Kuramitsu, S., Okamoto, A., Hirotsu, K., Higuchi, T., Morino, Y. & Kagamiyama, H. (1991). Tyr225 in aspartate aminotransferase: contribution of the hydrogen bond between Tyr225 and coenzyme to the catalytic reaction. *J. Biochem.* **109**, 570-576.

IUPAC-IUB Commission on Biochemical Nomenclature. (1973). Nomenclature for vitamin B6 and related compounds. *Eur. J. Biochem.* **40**, 325-327.

Isupov, M. N., Antson, A. A., Dodson, E. J., Dodson, G. G., Dementieva, I. S., Zakomirdina, L. N., Wilson, K. S., Dauter, Z., Lebedev, A. A. & Harutyunyan, E. H. (1998). Crystal structure of tryptophanase. *J. Mol. Biol.* **276**, 603-623.

Ivanov, V. I. & Karpeisky, M. Y. (1969). Dynamic three-dimensional model for enzymic transamination. *Adv. Enzymol. Relat. Areas Mol. Biol.* **32**, 21-53.

Jagath, J. R., Appaji Rao, N. & Savithri, H. S. (1997). Role of Arg-401 of cytosolic serine hydroxymethyltransferase in subunit assembly and interaction with the substrate carboxy group. *Biochem. J.* **327**, 877-882.

Janssen, A., Chen, X. J. & Clark-Walker, G. D. (1997). Sequence submitted to DDBJ/EMBL/GenBank databases.

Jenkins, W. T. (1964). Glutamic-aspartic transaminase. *J. Biol. Chem.* **239**, 1742-1747.

Kalyankar, G. D. & Snell, E. E. (1962). Pyridoxal-catalyzed decarboxylation of amino acids. *Biochemistry* **1**, 594-600.

Kaneko, T., Sato, S., Kotani, H., Tanaka, A., Asamizu, E., Nakamura, Y., Miyajima, N., Hirosawa, M., Sugiura, M., Sasamoto, S., Kimura, T., Hosouchi, T., Matsuno, A., Muraki, A., Nakazaki, N., Naruo, K., Okumura, S., Shimpo, S., Takeuchi, C., Wada, T., Watanabe, A., Yamada, M., Yasuda, M. & Tabata, S. (1996). I. Sequence analysis of the genome of the unicellular cyanobacterium *Synechocystis sp.* strain PCC6803. II. Sequence determination of the entire genome and assignment of potential protein-coding regions. *DNA Res.* **3**, 109-136.

Keller, J. W., Baurick, K. B., Rutt, G. C., O'Malley, M. V., Sonafrank, N. L., Reynolds, R. A., Ebbesson, L. O. & Vajdos, F. F. (1990). *Pseudomonas cepacia* 2,2-dialkylglycine decarboxylase sequence and expression in *Escherichia coli* of structural and repressor genes. *J. Biol. Chem.* **265**, 5531-5539.

Keller, J. W., Brayman, T. G. & Woon, S.-T. (1997). Genetic engineering of the *Burkholderia (Pseudomonas) cepacia* dialkylglycine decarboxylase. *International Workshop on New Trends in Biocatalysis Research*, 268-269.

Lamartiniere, C. A., Hajime, I. & Dempsey, W. B. (1971) α-Dialkylamino acid transaminase from *Pseudomonas cepacia*. Purification, crystallization, physical, and kinetic properties. *Biochemistry* **10**, 4783-4788.

Lee, I. S., Muragaki, Y., Ideguchi, T., Hase, T., Tsuji, M., Ooshima, A., Okuno, E. & Kido, R. (1995). Molecular cloning and sequencing of a cDNA encoding alanine-glyoxylate aminotransferase 2 from rat kidney. *J. Biochem.* **117**, 856-862.

Leklem, J. K. (1991). Vitamin B6. In *Handboook of Vitamins* (Machlin, L. J., ed), pp. 341–392, Marcel Dekker, New York.

Leussing, D. L. (1986). Model reactions. In *Coenzymes and Cofactors, vol 1* (Dolphin, D., Poulson, R. & Avramovic, O., eds), pp. 69-115, Wiley & Sons, New York.

Lowe, D. M., Fersht, A. R. & Wilkinson, A. J. (1985). Probing hisitidine-substrate interactions in tyrosyl-tRNA synthetase using asparagine and glutamine replacements. *Biochemistry* **24**, 5106-5109.

Lu, Z., Nagata, S., McPhie, P. & Miles, E. W. (1993). Lysine 87 in the α-subunit of tryptophan synthase that forms an internal aldimine with pyridoxal phosphate serves critical roles in transimination, catalysis, and product release. *J. Biol. Chem.* **268**, 8727-8734.

Lukacin, R. & Britsch, L. (1997). Identification of strictly conserved histidine and arginine residues as part of the active site in *Petunia hydrida* flavanone 3α-hydroxylase. *Eur. J. Biochem.* **249**, 748-757.

Marlier, J. F. & O'Leary, M. H. (1986). Solvent dependence of the carbon kinetic isotope effect on the decarboxylation of 4-pyridylacetic acid. A model for enzymatic decarboxylations. *J. Am. Chem. Soc.* **108**, 4896-4899.

Mayer, S. M., Rieble, S. & Beale, S. I. (1994). Metal requirements of the enzymes catalyzing conversion of glutamate to delta-aminolevulinic acid in extracts of *Chlorella vulgaris* and *Synechocystis sp.* PCC 6803. *Arch. Biochem. Biophys.* **312**, 203-209.

McPhalen, C. A., Vincent, M. G. & Jansonius, J. N. (1992). X-ray structure refinement and comparison of three forms of mitochondrial aspartate aminotransferase. *J. Mol. Biol.* **225**, 495–517.

Mehta, P. K., Hale, T. I. & Christen, P. (1993). Aminotransferases: demonstration of homology and division into evolutionary subgroups. *Eur. J. Biochem.* **214**, 549-561.

Mehta, P. K. & Christen, P. (1994). Homology of 1-aminocyclopropane-1-carboxylate synthase, 8-amino-7-oxononanoate synthase, 2-amino-6-caprolactam racemase, 2,2-diakylglycine decarboxylase, glutamate-1-semialdehyde 2,1-aminomutase and isopenicillin-*N*-epimerase with aminotransferases. *Biochem. Biophys. Res. Comm.* **198**, 138-143.

Metzler, C. M. & Metzler, D. E. (1987). Quantitative description of absorption spectra of a pyridoxal phosphate-dependent enzyme using lognormal distribution curves. *Anal. Biochem.* **166**, 313-327.

Momany, C., Ghosh, R. & Hackert, M. L. (1995). Structural motifs for pyridoxal-5'-phosphate binding in decarboxylases: An analysis based on the crystal structure of the Lactobacillus 30a ornithine decarboxylase. *Pro. Sci.* **4**, 849-854.

Morino, Y. & Snell, E. E. (1967). The relation of spectral changes and tritium exchange reactions to the mechanism of tryptophanase-catalyzed reactions. *J. Biol. Chem.* **242**, 2800-2809.

Mueckler, M. M. & Pitot, H. C. (1985). Sequence of the precursor to rat ornithine aminotransferase from a cDNA clone. *J. Biol. Chem.* **260**, 12993-12997.

Mumford, J. P. & Cannon, D. J. (1994). Vigabatrin. *Epilepsia* **35**(Suppl 5), 25-28.

New England Biolabs. (1994). RbCl transformation procedure for improved efficiency. *NEB Transcript* **6**, no 1, pp. 7.

Nishimura, K., Tanizawa, K., Yoshimura, T., Esaki, N., Futaki, S., Manning, J. M. & Soda, K. (1991). Effect of substitution of a lysyl residue that binds pyridoxal phosphate in thermostable D-amino acid aminotransferase by arginine and alanine. *Biochemistry* **30**, 4072-4077.

Nishino, J., Hayashi, H., Ishii, S. & Kagamiyama, H. (1997). An anomalous side reaction of the Lys303 mutant aromatic L-amino acid decarboxylase unravels the role of the residue in catalysis. *J. Biochem.* **121**, 604-611.

Okamoto, A., Higuchi, T., Hirotsu, K., Kuramitsu, S. & Kagamiyama, H. (1994). X-ray crystallographic study of pyridoxal 5'-phosphate-type aspartate aminotransferases from *Escherichia coli* in open and closed form. *J. Biochem.* **116**, 95-107.

Otsuka, A. J., Buoncristiani, M. R., Howard, P. K., Flamm, J., Johnson, C., Yamamoto, R., Uchida, K., Cook, C., Ruppert, J. & Matsuzaki, J. (1988). The *Escherichia coli* biotin biosynthetic enzyme sequences predicted from the nucleotide sequence of the bio operon. *J. Biol. Chem.* **263**, 19577-19585.

Palcic, M. M. & Floss, H. G. (1986). Conformation and stereochemistry of free and bound pyridoxal phsophate and its derivatives. In *Coenzymes and Cofactors, vol I* (Dolphin, D., Poulson, R. & Avramovic, O., eds), pp. 26-68, Wiley & Sons, New York.

Philips, R. S., Richter, I., Gollnick, P., Brzovic, P. & Dunn, M. F. (1991). Replacement of lysine 269 by arginine in *Escherichia coli* tryptophan indole-lyase affects the formation and breakdown of quinonoid complexes. *J. Biol. Chem.* **266**, 18642-18648.

Philips, R. S., von Tersch, R. L. & Secundo, F. (1997). Effects of tyrosine ring fluorination on rates and equilibria of formation of intermediates in the reactions of carbon-carbon lyases. *Eur. J. Biochem.* **244**, 658-663.

Quirk, P. G. & Krulwich, T. A. (1991). Sequence submitted to DDBJ/EMBL/GenBank databases.

Richardson, I. B., Hurley, S. K. & Hynes, M. J. (1989). Cloning and molecular characterisation of the amdR controlled gatA gene of *Aspergillus nidulans*. *Mol. Gen. Genet.* **217**, 118-125.

Sato, S., Mamoru, H. & Shimomura, T. (1978). The conversion of α-aminoisobutyrate decomposing enzyme into simple L-alanine : α-ketobutyrate aminotransferase by chemical modification. *Agr. Biol. Chem.* **42**, 2341-2346.

Sauberlich, H. E. (1985). Interaction of vitamin B6 with other nutrients. In *Vitamin B6: Its Role in Health and Disease* (Reynolds, R. D. & Leklem, J. K., eds.), pp. 193-217, A. R. Liss, New York.

Shah, S. A., Shen, B.W. & Brunger, A. T. (1997). Human ornithine aminotransferase complexed with L-canaline and gabaculine: structural basis for substrate recognition. *Structure* **5**, 1067-1075.

Shen, B. W., Henning, M., Hohenester, E., Jansonius, J. & Schirmer, T. (1998). Crystal structure of human recombinant ornithine aminotranferase. *J. Mol. Biol.* **277**, 81-102.

Snell, E. E., Guirard, B. M. & Williams, R. J. (1942). Occurrence in natural products of a physiologically active metabolite of pyridoxine. *J. Biol. Chem.* **143**, 519-530.

Snell, E. E. (1944). The vitamin activities of pyridoxal and pyridoxamine. *J. Biol. Chem.* **154**, 313-314.

Snell, E. E. (1986). Pyridoxal phosphate: history and nomenclature. In *Coenzymes and Cofactors, vol I* (Dolphin, D., Poulson, R. & Avramovic, O., eds), pp. 1-12, Wiley & Sons, New York.

Snell, E. E. (1994). History of vitamin B. In *Biochemistry of Vitamin B6 and PQQ* (Marino, G., Sannia, G. & Bossa, F., eds.), pp. 1-5, Birkhauser Verlag, Switzerland.

Sugio, S., Petsko, G. A., Manning, J. M., Soda, K. & Ringe, D. (1995). Crystal structure of a D-amino acid aminotransferase: how the protein controls stereoselectivity. *Biochemistry* **34**, 9661-9669.

Sun, S., Zabinski, R. F. & Toney, M. D. (1998) Reactions of alternative substrates demonstrate stereoelectronic control of reactivity in dialkylglycine decarboxylase. *Biochemistry* **37**, 3865-3875.

Tilley, K., Akhtar, M. & Gani, D. (1994). The stereochemical course of decarboxylation, transamination and elimination reactions catalysed by *Escherichia coli* glutamic acid decarboxylase. *J. Chem. Soc. Perkin Trans.* **1**, 3079-3087.

Toney, M. D. & Kirsch, J. F. (1989). Direct Bronsted analysis of the restoration of activity to a mutant enzyme by exogenous amines. *Science* **243**, 1485-1488.

Toney, M. D. & Kirsch, J. F. (1991). The K258R mutant of aspartate aminotransferase stabilizes the quinonoid intermediate. *J. Biol. Chem.* **266**, 23900-23903.

Toney, M. D. & Kirsch, J. F. (1993). Lysine 258 in aspartate aminotransferase: Enforcer of the Circe effect for amino acid substrates and general-base catalyst for the 1,3-prototropic shift. *Biochemistry* **32**, 1471-1479.

Toney, M. D., Hohenester, E., Keller, J. W. & Jansonius, J. N. (1995a). Structural and mechanistic analysis of two refined crystal structures of the pyridoxal phosphate-dependent enzyme dialkylglycine decarboxylase. *J. Mol. Biol.* **245**, 151-179.

Toney, M. D., Pascarella, S. & de Biase, D. (1995b). Active site model for γ-aminobutyrate aminotransferase explains substrate specificity and inhibitor reactivities. *Pro. Sci.* 4, 2366-2374.

Tramonti, A., de Biase, D., Giartosio, A., Bossa, F. & John, R. (1998). The roles of His167 and His275 in the reaction catalyzed by glutamate decarboxylase from *Escherichia coli*. *J. Biol. Chem.* **273**, 1939-1945.

United States Biochemical. (1993). *Topics in DNA sequencing: sequencing gel compressions*. In Nucleic acid sequencing, pp. 69.

Vaalar, G. L. & Snell, E. E. (1989). Pyridoxal 5'-phosphate dependent histidine decarboxylase: overproduction, purification, biosynthesis of soluble site-directed mutant proteins, and replacement of conserved residues. *Biochemistry* **28**, 7306-7313.

van Poelje, P. D., Kamath, A. V. & Snell, E. E. (1990). Site-directed alteration of the active-site residues of histidine decarboxylase from *Clostridium perfringens*. *Biochemistry* **29**, 10413-10418.

Watanabe, N., Sakabe, K., Higashi, T., Sasaki, K., Aibara, S., Morita, Y., Yonaha, K., Toyama, S. & Fukutani, H. (1989). Crystal structure analysis of omega-amino acid:pyruvate aminotransferase with a newly developed Weissenberg camera and an imaging plate using synchrotron radiation. *J. Biochem.* **105**, 1-3.

Wilson, R., Ainscough, R., Anderson, K., Baynes, C., Berks, M., Bonfield, J., Burton, J., Connell, M., Copsey, T., Cooper, J., Coulson, A., Craxton, M., Dear, S., Du, Z., Durbin, R., Favello, A., Fulton, L., Gardner, A., Green, P., Hawkins, T., Hillier, L., Jier, M., Johnston, L., Jones, M., Kershaw, J., Kirsten, J., Laister, N., Latreille, P., Lightning, J., Lloyd, C., McMurray, A., Mortimore, B., O'Callaghan, M., Parsons, J., Percy, C., Rifken, L., Roopra, A., Saunders, D., Shownkeen, R., Smaldon, N., Smith, A., Sonnhammer, E., Staden, R., Sulston, J., Thierry-Mieg, J., Thomas, K., Vaudin, M., Vaughan, K., Waterston, R., Watson, A., Weinstock, L., Wilkinson-Sproat, J. & Wohldman, P. (1994). 2.2 Mb of contiguous nucleotide sequence from chromosome III of *C. elegans*. *Nature* **368**, 32-38.

Wragg, S., Hagen, F. K. & Tabak, L. A. (1997). Identification of essential histidine residues in UDP-*N*-acetyl-D-galactosamine : polypeptide N-acetylgalactosaminyl-transferase-T1. *Biochem. J.* **328**, 193-197.

Yano, T., Hinoue, Y., Chen, V. J., Metzler, D. E., Miyahara, I., Hirotsu, K. & Kagamiyama, H. (1993). Role of an active site residue analyzed by combination of mutagenesis and coenzyme analog. *J. Mol. Biol.* **234**, 1218-1229.

Yonaha, K., Nishie, M. & Aibara, S. (1992). The primary structure of omega-amino acid:pyruvate aminotransferase. *J. Biol. Chem.* **267**, 12506-12510.

Yoshimura, T., Bhatia, M. B., Manning, J. M., Ringe, D. & Soda, K. (1992). Partial reactions of bacterial D-amino acid transaminase with asparagine substituted for the lysine that binds coenzyme pyridoxal 5'-phosphate. *Biochemistry* **31**, 11748-11754.

Zakomirdina L. N., Sakharova, I. S. & Torchinsky Y. M. (1989). Conformational changes in the active site of tryptophanase revealed by the circular dichroism method. *Biochimie* **71**, 545-550.

APPENDIX 1

E. coli codon usage table

Codon usage database compiled from CUTG (Codon Usage Tabulated from Genbank)
Source : Genbank release 102 (15 Aug 97)
Fields : [amino acid] [triplet] [frequency per thousand]

Phe	UUU	21.8	Ser	UCU	9.1	Tyr	UAU	16.2	Cys	UGU	5.1
Phe	UUC	16.7	Ser	UCC	8.9	Tyr	UAC	12.4	Cys	UGC	6.4
Leu	UUA	13.5	Ser	UCA	7.6	Stop	UAA	2.0	Stop	UGA	1.0
Leu	UUG	13.2	Ser	UCG	8.7	Stop	UAG	0.3	Trp	UGG	14.5
Leu	CUU	11.1	Pro	CCU	7.0	His	CAU	12.7	Arg	CGU	21.0
Leu	CUC	10.7	Pro	CCC	5.3	His	CAC	9.8	Arg	CGC	21.6
Leu	CUA	3.9	Pro	CCA	8.5	Gln	CAA	14.7	Arg	CGA	3.6
Leu	CUG	52.0	Pro	CCG	22.8	Gln	CAG	29.0	Arg	CGG	5.5
Ile	AUU	29.8	Thr	ACU	9.4	Asn	AAU	18.0	Ser	AGU	8.8
Ile	AUC	25.0	Thr	ACC	23.1	Asn	AAC	21.8	Ser	AGC	15.7
Ile	AUA	4.8	Thr	ACA	7.5	Lys	AAA	34.3	Arg	AGA	2.5
Met	AUG	27.5	Thr	ACG	14.0	Lys	AAG	11.2	Arg	AGG	1.5
Val	GUU	18.9	Ala	GCU	16.0	Asp	GAU	32.1	Gly	GGU	25.2
Val	GUC	14.9	Ala	GCC	25.3	Asp	GAC	19.5	Gly	GGC	29.2
Val	GUA	11.2	Ala	GCA	20.4	Glu	GAA	39.8	Gly	GGA	8.3
Val	GUG	25.8	Ala	GCG	32.9	Glu	GAG	18.4	Gly	GGG	11.0

APPENDIX 2

Correlation between codon usage with DGD production

DGD		codon	codon usage	g of cells	mg DGD	mg DGD/g of cells
WT	Gln	CAG	29.0	13.2	51.0	3.86
Q52A	Ala	GCG	32.9	11.4	18.4	1.62
Q52D	Asp	GAT	32.1	12.0	45.5	3.79
Q52E	Glu	GAA	39.8	12.4	40.0	3.23
Q52G	Gly	GGC	29.2	18.0	23.8	1.32
Q52H	His	CAC	9.8	16.7	28.8	1.72
Q52K	Lys	AAG	11.2	9.0	19.8	2.20
Q52L	Leu	CTA	3.9	19.0	46.4	2.44
Q52N	Asn	AAT	18.0	8.2	16.8	2.04
Q52R	Arg	CGA	3.6	15.4	35.0	2.27
Q52W	Trp	TGG	14.5	16.2	15.6	0.96

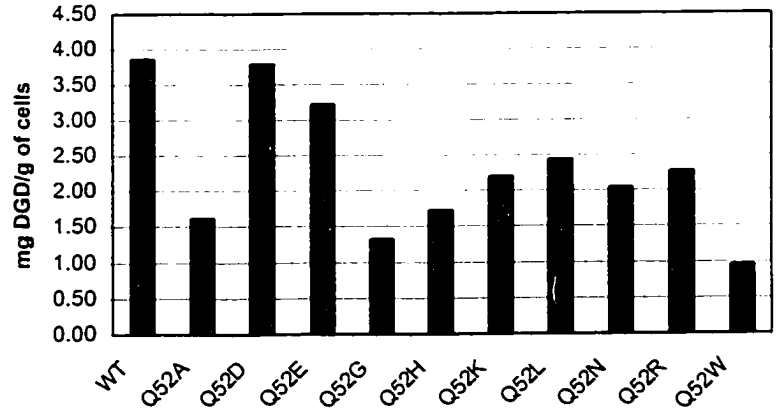

IMAGE EVALUATION TEST TARGET (QA-3)

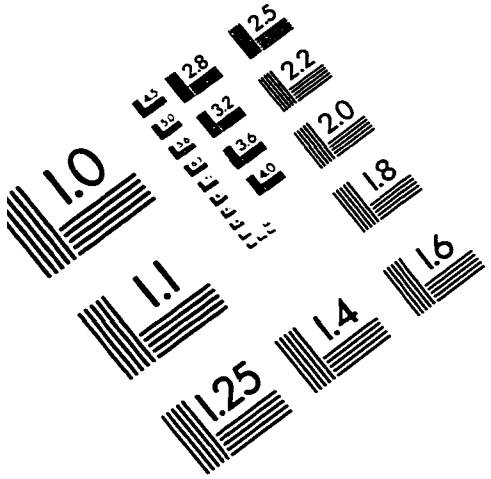

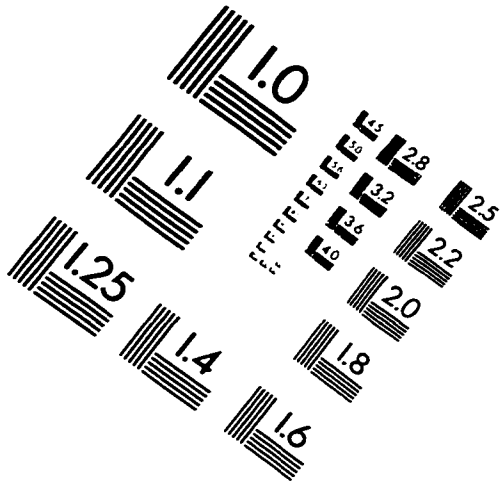

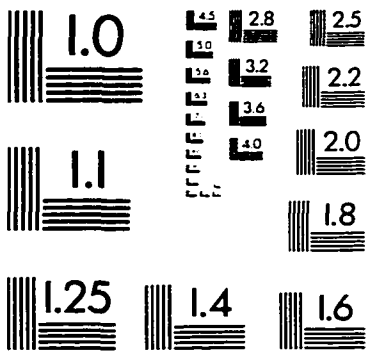

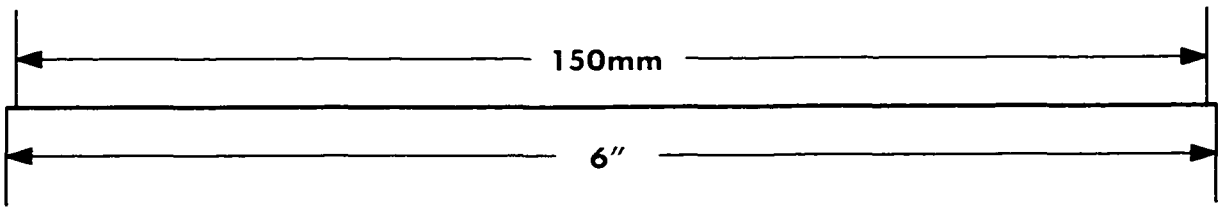

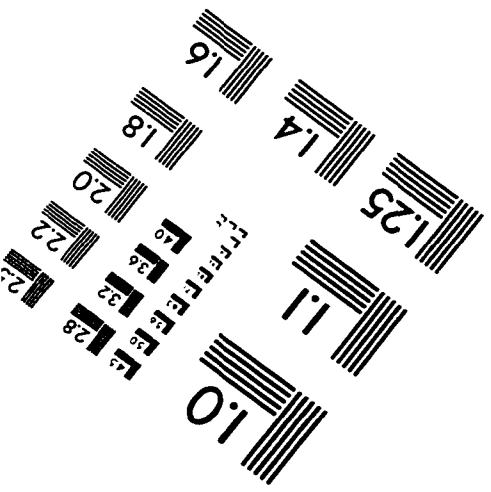

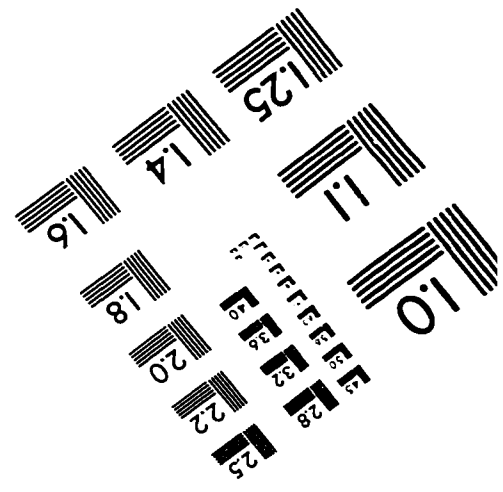

APPLIED IMAGE . Inc
1653 East Main Street
Rochester, NY 14609 USA
Phone: 716/482-0300
Fax: 716/288-5989